NANOSCALE SILVER AND GOLD FOR CHEMICAL AND BIOLOGICAL APPLICATIONS

A THESIS SUBMITTED IN PARTIAL FULFILMENT OF THE REQUIREMENTS FOR THE AWARD OF THE DEGREE OF

DOCTOR OF PHILOSOPHY

By

SONIT KUMAR GOGOI

ROLL NO. 04612208

DEPARTMENT OF CHEMISTRY

INDIAN INSTITUTE OF TECHNOLOGY GUWAHATI

GUWAHATI – 781039, INDIA

DECEMBER 2010

Dedicated to my parents

Mrs. Kamal Prova Gogoi
&
Mr. Nirmal Chandra Gogoi

INDIAN INSTITUTE OF TECHNOLOGY

GUWAHATI

Department of Chemistry

STATEMENT

I hereby declare that the matter embodied in this thesis is the result of investigations carried out by me in the Department of Chemistry, Indian Institute of Technology Guwahati, India under the guidance of Dr. Anumita Paul, Associate Professor of Chemistry.

In keeping with the general practice of reporting observations, due acknowledgements have been made wherever the work described is based on the findings of other investigators.

I. I. T. Guwahati **Sonit Kumar Gogoi**

December, 2010

INDIAN INSTITUTE OF TECHNOLOGY

GUWAHATI

Department of Chemistry

CERTIFICATE

It is certified that the work described in this thesis, entitled "*Nanoscale Silver and Gold for Chemical and Biological Applications*", done by Mr. Sonit Kumar Gogoi for the award of degree of Doctor of Philosophy is an authentic record of the results obtained from the research work carried out under my supervision in the Department of Chemistry, Indian Institute of Technology Guwahati, India, and this work has not been submitted elsewhere for a degree.

I. I. T. Guwahati
December, 2010

Anumita Paul
Associate Professor
(Thesis Supervisor)

INDIAN INSTITUTE OF TECHNOLOGY

GUWAHATI

Department of Chemistry

COURSE CERTIFICATE

This to certify that Mr. Sonit Kumar Gogoi has satisfactorily completed all the courses required for the Ph. D. degree programme. These courses include

CH 603	Supramolecules: Concept and Application
CH 621	New Reagents for Organic Synthesis
CH 601	Physical Methods in Chemistry
CH 632	Advanced Group Theory & Application

Mr. Sonit Kumar Gogoi has successfully completed his Ph. D. qualifying examination in April 2005.

Prof. Arun Chattopadhyay
Head, Department of Chemistry

Prof. T. Punniyamurthy
Secretary, DPPC

Acknowledgement

Writing the acknowledgement now fills my heart with gratitude. This is the opportunity I must take to offer my sincere thanks to Dr. Anumita Paul under whose guidance I had the honour to work for the degree of Doctor of Philosophy. Pleasure of scientific research was introduced to me and was always encouraged to explore new areas. I am also thankful to her for providing me with the opportunity to learn many instrumental methods vital for the research work.

Words seem dwarfed when I am trying to express my gratitude towards Prof. Arun Chattopadhyay who has been a driving force in shaping my thesis work. He has always been an inspirational figure to the young people like me coming into the scientific community. His encouragement and suggestions have shown light in my venture into the world of science.

I offer my heartfelt thanks to Dr. Siddhartha Sankar Ghosh of Department of Biotechnology, I. I. T. Guwahati. Without his support my research work would not have been complete and I would not have the opportunity to venture into the exciting field of nanobiotechnology. I am also indebted to Dr. A. Ramesh of the same department for his valuable suggestions. Doctoral committee member Dr. P. K. Iyer's suggestions were valuable and accepted with gratitude.

I am obliged to all the faculty members of Department of Chemistry, I. I. T. Guwahati for extending their helping hands whenever I approached. Special mention must be made of the teachers of the department who taught me during my M. Sc. for they made me like the department and stay longer for the Ph. D. work. Also I must thank Mr. Babulal Das, Mrs. Lipika Nath, Mr. Parikshit Gogoi, Mrs. Abhilasa Barua, Mr. Aniruddha Gogoi, Mr. Nilotpal Deka, Mr. Diganta K. Hira, Mr. Shyamal K. Mondol,

Mr. Santanu Deka and Mr. Subal Das for their help and support all the time. It has been a wonderful experience being associated with the department.

My sincere thanks to all the faculty members of the Department of Chemistry, Gauhati University for their help and cooperation during the last one and half year of my relationship with the department.

Let me also offer my gratitude to Mr. Chandan Borgohain and Mr. Kula Kamal Senapati of Central Instruments Facility for helping me with their technical support. I must also thank here Dr. Manoranjan Kar, Mr. Kaustubh Acharyya, Mr. Indrajit Talukdar, Mr. Paran Jyoti Dutta of Centre for Nanotechnology, I. I. T. Guwahati and Mr. Sidananda Sarma of Department of Physics, I. I. T. Guwahati. Sincere thanks are also to SAIF, NEHU Shillong, IIT Kharagpur and IACS Kolkata.

May be our laboratory is the best place to work in the whole world for the people I got the pleasure to share time and knowledge with. Some of the best labmates possible, starting from the seniors Dr. Tridib K Sarma, Dr. Devasish Choudhury, Dr. Gitanjali Majumdar, Dr. Biswa Ranjan Panda to friends Jashmini, Krishna, Muruga, Deba, Sankar da, Ali, Partha and juniors Sadhu, Subhojit, Raihana, Pallab, Palash, Rumi, Satyapriya, Amaresh and Roma. These are the people who made lab-work fun. Dr. P. Gopinath, a dear friend with whom I had the satisfaction of working in collaboration and learning many new techniques.

Stay in I. I. T. Guwahati has been a memorable part of my life both from the personal and the professional point of view. This would not have been so without my friends here. Many sweet things flood my mind when I try to thank these people and I am confused where to start. I think it would be appropriate to say 'thank you' to all my friends to start with and mention a few names that flash in. It has been a great pleasure being able to share my personal and professional life with you people and a

great learning experience. I extend my sincere thanks to Prasanta, Gunin da, Madhurjya, Ballav, Dhruba, Bolin da, Pranjal da, Lokman, Sahid da, Biplab, Santanu, Manash, Raju bhaiya, Babu bhaiya, Rupam da, Atul, Satish, Bimlesh, Dilip, Rama, Anto, Rupam, Deep, Sumantra, Saitanya, Soumya, Nihar, Ramesh and all the research scholars of the department for their constant help, motivation and enthusiastic company. I must also thank Dr. Arup Purakayastha, Anupam, Nirupam, Bani, Angshuman, Nayan, Sagar, Dipankar and Bhaskar for their help in providing me with the journal publications unavailable here at the earliest.

During the course of Ph. D. work financial assistance was provided by I. I. T. Guwahati and CSIR New Delhi in parts. I would like to thank them on this occasion. I also acknowledge I. I. T. Guwahati for providing the necessary infrastructure for successful completion of my Ph. D. work.

This work would not have come to this stage without the constant love, support and blessings of my parents, my in laws and my brother Sourabh and brother in laws Dr. Bhaskar J. Baruah , Rishav. I am also thankful to my wife Akashi for helping and supporting me in every step of my work as well as life.

I. I. T. Guwahati **Sonit Kumar Gogoi**

December, 2010

List of Publications

1. **Green Fluorescent Protein-Expressing *Escherichia coli* as a Model System for Investigating the Antimicrobial Activities of Silver Nanoparticles**
   Sonit Kumar Gogoi, P. Gopinath, Anumita Paul, A. Ramesh, Siddhartha Sankar Ghosh, and Arun Chattopadhyay *Langmuir* **2006**, *22*, 9322-9328.

2. **Implications of silver nanoparticle induced cell apoptosis for *in vitro* gene therapy**
   P Gopinath, Sonit Kumar Gogoi, Arun Chattopadhyay and Siddhartha Sankar Ghosh. *Nanotechnology*, **2008**, *19*, 075104.

3. **Signaling gene cascade in silver nanoparticle induced apoptosis**
   P. Gopinath, Sonit Kumar Gogoi, Pallab Sanpui, Anumita Paul, Arun Chattopadhyay and Siddhartha Sankar Ghosh. *Colloids and Surfaces B: Biointerfaces*, **2010**, *77*, 240-245.

4. **Generation of Ag-Au Bimetallic Nanoparticle Patterns on a Templated Surface by Chemical Reaction**
   Sonit Kumar Gogoi, Anumita Paul, Arun Chattopadhyay (manuscript under preparation)

5. **Chemical Reaction Based Generation of Electronically Transparent AgAu Thin Films**
   Sonit Kumar Gogoi, Anumita Paul, Arun Chattopadhyay (manuscript under preparation)

Not Included in Thesis

6. **Lithography for Imprinting Colored Patterns with Quantum Dots**
   Gitanjali Majumdar, Sonit Kumar Gogoi, Anumita Paul and Arun Chattopadhyay. *Langmuir* **2006,** *22*, 3439-3444.

TABLE OF CONTENTS

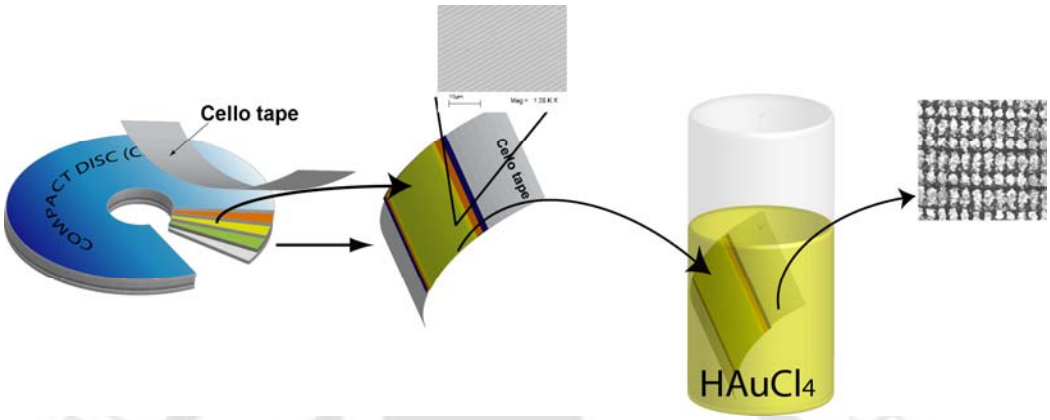

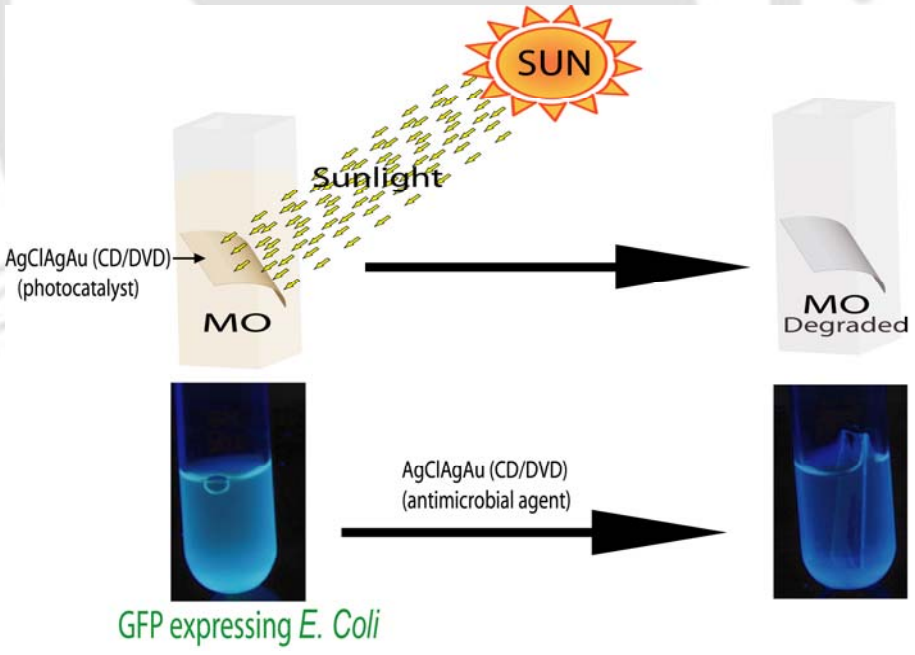

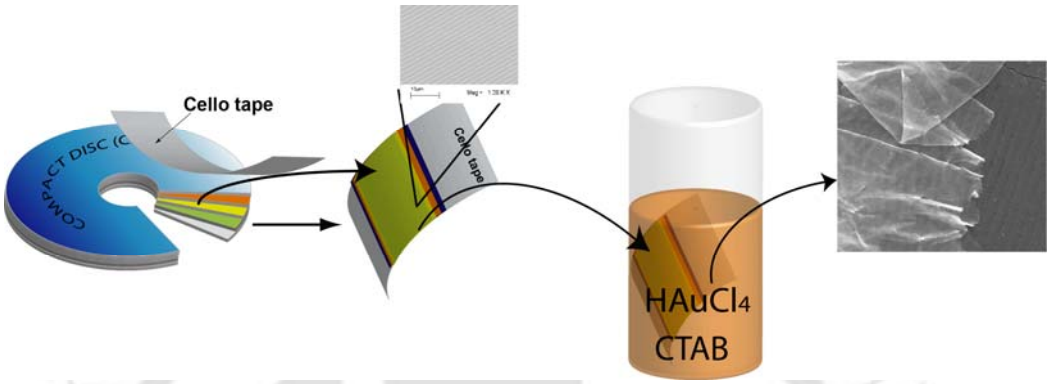

Chapter I

Introduction

1.1:Introduction - Overview of Research in Nanotechnology Relevant to the Thesis

Nanotechnology can be called the technology of this century [1, 2]. There has been an ever growing interest in this field for its potential, both in theory [3] and application [4]. The field has generated rare excitement with the hope for generation of newer technology for human health [5-7], energy [8], environment [9,10] and for other areas such as information technology, computers with higher memory[11-13] and better speed [14], electronics [15- 17] and photonics devices [18,19]. There have been up and coming nanotechnology based solutions to some of the fundamental challenges which currently confront the human civilization. For example, in the energy sector, photovoltaics (PVs) are promising alternatives to the traditional modes of generation and storage of electricity. Because PVs take advantage of the abundant solar radiation reaching the earth surface, research on and development of efficient devices would provide better alternatives. It is important to mention here that currently the conversion efficiency of most of the PVs is not very high, although lead selenide nanocrystals (NCs) have been shown to increase the efficiency of PV cells to 65%[8]. However, there remains much to be developed not only in terms of conversion efficiency but also in the development of devices based on abundant and environmentally benign materials. Also, mechanical flexibility of the device provided primarily by polymers and fabrics bring in newer opportunity for further development in this regard[20, 21]. Similarly for curing life threatening diseases like cancer, AIDS etc., extensive research is going on in nano-enabled techniques [22-25]. Scientific community is looking back in to the already practiced nanomedicines in Indian, Chinese and many other traditional treatments where gold and silver nanoparticles (NPs) are very widely used [26,27]. There are other wide spectrum of applications of

nanotechnology related materials and approaches that are under production[28] or are advanced stages of research and development like nanobiotechnology[29], electronics [30], optoelectronics [30], polymer nanocomposites [31], nanofabrication for various uses [32], photonic devices [18], chemical sensors [33,34], biosensors [28,33], high strength materials [35,36], high capacity data storage [11,13], catalysis [37, 38] and many more[39]. At present there are more than a thousand nanotechnology related products already available in the market [39].

Before we go into further details it would be appropriate to define nanotechnology at this point.[40] The National Nanotechnology Initiative of NSF (USA) defines nanotechnology as "the understanding and control of matter at dimensions of roughly 1 to 100 nanometers (nm), where unique phenomena enable novel applications". So, nanotechnology is a multidisciplinary area with diverse fields of research from nanometer size particles to large scale assemblies of NPs. Considering from the dimensional point of view the importance of the physical boundary defined for nanomaterials, i.e. 1-100 nm lies in the fact that in these size regime quantum mechanical effects and the surface effects are very much dominant and they are primarily responsible for the unusual properties of nanomaterials [3]. Apart from the various possible applications luring researchers from diverse background to pour into nanotechnology research, the fundamental properties of the nanomaterials and scientific theories behind them are equally interesting. Both physical and chemical properties of nanomaterials are very different from their atomic or bulk counterparts. For example, Au in bulk form is very inert but Au NPs are known to be good catalysts in different organic transformations or even catalytic conversion of CO to CO_2 [41,42].

A thrust area in nanotechnology research is based on exploiting the size dependent properties of nanomaterials [43-45] to create new functional materials and advanced

devices. For example, the surface plasmon resonance (SPR) of the metal NPs is one of the most studied properties. SPR is the collective oscillation of the conduction electrons in an NP in resonance with the oscillating electric field due to the interaction of electromagnetic radiation with these particles [44]. The SPR frequencies of metal NPs vary as a function of their size[46, 47], shape,[48] structure[49,50], aggregate morphology[51], surface chemistry [52] and the dielectric constant of the surrounding medium[53]. Such optical properties of the NPs has led to the development of new types of biosensors[54,55], bioprobes[56,57], chemical sensors[58,59], optical devices [60,61] filters[62,63], and substrates for surface-enhanced spectroscopies [64-67], etc.. Similarly the magnetic properties of NPs have application potential in new data storage media[68] and biological probes[69]. Further understanding of the heterogeneous catalysis has being gained from the NP based model systems[70].

In order to explore novel physical and chemical properties and phenomena to realize potential applications of nanostructures and nanomaterials, the ability to synthesize, fabricate and process nanomaterials and nanostructures is the first corner stone in nanotechnology. At present with the vast development of synthetic methods almost all desirable size [71] and shapes [72-77] and types [78] of NPs can be synthesized with a good deal of monodispersity of the particles. Still one cannot deny the requirement for new synthetic method to meet special requirements. For example, for a particular NP to be tested for medical diagnostics or for some bioactivity tests it is always desirable that the particular NP should be free from any material that can cause harm to the biological system under test. Therefore, NPs synthesized in bio-friendly media offer better and more suitable options.

At the same time surface immobilized NPs or nanostructured surfaces are of great importance in catalysis, medical diagnostics, photonics, surface enhanced

spectroscopies, sensors etc. 'Bottom up' and 'top down' are the two complimentary approaches followed for the generation of nanostructured surfaces. [32,67] In the "bottom up" approach, nanostructures are constructed from their respective atomic, the ionic or molecular precursors to get into the nano-dimensional regime, examples being gas phase cluster beam studies, condensed phase colloid synthesis etc. giving understanding of the size evolution properties of nanomaterials from bare atomic clusters to nanocrystals (NCs). On the other hand, 'top down' approach utilizes advanced lithographic techniques to reduce the dimensions of the bulk materials from microns to nanometer regime. Both conventional and unconventional lithographic techniques are being explored to achieve these goals [32, 79]. Some of the routinely used lithographic techniques to create surface nanostructures with controlled size, shape and spacing are photolithography [32,80], electron beam lithography (EBL) [81], X-ray lithography (XRL) [82] and ion beam lithography (IBL) [83]. Some other lithographic techniques explored recently are plasmonic lithography [8], nanosphere lithography [85], dip-pen nanolithography [86], lithography using reaction diffusion [87] etc. All these techniques come with their inherent advantages and disadvantages.

As mentioned earlier one of the prime attractions of the scientific community towards nanomaterials is for their exciting optical properties and noble metal NPs are at the centre of these new optical properties [44, 88]. For example gold and silver shows surface plasmon resonance based extinction of light at around 400 nm and 550 nm respectively i.e. in the visible region of light .[89] This leaves ample scope to pursue surface plasmon coupled spectroscopic studies for different applications like metal enhanced fluorescence (MEF) [90], surface enhanced Raman spectroscopy (SERS) [91-93]etc. Moreover there is also scope for manipulation of these optical properties by change in size, shape, stabilizer, and dielectric medium around the NPs etc. [30, 44].

Similarly, nanostructured thin films of metal NPs are of special interests in the fields of photonics, sensing, membrane technologies etc. [94]

Silver as antimicrobial agent is known for long time, and with the development of nanotechnology there is a new surge in exploring the possibility of silver nanomaterials being used as efficient antimicrobial agent [95]. Presently there are more than a thousand nanotechnology related products in the market and of them there are more than 200 products that are based on Ag NP in some way or other and are related to the antimicrobial activity of silver [39]. Now with all these products in the market it makes eminent sense for the scientific community to find out the exact course of action of the Ag nanomaterials. Clothing, respirators, household water filters, antibacterial sprays, cosmetics, detergent, dietary supplements, cutting boards, sox, shoes, cell phones, laptop keyboards, and children's toys are among the retail products that purportedly exploit the antimicrobial properties of Ag nanomaterials. [39,95]

On the other hand, Ag NPs may be released to the environment from discharges at the point of production, from erosion of engineered materials in household products [95] (e.g., antibacterial coatings and silver-impregnated water filters), and from washing or disposal of silver-containing products [96]. There is no doubt about the excellent antimicrobial activity of the Ag NPs, but at the same time there are certain negatives attached to the wide use of it, for this may also result in unintended exposure to the higher organisms including humans. Though eukaryotic and prokaryotic cells are different in many ways, understanding the fundamental mechanisms governing Ag NP toxicity in bacterial cells may shed light on the potential effects of Ag NPs. Simultaneously, detailed studies on the effect of Ag NPs on eukaryotic cells need to be undertaken to have a more complete understanding of the effect of Ag NPs on human health and the environment. Apart from the products available in the market a

great deal of research is going on to develop nanomaterials to be used in medical biology applications like therapeutics, imaging, targeted drug delivery etc.[7]. Therefore, exploring the possibilities of minimizing the nanomaterials from diffusing into the biosystems is a vital area of the nanoparticle research. For this purpose, various approaches such are immobilizing the NPs onto a surface [97, 98] or encapsulating them in polymer matrix [99] are currently being explored. Immobilization of NPs onto a surface consists of two basic approaches, first immobilization of the pre synthesized NPs onto substrates like glass, zeolite, silica etc. by some kind of surface binder and secondly to directly synthesize the NP on the surface through selective etching, reduction of precursor ions, galvanic replacement etc. Broadly, these approaches are parts of "top down" and the "bottom up" methodologies.[94] These techniques have wider range of application possibilities apart from the use we are concerned about, which is the bioactive nanomaterial. Also many applications of nanomaterials require that they are bound to a macro surface so that the benefits of both the worlds can be gained. [8]

1.2: Our Specific Goals

Our aim exemplified in the thesis vis-à-vis nanotechnology is twofold. First is to synthesize Ag NPs in biological media for examining the activity of the NPs in eukaryotic and prokaryotic cells. Secondly, to synthesize AgAu bimetallic nanostructures directly onto a surface for different applications and generation of AgAu bimetallic thin films.

It is important to know how metal as well as semiconductor NPs affect eukaryotic and prokaryotic cells for the application of nanotechnology to medical biology. Among

the metal NPs, the bactericidal and bacteriostatic properties of Ag NPs are well known for quite some time [100], however, the exact mechanism of interaction needs to be established. This is important for exploration of therapeutic promises of the NPs. Recently, we have demonstrated that Ag NPs, of less than 10 nm diameters, get attached to the cell walls of *Escherichia coli* bacteria, resulting in the perforation of the wall, which leads to cell death[101] and without any discernible effect on the intracellular and extracellular proteins or nucleic acids of the bacteria. Furthermore, currently efforts are being made to investigate the use of nanomaterials in various therapeutic applications, where the NPs could be the active component or could just be the physical support for the functional moieties. The works embodied in this thesis try to delve into synthesis of Ag NPs in bacterial or cell culture media and also on two dimensional surfaces as composites the details of which are incorporated below and in subsequent chapters.

Moreover, nanomaterials that are either redox active or transport across cell membrane are of major toxicological concern for human health and the environment. Recent studies have shown that NPs easily pass through the blood–brain and blood–testis barriers in mouse models [95,102] and some NPs catalyze the production of reactive oxygen species (ROS) and thereby, induce cytotoxicity *in vitro*[103]. Interestingly, interactions of carbon nanoparticle with mammalian cells showed evidence of cytotoxicity with manifestation of lipid membrane peroxidation, gene down regulation of adhesive proteins and increased cell death[104], whereas functionalized carbon nanotubes were reported to be non-cytotoxic to primary immune cells[105].

Immobilization of nanoparticles or nanostructures onto a substrate is another emerging area of research for it can serve up with the benefits of both the nano and

the macro world. Development of an easier synthetic method combining "top down" and "bottom up" approaches for getting surface immobilized nanoparticles using a commonly available precursor was our aim. Contrary to the conventional approaches of synthesizing NPs first and then immobilizing on to a substrate, we tried to etch out a precursor (Ag) bound to the surface by a galvanic replacement reaction with another reactant ($HAuCl_4$). By immobilizing the nanocrystals of metals (Ag and Au) and semiconductors (AgCl) attached to a flexible surface we wanted to explore the possibilities of their use in water purification by exploiting the properties of the immobilized nanomaterial. The immobilized nanoparticles also hoist the scope of their use in metal enhanced spectroscopies as mentioned earlier.

For nanoparticle thin films can have many potential uses in diverse areas from electronics, photonics to sensing, we were again tempted to develop a method for easily generating such films. As it is well known that high concentration of surfactants help in forming superstructures of nanoparticles [106] by a process of self assembly, we wanted to explore the possibilities with a well known surfactant CTAB. We have also tried with other surfactants without much success.

1.3 Outline of This Thesis

This thesis is divided into six chapters. Apart from the first **Chapter I** which gives a general introduction to the current status of nanotechnology research, our specific goals and a broad outline of this thesis, there are other five chapters which describe our findings and observations.

Chapter II is devoted to our findings regarding the antimicrobial activity of Ag NPs and tries to establish green fluorescent protein (GFP) expressing *Escherichia coli* as a model system for investigating the antimicrobial activities of Ag NPs. This work was

carried out in collaboration with Dr. P. Gopinath of Department of Biotechnology, Indian Institute of Technology Guwahati. The salient features of this work include the synthesis of Ag NPs in Lauria-Bertani (LB) bacterial growth medium, use of GFP expressing *E. coli* bacteria as the model system and the findings on the molecular mechanism of the course of action of the Ag NPs. Synthesis of the Ag NPs in bacterial growth medium (LB medium) is important for it enables us to study the effects of bare NPs and avoids any effect of the stabilizers commonly used. Stability of these NPs throughout the course of action was monitored. Use of GFP expressing *E. coli* bacteria simplifies the monitoring of the morphological changes in the bacteria during the action of the Ag NPs at different time points and provides easy qualitative detection of the bactericidal activity of the NPs by simply observing the green fluorescence in the bacterial growth medium. We have used this property to a great benefit in our later studies also. Understanding the molecular mechanism of the mode of action of Ag NPs on the bacteria is essential from the scientific point of view for its use in commercial products. Our findings add to the state of knowledge till date available.

Chapter III is dedicated to the research work carried out by us in collaboration with Dr. P Gopinath and Mr. Pallab Sanpui, Centre for Nanotechnology, IIT Guwahati, in the area of the cytotoxic effects of Ag NPs towards cancerous and non cancerous eukaryotic cell lines. Our findings suggest that with a higher dose of Ag NPs the cell death follows a necrotic pathway while with lower doses the pathway is apoptotic. Apoptosis, also called 'the programmed cell death' is crucial in curing diseases caused by excessive cell growth or death. We also tried to study the effect of Ag NPs as a therapeutic drug when used synergistically with the common chemotherapeutic agent 5-fluorouracil (5-FU) on non cancerous baby hamster kidney (BHK21) and

cancerous human colon adenocarcinoma (HT29) cell lines. The experimental results presented here indicate that the apoptosis induced by Ag NPs follows the same pathway as that by 5-FU and UPRT expressing cells in the presence of 5-FU. In other words, the apoptosis initiated by damage to mitochondrial membranes by Ag NPs is similar to the mechanism induced by other drugs or gene therapy treatments. Thus Ag NPs by themselves may also act as a therapeutic drug. The present findings suggest that Ag NPs may assume significance in the development of a suitable anticancer drug and the approach described here may lead to novel nanomedicines with strong potential in therapeutic use for treatment of cancers in conjunction with conventional gene therapy. In brief, the primary aim has been to study the effect of Ag NPs alone and in combination with gene therapy on cells.

Chapter IV presents a novel method for generating bimetallic (Au-Ag) NPs containing micro structures bound to a flexible plastic substrate and their characterization. Here we have used economic and commonly available Ag foils from compact discs (CDs) and digital versatile discs (DVDs) as one of the chemical precursors reacting with aqueous solution of $HAuCl_4$ to generate first AgCl microcrystals bound to the CD/DVD lacquer surface. The AgCl microcrystals were the product of galvanic reaction at the solid liquid interface between Ag (0) from the Ag foil (solid) and the Au (III) from $HAuCl_4$ solution (liquid). AgCl microcrystals were bound to the surface in a definite pattern which may be governed by the distribution of the photoactive dye on the silver foil from CDs and reaction diffusion waves. The 1 μm parallel line patterned template of the CD silver foils may also have a role to play. These AgCl microcrystals could then be reduced electrochemically to AgAu bimetallic NPs (may be core-shell type!) with higher percentage of Ag than Au. Interestingly, the initial patterns of the AgCl microcrystals were retained following

reduction of AgCl to Ag. Further, the AgCl formed could be removed by washing either with a saturated solution of NaCl or a dilute ammonia solution. Here again AgAu bimetallic (may be AgAu alloy type!) NPs were present following the removal of AgCl, but this time with a higher percentage of Au than Ag. These AgAu bimetallic NPs also retained the initial pattern of the AgCl microcrystals. This suggests that the Au (0) deposition upon reduction of Au (III) by Ag(0) followed the same pattern as the AgCl deposition. The topography and the composition of these nanostructured surfaces were characterized primarily by scanning electron microscopy (SEM), energy dispersive X-ray (EDX) spectroscopy, X-ray diffraction (XRD) analysis and UV-vis spectroscopy.

Chapter V describes the potential application of the nanostructured surfaces reported in Chapter IV (AgClAgAu) for water purification. In this chapter we demonstrate as a proof of principle the use of AgClAgAu patterned surface in photocatalytic degradation of a representative azo-dye methyl orange (MO), where AgCl is known to be the photocatalytically active material, as well as its antimicrobial activity. We have studied the photodegradation activity of the AgClAgAu patterned surfaces directly under the sun light, contrary to the most studies reported on literature using high power xenon arc lamps. We got encouraging results in this study, though the time taken for complete degradation of the dye was a little longer than the literature reports. None the less in this case the photocatalytic AgCl was surface immobilized which helped in easy catalyst recovery and along with AgCl, AgAu bimetallic NPs were also present on the surface, which provided ample scope for further tuning of the photocatalytic activity of AgCl by coupling the surface plasmon resonance of the AgAu NPs. Interestingly, the AgClAgAu patterned surfaces also showed anti microbial activity. In order to test the antimicrobial activity we have utilized one of

our earlier reported methods [101], described in detail in Chapter II. Also, we have used GFP expressing *E. coli* as the model system for rapid and easy detection of antimicrobial activity of the AgClAgAu patterned surfaces. Cell viability tests were carried out with these AgClAgAu patterned surfaces following appropriate controls. The results showed that the films have the potential of being used as antimicrobial agents. The combined photocatalytic activity and the antimicrobial activity make the AgClAgAu patterned surfaces potential candidates for water purification.

In **Chapter VI** we report the synthesis and the characterization of AgAu bimetallic NP thin films using the Ag foils from CDs and DVDs. Here also we took the Ag foils from CDs and DVDs and reacted with an aqueous solution of $HAuCl_4$ in the presence of the cationic surfactant cetyltrimethylammoniumbromide (CTAB). This led to formation of an electronically translucent thin film of AgAu bimetallic NPs of approximately 80-100 nm in size. Typically, the thickness of the films generated with Ag foils from CDs was approximately 30 nm and those generated from the Ag foils of DVDs were 60 nm. Interestingly, the films retained the corrugated patterns of the CD/DVD tracks. As the DVD tracks are ~400 nm in dimension so the patterns on the films generated from silver foils from DVDs were smaller in dimension than the 1 μm patterns in the films from CDs. Thus we have been able to generate thin films retaining the initial template patterns at different scales. These three-dimensional, AgAu bimetallic and patterned thin films generated consisted of CTAB adsorbed onto it. The films appear golden colored when viewed in reflected light and blue colored in the transmitted light. The films could be easily transferred to any surface by using a floatation technique, without any damage to the patterns thus supporting the robustness of the films. For the characterization purpose techniques like SEM,

transmission electron microscopy (TEM), EDX, atomic force microscopy (AFM), FTIR-spectroscopy and UV-visible spectroscopy were extensively used.

References

1. Buchachenko, A. L. Russ. Chem. Rev. **2003**, *72*, pp375 – 391.
2. Tegart, G. *Nanotechnology: The Technology for the 21st Century*, http://www.nistep.go.jp/IC/ic030227/pdf/p2-3.pdf
3. *The Science of Nanotechnology: An Introductory Text*; T. Luanne; Broughton S. A.; S. Tanke, R.; Jelski, D.; French, V. ; Zhang, G.; Popov, A. K.; A. B. Western; George, T. F., Eds.; Nova Science Publishers Inc.:New York, 2008.
4. *Nanotechnology: Science, Innovation, and Opportunity*; Foster, L. E., Ed.; Prentice Hall: New Jersey, 2005.
5. *Nanotechnology Applications for Clean Water;* Savage, N.; Diallo, M.; Duncan, J.; Sustich, R., Eds.; William Andrew Inc: New York, 2009.
6. Kraus, R. H. Jr.; Wright, B. Magnetic Nanoparticles in Cancer Diagnosis and Hyperthermic Treatment. In *Biomedical Applications of Nanotechnology*; Labhasetwar, V.; Leslie-Pelecky, D. L., Eds.; John Wiley & Sons, Inc.: New Jersey, 2007; pp 65-82.
7. *Biomedical Nanotechnology*; Malsch, N. H., Ed.; CRC Press: Boca Raton, FL, 2005.
8. Gasman, L. *Nanotechnology Applications and Markets*; Artech House, Inc.:Norwood, MA , 2006; pp101-125
9. Joo, S. H.; I. Francis Cheng, F.*Nanotechnology for Environmental Remediation*; Springer: New York, 2006.
10. Schimidt, K. F. *Green Nanotechnology*: *It's Easier Than You Think* , PEN 8 , The Phew Charitable Trust, April 2007, pp12-16. http://eprints.internano.org/68/
11. Chou, S. Y.; Krauss, P. R.; Kong, L. *J. Appl. Phys.* **1996**, *79*, pp 6101-6106
12. Thurn-Albrecht, T.; Schotter, J.; Kastle, G. A.; Emley, N.; Shibauchi, T.; Krusin-Elbaum, L.; Guarini, K.; Black, C. T.; Tuominen, M. T.; Russell, T. P. *Science*, **2000** , *290*, pp 2126-2129.

13. Hamann, H. F.**;** O'Boyle, M.; Martin, Y. C.; Rooks, M.; Wickramasinghe, H. K. *Nat. Mater*. **2006**, *5*, pp383 – 387.
14. *Intel introduces the fastest Processor based on nanotechnology* http://www.azonano.com/news.asp?newsID=8839
15. Huang, Y., Duan, X., Cui, Y., Lieber, C.M. *Nano Lett.* **2002**, *2*, pp101–104.
16. Cui, Y., Lieber, C.M. *Science* **2001**, *291*, pp851–853.
17. Duan, X., Huang, Y., Lieber, C.M. *Nano Lett.* **2002**, *2*, pp487–490.
18. Parviz, B. A.; Ryan, D.; Whitesides, G. M. *IEEE Trans. Adv. Packaging* **2003**, *26*, pp 233-241.
19. Willander, M.; Nur, O.; Zhao, Q. X.; Yang, L. L.; Lorenz, M.; Cao, B. Q.; Perez, J. Z. ; Czekalla, C.; Zimmermann,G.; Grundmann, M.; Bakin, A.; Behrends, A.; Al-Suleiman, M.; El-Shaer, A.; Mofor, A. C.; Postels, B. ; Waag, A.; Boukos, N.; Travlos, A. ; Kwack, H. S.; Guinard, J.; Dang, D. L. S. *Nanotechnology* **2009**, *20*, 332001 (40pp).
20. *Quantum Dot Materials Can Reduce Heat, Boost Electrical Outputs*, NREL News Release, May 23, 2005. http://www.nrel.gov/news/press/2005/350.html, Accessed on 8th December 2010.
21. Ellingson, r. J.; Beard, M. C.; Johnson, J. C.; Yu, P.; Micic, O. I.; Nozik, A. J.; Shabaev, A.; Efros, A. L. *Nano. Lett.* **2005**, 5, pp865-871.
22. Elechiguerra, J. L.; Burt, J. L.; Morones, J. R. ; Camacho-Bragado, A.; Gao, X.; Lara, H. H; Yacaman, M. J. *J. Nanobiotechnol.* **2005**, *3*, art. No. 6 .
23. Bailey, R. E.; Smith, A. M.; Nie, S. *Physica E*, **2004**, *25*, pp1–12.
24. *Nanotechnoogy for Cancer therapy*: Mansoor M. Amiji, M. M., Ed, CRC Press: Boca Raton, FL, 2007.
25. Koo, O. M.; Rubinstein, I.; Onyuksel, H. *Nanomedicine: Nanotech. Biol. Med.* **2005**, *1*, pp193-212.
26. Turkevich, J. *Gold Bull.* **1985**, *18*, pp 86-91.
27. Shankar, D.; Unnikrishnan, P. M.; Venkatasubramanian, P.*Curr. Sci.* **2007**, *92*, pp1499-1505.
28. *Commercializing Micro-Nanotechnology Products;* Tolfree, D. ; Jackson, M. J. CRC Press: Boca Raton, FL, 2008.
29. *Nanobiotechnology: Concepts, Applications and Perspectives*: Niemeyer, C. M.; Mirkin, C. A., Eds., Wiley-VCH: Weinheim, 2004.

30. Talapin, D. V.; Lee, J. S.; Kovalenko, M. V.; Shevchenko, E. V. *Chem. Rev.* **2010,** *110*, pp 389–458.
31. Gangopadhyay, R.; De, A. *Chem. Mater.* **2000**, *12*, pp 608-622.
32. Gates, B. D.; Xu, Q.; Stewart, M.; Ryan, D.; Willson,C. G.; Whitesides, G. M. *Chem. Rev*. **2005,** *105*, pp1171-1196.
33. Helmus, M. N.; Gammel, P.; Allen, F.; Migliorato, P. *American Laboratory*, 2006, *38*, pp 34-36.
34. McAlpine, M. C.; Ahmad, H.; Wang, D; Heath, J. R. *Nat. Mater.*, 2007,*6*, pp379 – 384.
35. Qian, L.; Hinestroza, J.P.; *Journal of Textile Apparel Technology and Management* 2004, *4*, pp 1–4.
36. Dzenis, Y. *Science* **2004**, *304*, pp 1917-1919.
37. Wong, M. S.; Alvarez, P. J. J.; Fang, Y. L.; Akcin, N.; Nutt, M. O.; Miller, J. T.; Heck, K. N. *J. Chem. Technol. Biotechnol.* **2009**, *84*, pp 158– 166
38. Tian, N., Zhou, Z. Y., Sun, S. G., Ding, Y., and Wang, Z. L. *Science* **2007**, *316*, pp732-735.
39. Nanotechnology and consumer products. http://www.nanotechproject.org/inventories/consumer/analysis_draft/ Accessed on 1st December, 2010.
40. *National Nanotechnology Initiative 2000 Leading to the Next Industrial Revolution***,** A Report by the Interagency Working Group on Nanoscience, Engineering and Technology (Washington, DC: Committee on Technology, National Science and Technology Council). www.nano.gov/html/facts/whatIsNano.html
41. Maye, M. M.; Lou, Y.; Zhong, C.-J. *Langmuir* **2000**, *16*, pp 7520-7523.
42. Daniel, M. C.; Didier Astruc, D. *Chem. Rev.* **2004**, *104*, pp 293-346**.**
43. Burda, C.; Chen, X.; Narayanan, R.; El-Sayed, M. A. *Chem. Rev.* **2005,** 105, pp 1025-1102.
44. Kelly, K. L.; Coronado, E.; Zhao, L. L.; Schatz, G. C. *J. Phys. Chem. B* **2003**, *107*, pp 668–677.
45. El-Sayed, M. A. *Acc. Chem. Res.* **2004**, *37*, pp 326-333
46. Stewart, M. E.; Anderton, C. R.; Thompson, L. B.; Maria, J.; Gray, S. K.; Rogers, J. A.; Nuzzo, R. G. *Chem. Rev.* **2008,** *108*, pp 494-521.
47. Yguerabide, J.; Yguerabide, E. E. *Anal. Biochem.* **1998**, *262*, pp 137–156.

48. Orendorff, C. J.; Sau, T. K.; Murphy, C. J. *Small* **2006**, *2*, pp 636–639.
49. Jackson, J. B.; Halas, N. J. *J. Phys. Chem. B* **2001**, *105*, pp 2743–2746.
50. Selvakannan, P. R.; Sastry, M. *Chem. Commun.* **2005**, pp 1684–1686.
51. Novak, J. P.; Nickerson, C.; Franzen, S.; Feldheim, D. L. *Anal. Chem.* **2001**, *73*, pp 5758–5761.
52. Caruso, R. A.; Antonietti, M. Sol_Gel *Chem. Mater.* **2001**, *13*, 3272–3282.
53. Kubo, S.; Diaz, A.; Tang, Y.; Mayer, T. S.; Khoo, I. C.; Mallouk, T. E. *Nano Lett.* **2007**, *7*, pp3418–3423.
54. Storhoff, J. J.; Elghanian, R.; Mucic, R. C.; Mirkin, C. A.; Letsinger, R. L. *J. Am. Chem. Soc.* **1998**, *120*, pp1959-1964.
55. Mucic, R. C.; Storhoff, J. J.; Letsinger, R. L.; Mirkin, C. A. *Nature* **1996**, *382*, pp 607-609.
56. Bruchez, M., Jr.; Moronne, M.; Gin, P.; Weiss, S.; Alivisatos, A. P. *Science* **1998**, *281*, pp 2013-2018.
57. Rosi, N. L.; Mirkin, C. A. *Chem. Rev.* **2005,** *105*, pp1547-1562.
58. Pan, G.; Kesavamoorthy, R.; Asher, S. A. *J. Am. Chem. Soc.* **1998**, *120*, pp 6525-6530.
59. Weissman, J. M.; Sunkara, H. B.; Tse, A. S.; Asher, S. A. *Science* **1996**, *274*, pp 959-960.
60. Asher, S.; Chang, S.-Y.; Tse, A.; Liu, L.; Pan, G.; Wu, Z.; Li, P. *Mater. Res. Soc. Symp. Proc.* **1995**, *374*, pp 305-310.
61. Mansour, K.; Soileau, M. J.; Van Stryland, E. W. *J. Opt. Soc. Am. B* **1992**, *9*, pp 1100-1109.
62. Flaugh, P. L.; O'Donnell, S. E.; Asher, S. A. *Appl. Spectrosc.* **1984**, *38*, pp 847-850.
63. Munro, C. H.; Pajcini, V.; Asher, S. A. *Appl. Spectrosc.* **1997**, *51*, pp1722-1729.
64. Zou, S.; Williams, C. T.; Chen, E. K.-Y.; Weaver, M. J. *J. Am. Chem. Soc.* **1998**, *120*, pp 3811-3812.
65. Caldwell, W. B.; Chen, K.; Herr, B. R.; Mirkin, C. A.; Hulteen, J. C.; Van Duyne, R. P. *Langmuir* **1994**, *10*, pp 4109-4115.
66. Howard, R. E.; Liao, P. F.; Skocpol, W. J.; Jackel, L. D.; Craighead, H. G. *Science* **1983**, *221*, pp 117-121.
67. Hulteen, J. C.;Treichel, D. A.; Smith,T. M.; Duval, M. L.; Jensen, T. R.; Van Duyne, R. P. *J. Phys. Chem. B* **1999**, *103*, pp 3854-3863.

68. Chou, S. Y.; Krauss, P. R.; Zhang, W.; Guo, L.; Zhuang, L. *J. Vac. Sci. Technol. B* **1997**, *15*, pp 2897-2904.
69. Baselt, D. R.; Lee, G. U.; Hansen, K. M.; Chrisey, L. A.; Colton, R. J. *Proc. IEEE* **1997**, *85*, pp 672-680.
70. Street, S. C.; Xu, C.; Goodman, D. W. *Annu. Re*V. *Phys. Chem.* **1997**, *48*, pp 43-68.
71. Jain, P. K.; Lee, K. S.; El-Sayed, I. H.; El-Sayed, M. A. *J. Phys. Chem. B* **2006**, *110*, pp7238-7248.
72. Teng, X; Yang, H. *Nano. Lett.* **2005**, *5*, pp 885-891.
73. Xia, Y.; Yang, P.; Sun, Y.; Wu, Y.; Mayers, B.; Gates, B.; Yin, Y.; Kim, F.; Yan, H. *Adv. Mater.*, **2003**, *15*, pp 353–389.
74. . Pileni, M. P. *Nat. Mater.* **2003**, *2*, pp145–149.
75. Murphy, C. J.; Sau, T. K.; Gole, A. M.; Orendorff, C. J. G.; Gou, J. L.; Hunyadi, S. E.; Li, T. *J. Phys. Chem. B*, **2005**, *109*, pp 13857–13870.
76. Crooks, R. M.; Zhao, M.; Sun, L.; Chechik, V.; Yeung, L. K. *Acc. Chem. Res.*, **2001**, *34*, pp 181–190.
77. J. Scott, R. W.; Wilson, O. M.; Crooks, R. M. *J. Phys. Chem. B*, **2005**, *109*, pp 692–704.
78. Wang, X.; Zhuang,J.; Peng, Q.; Li, Y. *Nature*, **2005**, *437*, pp 121-124.
79. Wouters, D.; Schubert, U. S. *Angew. Chem. Int. Ed.* **2004**, *43*, pp2480 – 2495.
80. Shao, D. B.; Chena, S. C. *Appl. Phys. Lett.* **2005**, *86*, 253107(pp3)
81. Tseng, A. A.; Chen, K.; Chen, C. D.; Ma, K. J. *IEEE Trans. Electron. Pack. Manuf.* **2003**, *26*, pp141-149.
82. Silverman, J. P. *J. Vac. Sci. Technol. B* **1997**, *15*, pp 2117-2124.
83. Watt, F.; Bettiol, A. A.; Van Kan, J. A.; Teo, E. J.; Breese, M. B. H. *Int. J. Nanosci.* **2005**, *4*, pp 269-286.
84. Srituravanich, W.; Fang, N.; Sun,C; Luo, Q; Zhang, X. *Nano. Lett.* **2004** , *4*, pp1085-1088.
85. Jensen, T. R.; Malinsky, M. D.;Haynes, C. L.; Van Duyne, R. P. *J. Phys. Chem. B* **2000**, *104*, pp10549-10556.
86. Piner, R. D.; Zhu, J; Xu, F.;Hong, S.; Mirkin, C. A. *Science* **1999**, *283*, pp 661-663.
87. Grzybowski, B. A.; Bishop, K. J. M.; Campbell, C. J.; Fialkowski, M.; Smoukov, S. K. *Soft Matter* **2005**, *1*,pp 114-128.

88. Wan, D.; Chen, H. L.; Tseng, S. C.; Wang, L. A.; Chen, Y. p.; *ACS Nano* **2010,** *4,* pp165–173.
89. Link, S.; Wang, Z. L.; El-Sayed, M. A. *J. Phys. Chem. B* **1999**, *103*, pp 3529-3533.
90. Lakowicz, J. R.; Geddes, C. D.; Gryczynski, I.; Malicka, J.; Gryczynski, Z.; Aslan, K.; Lukomska, J.; Matveeva, E.; Zhang, J. A.; Badugu, R.; Huang, J. *J. Fluoresc.* **2004**, *14*, pp 425−441.
91. Litorja, M.; Haynes, C. L.; Haes, A. J.; Jensen, T. R.; Van Duyne, R. P. *J. Phys. Chem. B* **2001**, *105*, pp 6907−6915.
92. Dick, L. A.; McFarland, A. D.; Haynes, C. L.; Van Duyne, R. P. *J. Phys. Chem. B* **2002**, *106*, pp 853-860.
93. Roberta Brayner,; Ruth Iglesias,;Stephanie Truong,; Zyed Beji, Z.; Felidj, N.; Fievet, F.; Aubard, J. *Langmuir*, **2010**, *26* , pp 17465–17469.
94. Cao, G. *Nanostructures and Nanomaterials;* Imperial College Press: London, 2004.
95. Catalina Marambio-Jones, C.; Hoek, E. M. V. *J. Nanopart. Res.* 2010**,** *12*, pp1531-1551.
96. Benn, T.; Westerhoff, P. *Environ. Sc.i Technol.* **2008**, *42*, pp4133–4139.
97. Malynych, S.; Luzinov, I.; Chumanov, G. *J. Phys. Chem. B*, **2002**, *106*, pp 1280–1285.
98. Oh, S. K.; Kim, Y. G.; Ye, H.; Crooks, R. M. *Langmuir*, **2003**, *19*, pp 10420–10425.
99. Radetic, M.; Ilic, V.; Vodnik, V.; Dimitrijevic, S.; Jovancic´, P.; Saponjic´, Z.; Nedeljkovic´, J. M. *Polym. Adv. Technol.* **2008**, *19*, pp 1816–1821
100. Baker, C.; Pradhan, A.; Pakstis, L.; Pochan, D. J.; Shah, S. I. *J. Nanosci. Nanotechnol*. **2005**, *5*, pp 244-249.
101. Gogoi, S. K.; Gopinath, P.; Paul, A.; Ramesh, A.; Ghosh, S. S.; Chattopadhyay, A. *Langmuir* **2006**, *22*, pp 9322-9328.
102. Borm, P. J.; Kreyling, W. J. *J. Nanosci. Nanotechnol*. **2004**, *4*, pp 521–531.
103. Xia, T; Kovochich, M.; Brant, J.; Hotze, M.; Sempf, J.; Oberley, T.; Sioutas, C.; Yeh, J. I.; Wiesner, M. R.; Nel, A. E. *Nano Lett.* **2006**, *8*, pp 1794-1807.
104. Magrez, A.; Kasas, S.; Salicio, V.; Pasquier, N.; Seo, J. W.; Celio, M.; Catsicas, S.; Schwaller, B.; Forro, L. *Nano Lett.***2006**, *6*, pp 1121-1125.
105. Dumortier, H; Lacotte, S.; Pastorin, G.; Marega, R.; Wu, W.; Bonifazi, D.; Brinad, J. P.; Prato, M.; Muller, S.; Bianco, A. *Nano Lett.* **2006**, 6, pp 1522-1528.

106. Kotov, N.; Tang, Z. Organization of Nanoparticles and Nanowires in Electronic Devices: Challenges, Methods and Perspectives. In *Nanoparticle Assemblies and Superstructures;* Kotov, N. Ed., CRC Press: Boca Raton, FL, 2006, pp 3-73.

Chapter II

Synthesis of Ag Nanoparticles in Bacterial Growth Medium and their Bactericidal Activity

2.1: Introduction

The investigations related to interactions between metal or semiconductor nanoparticles (NPs) with eukaryotic and prokaryotic cells are of primary concern for further development in medical biology, especially using the tools of nanoscale science and technology.[1-4] Although the bacteriostatic and bactericidal properties of Ag^+ (silver) ions have been known for centuries,[5-7] those of Ag NPs have been studied only recently owing to the demands of the development of nanotechnology.[7-16] The primary development with respect to the properties of Ag NPs has been the generation of size-selected NPs, their incorporation into polymer or other devices for delivery, and the study of their effect on prokaryotic biological systems.[12,13,14] The general understanding is that Ag NPs of typically less than 20 nm diameters get attached to sulfur-containing proteins of bacterial cell membranes leading to greater permeability of the membrane, which causes the death of the bacteria. In addition, it has been reported that NPs enter the cell and therefore presumably get attached to DNA.[11] However, these conclusions are based on indirect evidences, and further investigations are needed to understand the detailed mechanism of the processes of NP attachment to the cell wall and other parts of the cell so that other more stable, cheaper, and specific materials could be developed against various pathogens. One of the hindrances of *in vivo* study of the interaction of NPs with bacteria is the lack of a suitable probe either for the organism or for the NP. Although NPs have very high oscillator strength, it is still difficult to make a routine probe involving the interaction between an individual NP and cell using ordinary microscopic or spectroscopic techniques, especially using metal NPs. On the other hand, green fluorescent proteins (GFPs) have been used extensively as spectroscopic and microscopic probes in

various physiological systems, leading to greater understanding of the systems.[17,18] In addition, GFPs have been used to study protein mobility and pattern formation in various chemical and biological systems using its intrinsic fluorescence as the probe.[19,20]

Herein, we report the results of the investigation of the bactericidal effect of Ag NPs on GFP-expressing recombinant *Escherichia coli* (*E. coli*). Although the antagonistic property of Ag NPs is known, [3] the application of fluorescent bacteria facilitates rapid monitoring of cause-effect phenomena by spectroscopic and microscopic techniques. An easy and convenient *in vitro* synthesis of Ag NPs in bacterial growth medium has been adopted in the present study. In addition to conventional viability tests, transmission electron microscopic (TEM), X-ray diffraction (XRD), UV-visible (UV-vis) spectroscopic analysis, the morphological changes of the fluorescent bacteria and electrophoretic analysis of cellular DNA and protein migration profile have been performed to establish the effect of Ag NPs on GFP bacteria. Our essential observation is that Ag NPs of less than 10 nm diameters get attached to the bacterial cell wall, resulting in the perforation of the wall, which leads to the cell death. On the other hand, our evidences suggest that the Ag NPs did not affect the plasmid DNA or the proteins of the bacteria, which is contrary to the conventional view. This work has been carried out in collaboration with Dr P. Gopinath, Department of Biotechnology, IIT Guwahati and his contributions are duly acknowledged.

2.2: Experimental Section

2.2.1: Growth Media and Chemicals: GFP-expressing recombinant *E. coli* was grown in Luria-Bertani (LB) medium (HiMedia, Mumbai, India). Silver nitrate

($AgNO_3$) and sodium borohydride ($NaBH_4$) used for silver NP preparation were procured from Merck India, Ltd. High-purity molecular biology grade chemicals and reagents used for sodium dodecyl sulfate-polyacrylamide gel electrophoresis (SDS-PAGE) and agarose gel electrophoresis were obtained from Sigma-Aldrich chemicals.

2.2.2: Ag NP Preparation. Ag NPs were prepared by slight modification of the standard NaBH4 reduction of $AgNO_3$ [21,22]. In a typical Ag NPs synthesis, different concentrations of Ag NPs were prepared in LB media and Tris-EDTA buffer (TE buffer, pH=8) where, the final concentration of $AgNO_3$ was in the range of 10^{-4}-10^{-5} M and $NaBH_4$ on the order of 10^{-4}. In order to represent the concentrations of Ag NPs we will use the respective concentrations of $AgNO_3$ used for the syntheses.

2.2.3: GFP Construct.* The recombinant GFP-expressing *E. coli* (DH5α) was generated by cloning of the GFP gene into an ampicillin-resistant pUC-derived plasmid vector driven by bacterial promoter.

2.2.4: Determination of Minimum Inhibitory Concentration (MIC) and Minimum Killing Concentration (MKC). Minimum inhibitory concentration is defined as the minimum concentration of the antimicrobial agent that is required to inhibit the visible growth of the microorganism in question after overnight incubation. [23] While minimum killing concentration (MKC) is the concentration of the test compound that prevents growth of the bacterial cells following reinoculation, as observed by the lack of visual turbidity. MIC and MKC for the Ag NPs were determined by growing 2.0 x 10^8 CFU of GFP expressing *E.coli* (DH5α) cells with 5.66 µg mL^{-1} , 11.32 µg mL^{-1}, 16.98 µg mL^{-1}, 22.64 µg mL^{-1}, 28.3 µg mL^{-1} of preformed NP in LB medium(Ampicillin). MIC was found to be 22.64 µg mL^{-1} and MKC 28.3 µg mL^{-1} of Ag NPs.

2.2.5: Bactericidal Activity of Silver NPs. GFP expressing *E.coli* (DH5α) cells were grown overnight (12 hrs) in a 300 mL LB medium. The overnight grown culture was centrifuged at 8000 rpm (Sigma 4K15C, Rotor No.12256) for 10 min and the pellet was resuspended in 3 mL of LB medium. 1.0 mL each of resuspended cells was added to 100 mL fresh LB medium (control) and LB medium with preformed NP of two different concentrations i.e. 56.5 μg mL^{-1} and 84.83 μg mL^{-1} of Ag NPs. Samples were incubated at 37°C and 180 rpm and at every 1 hour optical density (O.D.) at 595 nm was measured using a Analytikjena SPEKOL1200 UV-vis spectrophotometer. The viability of the bacterial cells was determined by several batches of viability count experiment. In a typical experiment a pre-grown culture was diluted and plated on a solid medium (LB agar ampicilin plate). The viable cell number was determined by colony count on the plate and multiplied by the dilution factor expressing in CFU/mL units.

It may be mentioned here that an excess of $NaBH_4$ was used as a reducing agent in the preparation of Ag NPs in the LB medium. Thus, the number of Ag^+ ions that would be present in the medium in addition to the Ag NPs would be significantly small. Even then, we have performed experiments to assess the effect of Ag^+ ions at various concentrations on the growth of recombinant GFP-expressing bacterial cells. We observed that when the concentration of Ag^+ ions was on the order of 10^{-4} M (in the absence of $NaBH_4$), the bacterial growth was significantly reduced. However, when the Ag^+ concentrations were kept at 10^{-6} and 10^{-8} M, there was no observable effect on the growth of the bacterial colony. Since the excess concentration of Ag^+ ions in the present experimental conditions would be less than 10^{-6} M, one can assume that the additional Ag^+ ions present in the medium, if any, would have no significant effect on the growth of the colony.

2.2.6: Fluorescence Microscopy: Fluorescence from the GFP -expressing *E. coli* cells was advantageously utilized to monitor the population growth and the overall shape of the bacteria by observing the Ag NP treated samples under an epifluorescence microscope (Axioskop2MAT, Carl Zeiss) at different time points. Samples for fluorescence microscopic studies were prepared by taking out 5 µL aliquots from the GFP-expressing *E. coli* incubated with and without Ag NPs in LB medium and then spreading the aliquots on microscopic slides. The excitation wavelength used was controlled by a band pass filter of 445-495 nm, and the observation filter had a long-pass filter wavelength above 515 nm.

2.2.7: Fluorescence Spectroscopy: To complement the fluorescence microscopic observations fluorescence spectroscopic studies were also carried out using a Cary Eclipse Fluorescence spectrophotometer. Fluorescence spectra of the GFP expressing *E. coli* were recorded for the samples treated with 55.6 mg mL^{-1}, 84.83 µg mL^{-1} of Ag NPs and the control without the Ag NPs, at different time points starting from 0 hr to 12 hrs. Samples for fluorescence spectroscopic investigations were prepared by following a similar procedure as mentioned before for the O. D. measurements. The excitation wavelength for fluorescence studies was set at 400 nm[17]. Also the fluorescence spectra of the supernatant, obtained upon centrifugation, were recorded in order to monitor the leakage of GFP on to the bacterial growth medium due to the action of Ag NPs.

2.2.8: TEM Analysis: Ag NPs and the bacteria were observed by a Hitachi H-600 TEM instrument operating at a maximum accelerating voltage of 200 kV. In order to confirm the formation of the NPs and their presence in the cells during the course of the experiments TEM images were recorded at different time points. 10 µL each of

Ag NPs as synthesized in LB media and at time point 0 hr, 1 hr and 10 hr of the bacterial growth in presence of Ag NPs was deposited on the carbon coated copper TEM grids and allowed to air - dry .

2.2.9: XRD and UV-Visible Spectroscopic Measurements: In order to confirm the presence of Ag NPs on the cell walls we have centrifuged at 1000 rpm, the bacterial solution treated with Ag NPs for 12 hrs. The bacterial cell pellet obtained was spread on a glass slide after washing twice with sterile deionised water and XRD was recorded with a Bruker Advance D8 XRD machine (Cu Kα source with 1.5406 Å wavelength). Also, UV-vis spectrum of the washing was recorded using a Cary 100 spectrophotometer to observe residual Ag NPs.

2.2.10: Agarose Electrophoresis:* Plasmid DNA was isolated by alkaline lyses method [24] from control and NP treated *E.coli* cells of every 1 hour sample and electrophoresed in 0.8% agarose gel.

2.2.11: SDS-PAGE: * For protein analysis GFP expressing *E. coli* (DH5α) sample collected from control and NP treated cells of every 1 hour sample were centrifuged at 8000 rpm for 2 min (using a Biofuge pico, Heraeus with Rotor No. 3328). 1 mL of PBS buffer was then added to the pellet and centrifuged at 8000 rpm for 2 minutes and the pellet was store at -20 °C until use. Then, the pellet was resuspended in 200 µL of 1X sample buffer (containing 60 mM Tris-HCl (pH 6.8), 25% glycerol, 2% SDS, 14.4 mM 2-mercaptoetanol and 0.1% bromophenol blue) [25] and the cell was lysed by boiling for 5 min to get the crude extract of protein. 10 µL of each sample was loaded in 10% SDS-PAGE and electrophoresed (using a Biorad machine). Gel was stained using coomasie blue stain for 2-3 hours and destained for 2-3 hours to visualize the bands.

2.2.12: DNA-Ag NPs Interaction: DNA-Ag NPs interaction was studied by incubating GFP plasmid (4 μg) with preformed Ag NPs at 37 °C. Samples were withdrawn periodically after 1, 2, and 3 h, and spectral changes were observed by UV-vis spectroscopy. NP treated plasmid DNA samples were also subjected to agarose gel electrophoresis. Untreated plasmid DNA was used as the control for both of the experiments.

2.3: Results and Discussion

It is known that smaller Ag NPs are more effective in killing *E. coli* bacteria than large ones, and typical diameters of less than 10 nm are the best in this regard.[11] In the present studies, Ag NPs were synthesized in the LB medium using $NaBH_4$ with a slight modification of the standard method[21, 22] of preparation. $AgNO_3$ concentrations of 56.5 and 84.83 μg mL^{-1} produced stable Ag NPs in the LB medium.

In general, when Ag NPs are synthesized in ordinary aqueous solution (in the presence of a stabilizer such as SDS), the UV-vis spectrum consists of a peak at around 400 nm that is characteristic of Ag NP formation. However, because the synthesis was carried out in the LB medium (to avoid effects such as dilution) and the medium absorbs strongly in the region of 400-500 nm, it was not possible to obtain a UV-vis absorption spectrum of Ag NPs thus synthesized. This was, however, pursued by TEM studies. A TEM micrograph obtained after 1 h of Ag NP synthesis and the corresponding particle size distribution is shown in **Figure 2.1 (A, B)**. The NPs were well-dispersed, and showed no aggregation. The sizes typically ranged from 2 to 5 nm and were smaller than the typical 10nmdiameter reported previously.[21] The NPs retained their sizes even after 10 h of synthesis, and there was no significant

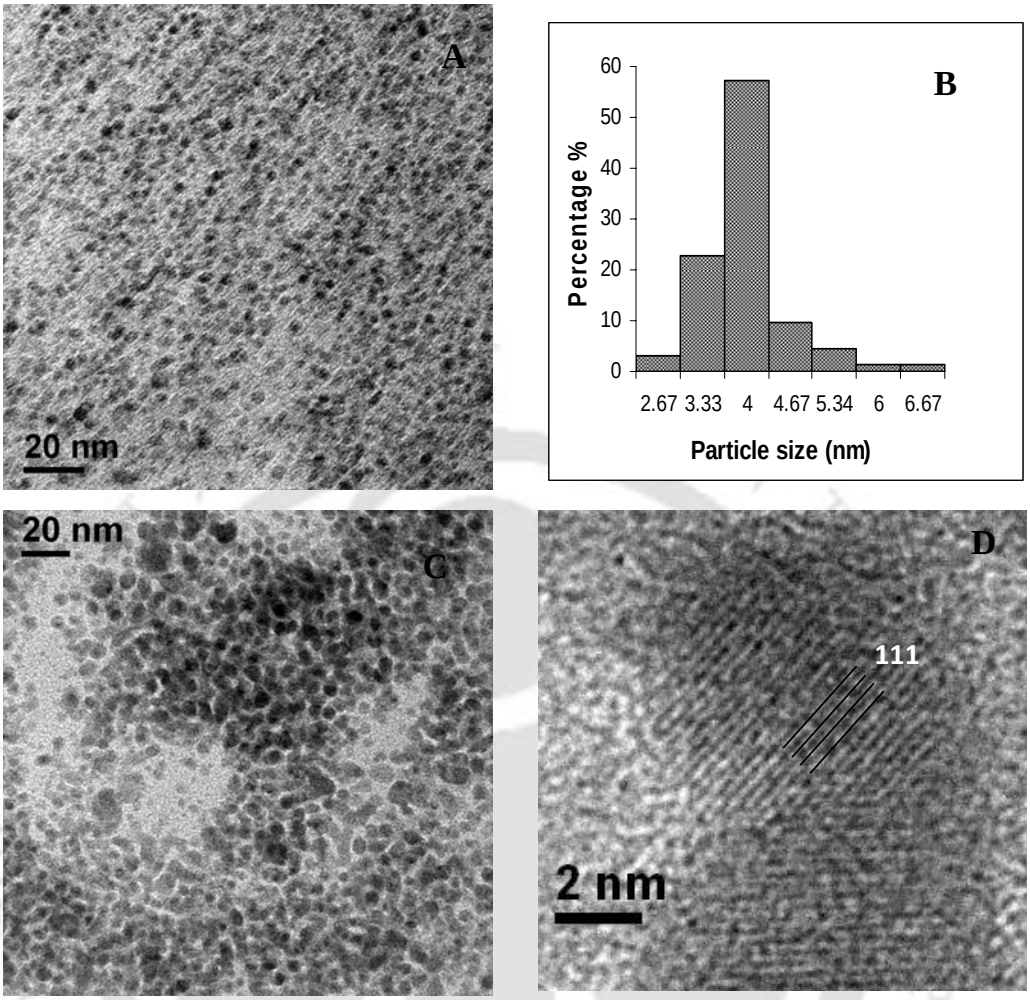

Figure 2.1. (A,B) TEM micrograph of the Ag NPs and the particle size distribution, respectively, at 1h. **(C)** TEM micrograph at 10 h. **(D)** Lattice planes of Ag NPs.

aggregation of particles, as is evident from **Figure 2.1(C)**. It may be mentioned here that, in **Figure 2.1(C)**, there seems to be particles that are apparently larger than 5 nm. However, if one looks carefully into the figure, one can see dark spots, which are less than 10 nm, surrounded by gray spots, which makes the overall sizes larger than 10 nm. It is possible that the gray background does not represent particles, whereas the dark spots do. The gray spots may be due to evaporated medium, bacterial debris, and so forth. However, another point that must be added here is that the measurement of

this particular sample was made at 10 h, when most of the bacteria were dead in the presence of the Ag NPs. Hence, some of the particles that were agglomerated because of the absence of any stabilizing agent in the medium were not effective in killing the bacteria (because of their large sizes) and were present in the medium. The high-resolution image of a single Ag NP shown in **Figure 2.1(D)** exhibits a lattice plane, indicating that Ag NPs remained intact and did not get oxidized in the medium. Also, the XRD of the Ag NP-treated bacteria (after 12 h) showed a peak characteristic of Ag NPs (discussed later). Thus Ag NPs produced in the LB medium under the present conditions provide a good system for studying their effect on bacteria. **Figure 2.2** depicts the effect of Ag NPs on the growth of recombinant GFP *E. coli*. The time-dependent changes in bacterial growth were monitored by measuring OD_{595}. The measurement of the OD was pursued at 595 nm to avoid strong absorption due to the Ag NPs in the region of 380-450 nm and from bacterial cellular components such as nucleic acids (A_{260}), proteins (A_{280}), and macromolecules present in the LB media such as sugar and carbohydrates that might absorb at $A_{400-500}$. The OD value at 595 nm is due to the scattering of light by the bacterial cells and is a function of bacterial cell density and thus correlates with the growth of the colony. As is clear from the figure, at Ag NPs concentrations of 22.64 and 28.3 μg mL^{-1} there was no bacterial growth, whereas a discernible growth was observed at a concentration of 5.66 μg mL^{-1}. The control sample (grown in the absence of Ag NPs and $NaBH_4$) and the sample treated with 6.66 X 10^{-4} M $NaBH_4$ used to synthesize Ag NPs showed no growth inhibition. Thus the present method involving the use of $NaBH_4$ for the synthesis of Ag NPs did not affect the bacterial growth in any way and provided a convenient tool

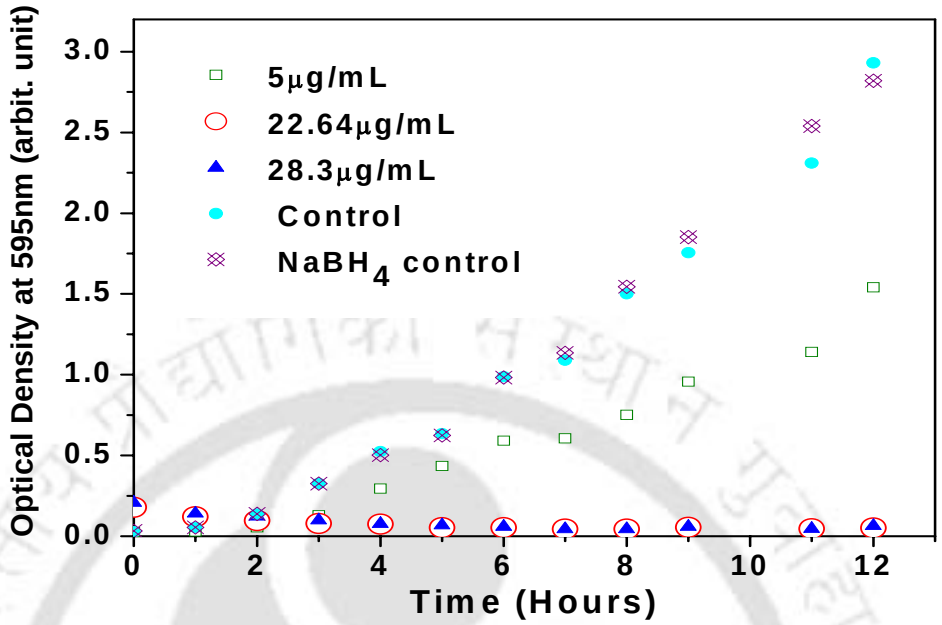

Figure 2.2: Effect of varying concentrations of Ag NPs on the growth of GFP recombinant *E. coli*.*

for the study of the antibacterial effect of preformed NPs. The MIC and MKC values were found to be 22.64 and 28.3 μg mL^{-1} in our studies and are less than those reported previously.[10] In the present investigation, Ag NPs were also smaller in size, with an average diameter of 4 nm. Reduced particle size could lead to efficient NP-bacteria surface interaction and augment bactericidal activity.[11] Previous investigations have reported chemical syntheses of silver NPs under stringent conditions and the subsequent study of their antimicrobial properties. In the present study, we achieved the synthesis of stable Ag NPs in a bacterial growth medium and monitored its bactericidal effect.

The results of fluorescence spectroscopic studies of the recombinant bacterial culture treated with different concentrations of Ag NPs are shown in **Figure 2.3**. The control (untreated) sample showed detectable fluorescence, which consistently increased with time (**Figure 2.3(A)**), whereas the samples treated with Ag NPs initially showed low

fluorescence that increased only marginally with time (**Figure 2.3(B,C)**). The final magnitude of fluorescence of the control sample was much higher than that of the samples treated with Ag NPs. Moreover, the magnitudes of fluorescence of the treated samples at 12 h are either close to or less than the value of the control samples at 0 h. These observations can be understood in the following way. Initially, the OD_{595} of the untreated samples (control) was low in comparison to the values of the Ag NP treated samples (**Figure 2.2**). Hence, the fluorescence for the control sample was conspicuous. On the other hand, the initial fluorescence of the treated samples could not be observed because of high background absorption in the presence of Ag NPs. The concentration of Ag NPs in the medium got depleted progressively with time as the NPs got attached to bacterial cells. Consequently, the background absorbance was reduced, resulting in increased fluorescence. In other words, it is expected that the emission intensities of all the samples should ideally be identical at time 0 h, since all the samples had equal concentrations of bacteria to begin with. However, we could observe fluorescence at 0 h only from the sample that was devoid of the Ag NP synthesizing medium. This is due to intense absorption of the media (where Ag NPs were present) in the region of the excitation wavelength (400 nm), which possibly prevented significant excitation of the bacterial GFP protein, and thus no clear fluorescence was observed. On the other hand, when Ag NPs were attached to the bacteria, the OD of the media at the fluorescence excitation wavelength gradually decreased. This is possibly due to the attachment of free Ag NPs to the bacterial cell wall, which reduced its oscillator strength[26]. It is known that the oscillator strength of the plasmon resonance absorption of metal NPs strongly depends on the stabilizing

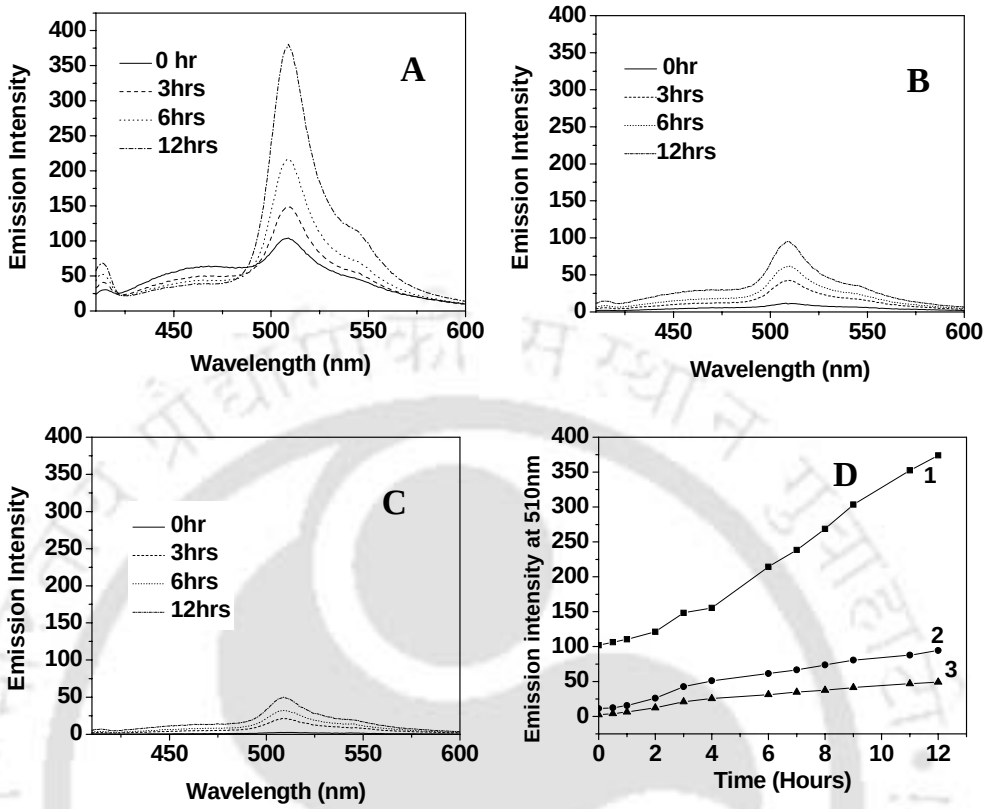

Figure2. 3: Time-dependent fluorescence spectra of GFP recombinant *E. coli*. Excitation wavelength was set at 400 nm. **(A)** In the absence of the NPs; **(B)** in the presence of 56.5 μg mL^{-1} of Ag NPs; **(C)** in the presence of 84.83 μg mL^{-1} of Ag NPs. **(D)** Rate of change of fluorescence (1) for the control, (2) in the presence of 56.5 μg $mL^{-1}$of Ag NPs, and (3) in the presence of 84.83 μg mL^{-1} of Ag NPs as marked in the graph.

agent, the dielectric constant of the medium, and the surfaces to which they get attached. In the present case, the attachment of the NPs to the cell wall may have reduced the oscillator strength considerably, thereby making the media optically less dense. Hence, the excitation of GFP (in bacteria) could be progressively achieved and consequent fluorescence. The time-dependent progressive decrease in the ODs of the media containing a higher amount of Ag NPs (**Figure 2.2**) is consistent with the progressive increase in fluorescence. One can also see that, while the OD values of

the untreated samples go up with time, the same goes down for treated samples at the MIC and MKC concentrations of the Ag NPs. Furthermore, the final fluorescence intensity of the bacteria treated with higher Ag NP concentrations was lower than that of samples treated with lower concentrations. This possibly indicates that, at higher Ag NP concentrations, the bacteria are killed at a higher rate, leading to a net reduction in fluorescence (**Figure 2.3**(**D**)) due to degradation of the dead bacteria with time.

Figure 2.4 reveals the time-dependent fluorescence microscopic studies of the control (untreated) and Ag NP-treated bacteria. As is clear from the **Figure 2.4 (A1)**, **(B1)**, and **(C1)**, there was comparable population of bacteria at 0 h in all three samples. The bacterial number increased with time for the control sample, as can be seen from **Figure 2.4 (A1), (A2), (A3),** and **(A4)**. On the other hand, the samples treated with 56.5 and 84.83 μg mL^{-1} of Ag NPs showed continuous decrease in fluorescence intensity with a simultaneous reduction in bacterial population (**Figure 2.4**, panels in the **B** and **C** series). Furthermore, Ag NP treatment of recombinant bacteria resulted in morphological deformation (**Figure 2.5**). In comparison to those of the control, the treated bacteria were slender and truncated with reduced fluorescence, possibly due to death and subsequent cell lysis. The fluorescence observed is mainly from residual GFP in lysed bacteria. TEM studies on a single bacterial cell showed perforation on the cell wall upon treatment with Ag NPs (**Figure 2.6(A)**). A large number of discrete Ag NPs in the range of 4-5 nm in size remained attached to the cell wall (**Figure 2.6(B)**). The NP sizes correspond to that of the Ag NPs prepared in the LB medium. It is also important to note here that there was no significant agglomeration of NPs once they were attached to the cell wall. This is evident from the typical particle sizes that

are less than 10 nm, as shown in **Figure 2.6(B)**. Furthermore, XRD measurement of

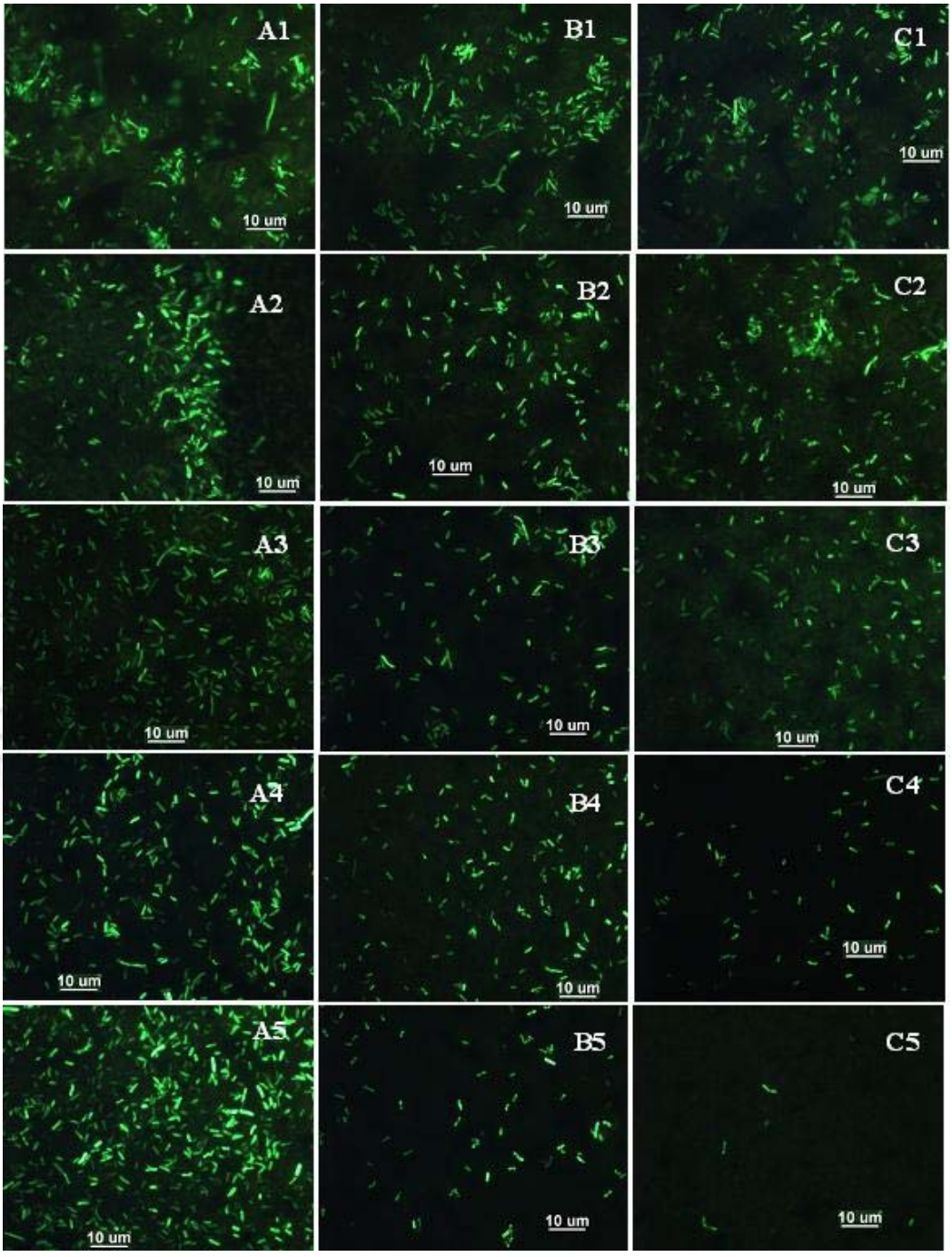

Figure 2.4: Time-dependent fluorescence micrograph of GFP recombinant *E. coli*. Series A, B, and C refer to the control, 56.5 μg mL^{-1} Ag NP-treated, and 84.83 μg mL^{-1}Ag NP-treated samples, respectively, while series 1, 2, 3, 4 and 5 refer to the samples at 0, 3, 6, 9 and 12 h time points, respectively.

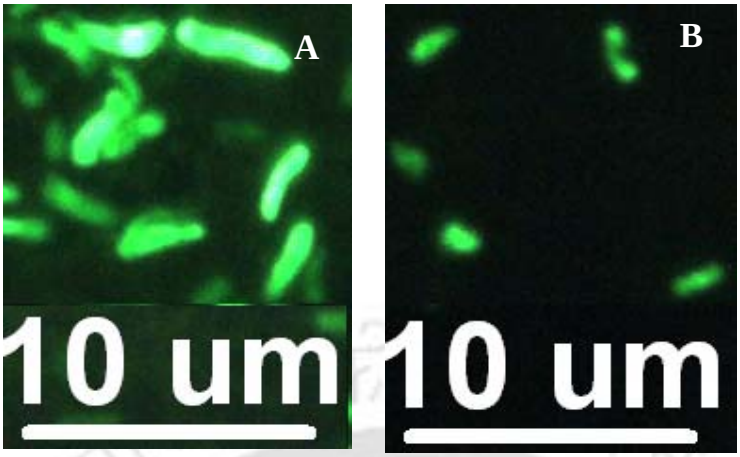

Figure 2.5: Fluorescence micrographs of GFP *E. coli*: (A) control, (B) 84.83 μ*g* mL^{-1} Ag NP-treated up to 12 h.

the centrifuged bacterial medium at 12 h indicates the presence of a peak characteristic of AgNPs (**Figure 2.6(C)**). Using the Debye-Scherrer[7] formula, the average particle size was calculated to be 9 nm, which is close to the sizes observed using TEM. In addition, the UV-vis spectrum of the washed pellet supernatant of the above bacteria showed a broad peak at 393 nm, which is characteristic of Ag NPs. Thus TEM, XRD, and UV-vis studies showed that, indeed, Ag NPs were formed in the medium and are present in the bacterial cell wall, which is responsible for the bactericidal activity of the NPs. Accumulation of NPs in the vicinity of the bacterial cell wall and the formation of pits has also been reported previously.[8] However, in the present study, the perforation of the cell wall is clear, which was not reported previously. The high affinity of Ag NPs for attachment to the bacterial cell wall could be due to the presence of thiol groups in the cell wall proteins. The loss of viability of bacterial cells upon treatment with Ag NPs (56.5 and 84.8 μg mL^{-1}) was observed by the viable cell count method (**Figure 2.7**). After 6 h of treatment, bacterial growth

was totally obliterated in comparison to that of the control sample, clearly reflecting the lethal effect of Ag NP treatment. Furthermore, the effect of Ag NPs on recombinant bacteria was studied by measuring the fluorescence of the cell-free

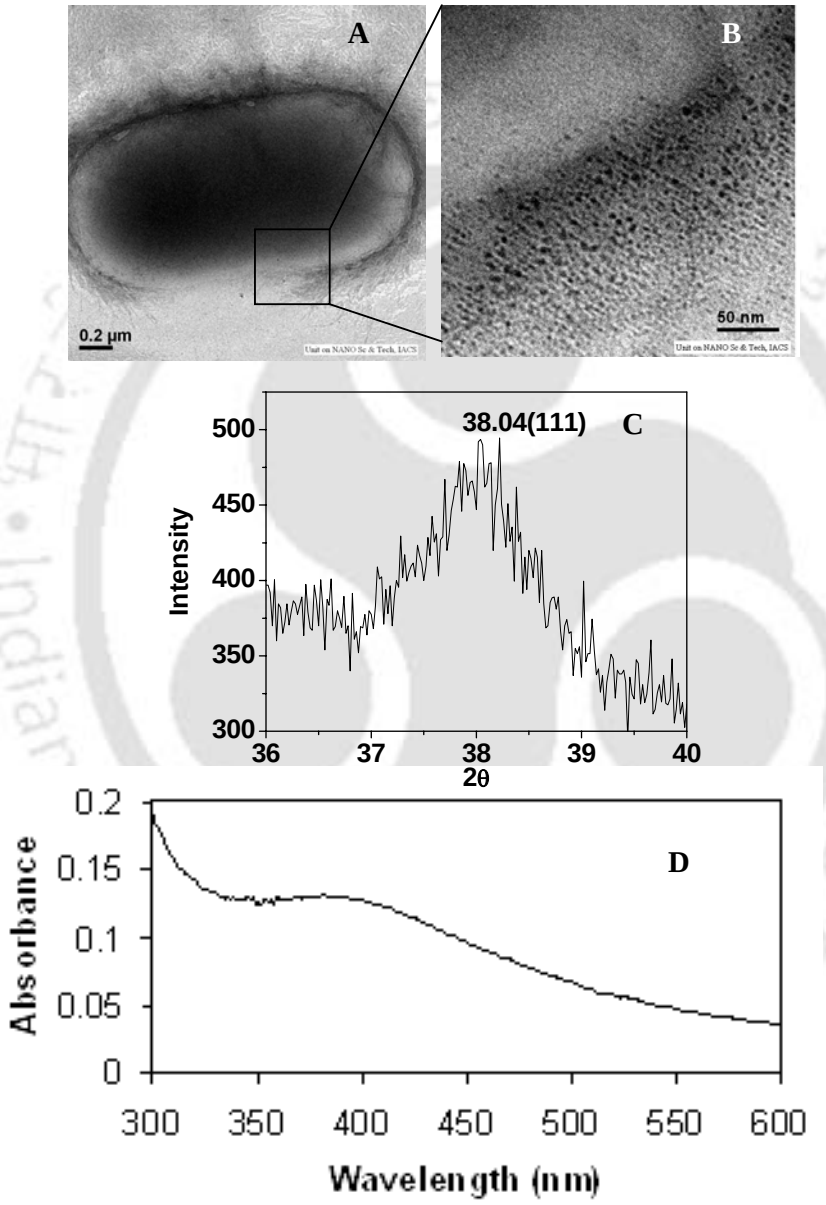

Figure 2. 6: TEM micrograph of (**A**) a single bacterial cell and (**B**) an expanded view indicating the presence of Ag NPs on the cell membrane. (**C**) XRD of the Ag NPs containing bacterial pellet at 12 h. (**D**) UV-vis spectrum of the supernatant.

supernatant and the bacterial cell pellet for the treated and control samples (**Figure 2.8**). The relative fluorescence intensity of the supernatant in comparison to the bacterial pellet was higher for the Ag NP-treated samples compared to that of the

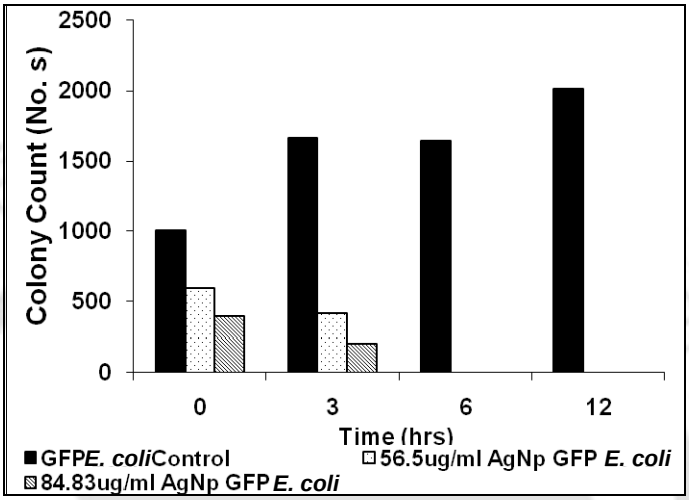

Figure 2.7: Effect of Ag NPs on the viability of GFP-expressing *E. coli* at 0, 3, 6, and 12 h.

control. Moreover, the fluorescence intensity of the supernatant increased proportionately with higher concentrations of Ag NPs. This indicates efficient bacterial cell lysis and leakage of copious amounts of GFP protein into the medium.

The SDS-PAGE* analysis showed greater protein turnover for the control sample compared to the treated samples where the protein profile remained same but with a lower protein turnover (as a result of fewer bacteria). This signifes that the Ag NPs had no qualitative impact on the protein expression. At the same time the agarose gel electrophoresis* of the plasmid DNA isolated from the control and treated samples at different time points indicated a relative decrease in plasmid DNA in the treated samples while the DNA migration pattern remained the same.

UV-vis spectroscopic studies of Ag NP-pure plasmid DNA suggested a minimal absorbance spectral shift due to the possible binding of Ag NPs on DNA (**Figure 2.9(A)**), whereas the corresponding agarose gel migration pattern did not

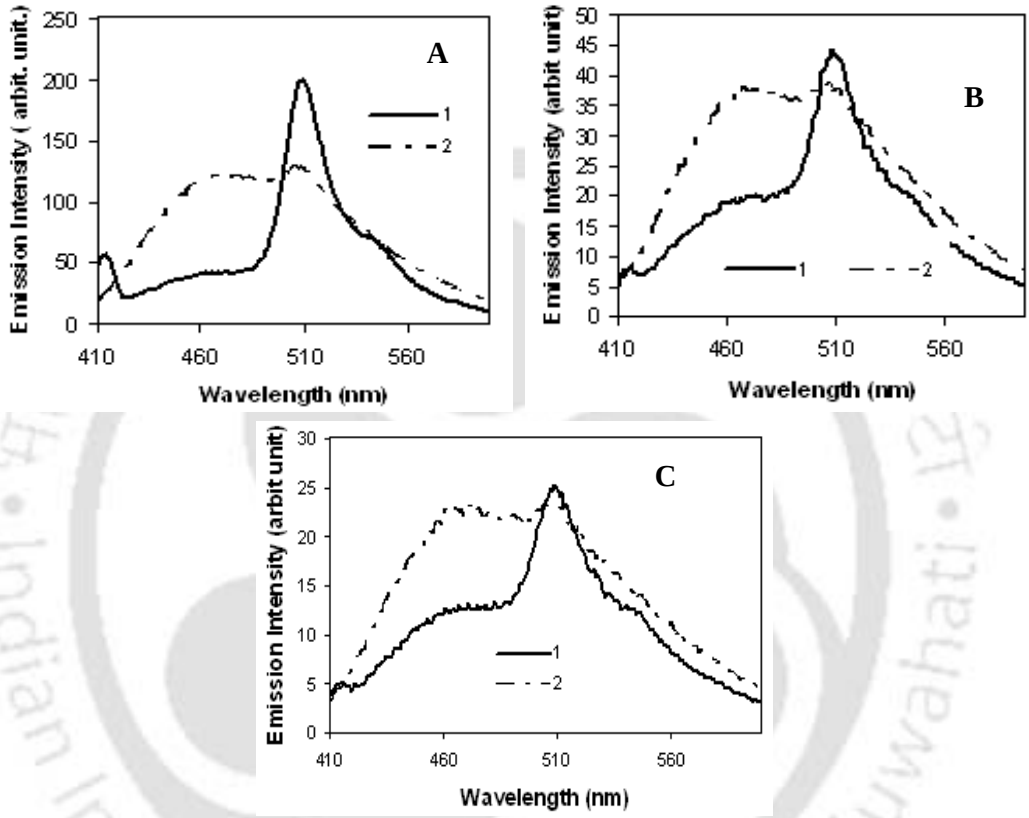

Figure 2. 8: Fluorescence spectra of GFP *E. coli*: (A) control, (B) 56.5 μg L^{-1} Ag NPs-treated, (C) 84.83 μg L^{-1} Ag NPs-treated, where 1 and 2 in each spectra are the GFP *E. coli* in the media and supernatant, respectively.

show any variation (**Figure 2.9B**). Interaction of Ag NPs and pure plasmid DNA was indicated by spectrophotometric studies, but Ag NPs had no effect on DNA isolated from treated bacteria. Previously, Feng et al.[5] observed a low electron density region rich in agglomerated DNA based on TEM analysis of bacteria treated with Ag^{+} ions.

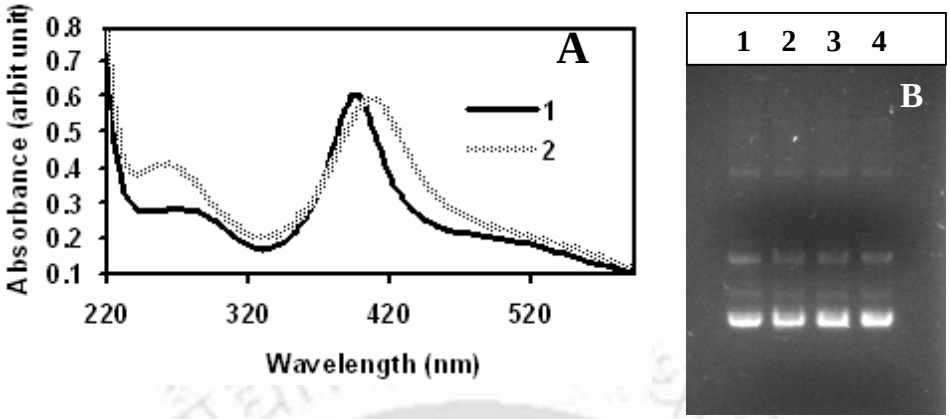

Figure 2.9: Ag NP plasmid DNA interaction. (**A**) UV-vis spectroscopic measurements. The solid line is the control plasmid DNA, and the dashed line is DNA treated with 84.83 μg.mL^{-1} of Ag NPs. (**B**) Agarose gel electrophoresis of plasmid DNA treated with 84.83 μg.mL^{-1} of Ag NPs *in* V*itro*. Lane 1: control; lane 2: 1 h; lane 3: 2 h; and lane 4: 3 h.

They also suggested the loss of DNA replication ability and inactivation of cellular proteins due to Ag^{+} ion interaction with those macromolecules. On the other hand, Morones et al.[11] reported a large accumulation of Ag NPs in bacteria without finding any low-density region rich in agglomerated DNA, but no direct analysis of DNA or proteins had been done in previous studies. In our study, the electrophoretic mobility of DNA and protein isolated from Ag NP treated bacteria did not reveal any gross anomaly in structure or migration pattern, which indicates that Ag NPs possibly had no direct effect on either cellular DNA or protein.

2.4: Conclusion

The present study, for the first time, shows the feasibility of using fluorescent bacteria as a prototype to investigate the antibacterial properties of Ag NPs. The synthesis of NPs achieved in the bacterial growth medium circumvented additional stringent

conditions for chemical methods of NP synthesis and minimized the artifact effects. Earlier studies using wild-type bacterial strains relied essentially on viability tests, which are time-consuming and error prone. Moreover, the direct effect of Ag NPs on cellular DNA/protein migration profiles, which has been included in the current studies, had not been shown previously. Our work embraces nanotechnology and rDNA technology and demonstrates a reliable model system to study the antibacterial efficacy of NPs. The choice of a GFP-expressing *E. coli* to test the antibacterial effect of Ag NPs is superior because of the intrinsic stable property of fluorescence, minimal photobleaching effect, easy morphological identification by fluorescence microscopy, and the possibility of a noninvasive detection method.

References

1. Spatz, J. P. *Nanobiotechnology*; Niymeyer, C. M., Mirkin, C. A., Eds.; Wiley-VCH: New York, 2004; pp 53-65.
2. Bharali, D. J.; Lucey, D. W.; Jayakumar, H.; Pudavar, H. E.; Prasad, P. N. *J. Am. Chem. Soc.* **2005**, *127*, pp 11364-11371.
3. El-Sayed, I. H.; Huang, X.; El-Sayed, M. A. *Nano Lett.* **2005**, *5*, pp 829-834.
4. Rosi, N. L.; Mirkin, C. A. *Chem. Rev.* **2005**, *105*, pp 1547-1562.
5. Feng, Q. L.; Wu, J.; Chen, G. Q.; Cui, F. Z.; Kim, T. N.; Kim, J. O. *J. Biomed. Mater. Res.* **2000**, *52*, pp 662-668.
6. Batarseh, K. I. *J. Antimicrob. Chemother.* **2004**, *54*, pp 546-548.
7. Baker, C.; Pradhan, A.; Pakstis, L.; Pochan, D. J.; Shah, S. I. *J. Nanosci. Nanotechnol.* **2005**, *5*, pp 244-249.
8. Sondi, I.; Salopek-Sondi, B. *J. Colloid Interface Sci.* **2004**, *275*, pp 177-182.

9. Jain, P.; Pradeep, T. *Biotechnol. Bioeng.* **2005**, *90*, pp 59-63.

10. Li, P.; Li, J.; Wu, C.; Wu, Q.; Li, J. *Nanotechnology* **2005**, *16*, pp 1912- 1917.

11. Morones, J. R.; Elechiguerra, J. L.; Camacho, A.; Holt, K.; Kouri, J. B.; Ramirez, J. T.; Yacaman, M. J. *Nanotechnology* **2005**, *16*, pp 2346-2353.

12. Lee, D.; Cohen, R. E.; Rubner, M. F.; *Langmuir* **2005**, *21*, pp 9651-9659.

13. Jeong, S. H.; Hwang, Y. H.; Yi, S. C. *J. Mater. Sci.* **2005**, *40*, pp 5413-5418.

14. Aymonier, C.; Schlotterbeck, U.; Antonietti, L.; Zacharias, P.; Thomann, R.; Tiller, J. C.; Mecking, S. *Chem. Commun*. **2002**, *24*, pp 3018-3019.

15. Elchiguuerra, J. L.; Burt, J. L.; Morones, J. R.; Camacho-Bragado, A.; Gao, X.; Lara, H. H.; Yacaman, M. J. *J. Nanobiotechnol.* **2005**, *3*, pp 1477-3155.

16. Shi, Z.; Neoh, K. G.; Kang, E. T. *Langmuir* **2004**, *20*, pp 6847-6852.

17. Tsien, R. Y. *Annu. Rev. Biochem.* **1998**, *67*, pp 509-544.

18. Niwa, H.; Inouye, S.; Hirano, T.; Matsuno, T.; Kojima, S.; Kubota, M.; Ohashi, M.; Tsuji F. I. *Proc. Natl. Acad. Sci. U.S.A.* **1996**, *93*, pp 13617-13622.

19. Shaner, N. C.; Steinbach, P. A.; Tsien, R. Y. *Nat. Methods* **2005**, *2*, pp 905-909.

20. Tavare´, J. M.; Fletcher, L. M.; Welsh, G. I. *J. Endocrinol.* **2001**, *170*, pp 297-306.

21. He, S.; Yao, J.; Jiang, P.; Shi, D.; Zhang, H.; Xie, S.; Pang, S.; Gao, H. *Langmuir* **2001**, *17*, 1571-1575.

22. Li, X.; Zhang, J.; Xu, W.; Jia, H.; Wang, X.; Yang, B.; Zhao, B.; Li, B.; Ozaki, Y. *Langmuir* **2003**, *19*, 4285-4290.

23. Andrews, J. M. *J. Antimicrobial Chemotherapy* **2001**, *48 suppl. S1*, pp 5-16.

24. Sambrook, J.; Russell, D. W. *Molecular Cloning-A Laboratory Manual, 3rd ed.*; Cold Spring Harbor Press: New York, 2001; Vol. 1, pp 1.31-1.34.

25. Bollag, D. M.; Rozycki, M. D.; Edelstein, S. J. *Protein Methods,2nd ed* ,Wiley-Liss, Inc.: New York, 1996.

26. Jensen, T. R.; Malinsky, M. D.; Haynes, C. L.; Van Duyne, R. P. *J. Phys. Chem. B* **2000,** *104,* pp10549-10556.

* *Prodrug Gene Therapy Vectors in Combination Therapies*, Ph D Thesis, Gopinath, P., Department of Biotechnology, Indian Institute of Technology Guwahati, 2008.

Chapter III

Synthesis of Ag Nanoparticles in Mammalian Cell Growth Medium and their Possible Anti-cell Proliferative Activity

3.1: Introduction

Understanding the behavior of eukaryotic and prokaryotic cells when exposed to metal as well as semiconductor nanoparticles (NPs) is crucial for application of nanotechnology to medical biology. Moreover, nanomaterials that are either redox active or transport across cell membrane are of major toxicological concern for human health and environment [1]. Recent studies have shown that NPs easily pass through the blood–brain and blood–testis barriers in mouse models[2]. Interestingly, interactions of carbon nanoparticle with biological cells showed evidence of cell cytotoxicity with manifestation of lipid membrane peroxidation, gene down regulation of adhesive proteins and increased cell death[3]. Among the metal NPs, the bactericidal and bacteriostatic properties of Ag NPs are well known for sometime [4,5], however, the exact mechanism of interaction is yet to be established. This is important for exploration of the therapeutic potentials of these NPs.

Genetically programmed cell death, known as apoptosis (**Schematic 3.1**), and which eliminates the unwanted/damaged cells in the process of development or in response to infection or DNA damage [6], holds the key to the development of viable therapeutics against killer diseases like cancer and autoimmune diseases [7]. Apoptosis is induced by extracellular or intracellular signals, which trigger onset of signaling cascade with characteristic biochemical and cytological signatures, including nuclear condensation, membrane blebbing and DNA fragmentation [8], leading ultimately to cell death [9]. On the other hand necrosis is the premature death of the cells and tissue caused by factors external to the cell or tissue, such as infection, toxins, or trauma. In contrast to the apoptosis, necrosis is accompanied by loss of membrane integrity, swelling and disrupture of the cells as shown in **Schematic 3.1**. In necrosis the

cellular materials are released uncontrollably to the cells environment resulting in damage of the surrounding cells and a strong inflammatory response in the corresponding tissue.[10] While apoptosis is often beneficial to the organisms necrosis is almost always damaging.

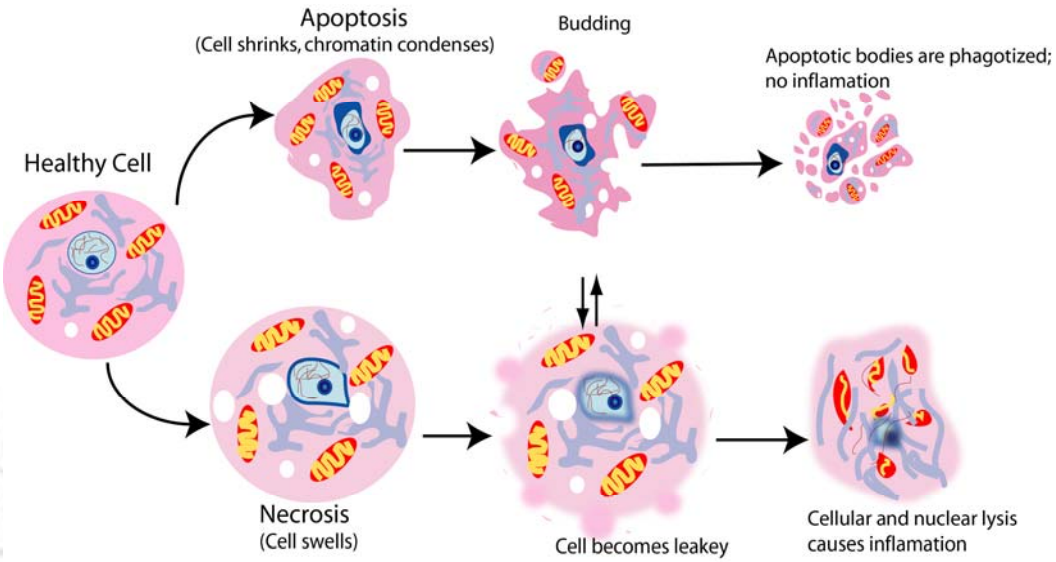

***Schematic 3.1*:** Schematic diagram showing the hallmarks of apoptotic and necrotic pathways of cell death. *(Source: Andreas Gewies (2003), ApoReview - Introduction to Apoptosis, 1-26.)*

In this regard, understanding the molecular mechanism of apoptosis is essential to develop newer drugs and therapeutic strategies [11]. Conventional anti-cancer therapies although abound, suffers from lack of generality, effectiveness in case of advanced stages of the disease and not to mention numerous toxic side effects left by radiation or chemicals used in the process. In addition, the importance of augmenting the performance of conventional drugs by incorporating the NPs cannot be overstated as the synergistic effect may offer valuable alternatives with minimization of harmful consequences. For example, the chemotherapeutic agent 5-fluorouracil (5-FU), which is widely used as anticancer drug, has little effect in the treatment of human solid

tumors due to their resistance to the cytotoxic effects of 5-FU[12,13]. Therefore, expression of *Escherichia coli* uracil phosphoribosyltransferase (UPRT) using gene therapy techniques is required to convert 5-FU to more toxic 5-flurouracilmonophosphate (5-FUMP), hence sensitizes colon, gastric, liver, and pancreas cancer cell lines at low concentrations of 5-FU *in vitro*[14,15]. On the other hand, the advent of synthetic inorganic, organic and biological nanomaterials has injected new enthusiasm in the development of newer therapies against cancer and also understanding their impact on cellular gene expressions. [16, 17] A potential candidate in this regard is Ag nanoparticle (NP), which has known antimicrobial activities either as it is or in composites with polymer.[5,18] We have been exploring the possibility of using Ag NPs by themselves or in combination with gene therapy to induce apoptosis in mammalian cells. [19] The combination therapy is especially attractive as the use of the component materials could possibly be made below their toxic doses and thus the best of both worlds could be achieved with minimum damage to the healthy cells. Moreover, most of the conventional anti-cancer drugs available commercially are known to be toxic to the cells. In that respect, the level of toxicity posed by the use of Ag NPs in the treatment may not necessarily be graver and thus could be considered for alternative therapy. However, fundamental to this is a clear understanding of mechanism of apoptosis induced by Ag NPs and thus their subsequent use would depend on their mode of function. Our observations indicated that the NPs disrupted normal cellular function through cytotoxic stress and were responsible for the membrane damage. Also, in the Ag NP induced apoptosis of mammalian cells, various signaling genes were involved in the process leading to programmed cell death. Essentially, interactions of Ag NPs with the mammalian cells

involve p53 dependent and mitochondria mediated DNA fragmentation leading to programmed cell death.

Herein we report that besides known cytotoxicity to mammalian cells, Ag NPs have apoptotic function and show that this can have important and new therapeutic values. We also observe that the augmentation of concentration dependent apoptotic effect makes Ag NPs a suitable candidate for gene therapy application. Synergistic effect on apoptosis is shown on UPRT expressing cells as well as on non UPRT expression cells upon 5-FU drug treatment. The important feature of the Ag NPs mediated apoptosis induction not only incur the benefits of cytotoxic effect, but also sensitizes cancer cells towards drug treatment even in absence of gene therapy. This switching behavior of Ag NPs can possibly have high impact therapeutic potential in conventional gene therapy. This work has been carried out in collaboration with Dr P. Gopinath, Department of biotechnology, IIT Guwahati and his contributions are duly acknowledged.

3.2: Experimental Methods

3.2.1: Materials and Growth media: High purity molecular biology grade chemicals, reagents and kits used for DNA isolation and agarose gel electrophoresis were obtained from Sigma-Aldrich, USA and Roche Applied science, Germany. Restriction enzymes were purchased from Promega Life science, USA and PCR reagents from Bio-line, USA. Luria-Bertani (LB) was purchased from HiMedia, India for bacterial growth. Cell culture media like Dulbecco's Modified Eagle's medium (DME), fetal bovine serum (FBS), penicillin, streptomycin were purchased from Sigma-Aldrich, USA. The baby hamster kidney (BHK21) and human colon

adenocarcinoma (HT29) cell lines were obtained from National Centre for Cell Science, India.

3.2.2: Ag NPs synthesized in DME media: Ag NPs were synthesized in DME medium by reduction of $AgNO_3$, at various concentrations, using $NaBH_4$ as the reducing agent following slight modification of a method developed earlier by our group to synthesize Ag NPs in bio-friendly media [5]. The concentration of Ag precursor $AgNO_3$ used at 10^{-6}-10^{-4} M, while the reducing agent concentration kept at 10^{-4} M. The advantage of synthesizing Ag NPs in cell growth media lies in the fact that it avoids any external stabilizer and the effect of dilution.

3.2.3: Transmission Electron Microscopy (TEM): For TEM investigation, 20 μL of as prepared Ag NPs in DME was drop-cast on a carbon-coated copper grid and subsequently dried in air. The cells treated with Ag NPs for 0 h and 16 h were washed gently with phosphate buffer saline (PBS) and removed from culture dish by rubber policeman. Cells were then resuspended in sterile water and immediately 20 μL of the suspension was deposited on carbon-coated copper TEM grid followed by air-drying. TEM images of Ag NPs were recorded by the Jeol 2100 HR-TEM operating at a maximum accelerating voltage of 200 keV. Selected area electron diffraction (SAED) was observed using the same TEM instrument.

3.2.4: Scanning Electron Microscopy (SEM). For scanning electron microscopy (SEM), cells were grown in 6 well tissue culture plates and washed with PBS. A heated metal cutter was used to cut out discs on which the cells had been grown. The cells attached on discs were dried, coated with gold film in the sputter coater and examined in LEO 1430VP SEM. The images were recorded at different time points to observe changes in cell morphology.

3.2.5: X-Ray diffraction (XRD) measurement. We performed X-ray diffraction measurements to confirm the presence of Ag NPs throughout the cytotoxicity experiments. Firstly, the Ag NPs synthesized in DME medium were spread on glass microslides and XRD was recorded using a Bruker Advance D8 XRD machine (Cu α source with 1.5406 Å wavelength). Again cells treated with Ag NPs for 12 h was centrifuged at 2000 rpm for 10 min. The cell pellet was washed twice with phosphate buffer saline and spread on a glass slide and XRD of the cell pellet was then recorded.

3.2.6: Construction of *E. coli* uracil phosphoribosyltransferase (UPRT) plasmid:[19,*] The UPRT gene was polymerase chain reaction (PCR) amplified from CD-UPRT plasmid with UPRT1 (5'GCCCATGGATGGCTAAGATCGTGGAAG3', with NcoI linker) and UPRT2 (5'GAGCTAGCGAATTTCGACAAGC 3', with NheI linker) linker primers. The amplicon was cloned into the NcoI and NheI sites of the pORF expression vector (*Invivogen*) and the recombinant pORF-UPRT clone was selected in LB ampicillin agar plate.

3.2.7: Cell Culture and Electroporation: [19,*] BHK21 and HT29 cell lines were propagated in complete DME medium supplemented with 10% FBS 50U mL^{-1} penicillin and 50mg mL^{-1} streptomycin in a humidified atmosphere containing 5% CO_2 at 37^0C. For the MTS (3-(4, 5-dimethylthiazol-2yl)-5-(3-carboxymethoxyphenyl)-2-(4 sulfophenyl)-2H-tetrazolium) and lactate dehydrogenase (LDH) assays, the cells were seeded in 96-well microplates at a density of $1x10^4$ cells per well. For apoptosis assay, the cells were seeded into 6-well plates at a density of $1x10^5$ cells per well and propagated for 2 days up to 80% confluency before the assay. Electroporation was performed on 60-70% confluent

cells with 2µg DNA/ 35mm plate in a BIO-RAD Gene Pulser Xcell. A square wave of 25 milliseconds at 140V for BHK-21 and an exponential wave of 500 µF at 160V for HT-29 cell lines were used.

3.2.8: PCR and RT –PCR analysis : [19,*] PCR was performed using UPRT1 and UPRT2 primers at the following cycle conditions denaturation at 94ºC for 30s, annealing at 55ºC for 1min and extension at 72ºC for 1min to amplify 651bp UPRT DNA. RNA was extracted with Tri reagent (Sigma, USA), and the RT PCR was performed with the same primers according to the manufacturer's instructions using Enhanced Avian HS RT-PCR kit (Sigma, USA) in Gene Amp PCR system 9700, Applied Biosystems.

3.2.9: Semi-quantitative RT-PCR : [19,*] Apoptotic signaling genes were detected by semi-quantitative RT-PCR. cDNA was generated from total RNA by reverse transcription of 3µg denatured RNA. The reaction was performed at 37 ◦C for 50 min using M-MLV Reverse Transcriptase (Sigma, USA) in a total mixture of 20µL. 2µL from the product was used for PCR using gene specific upstream and downstream primers [20] in Gene Amp PCR system 9700, Applied Biosystems. Initial denaturation at 94 ◦C for 2min was followed by a PCR cycle of denaturation at 94 ◦C for 15 s, annealing at 55 ^{o}C for 30 s, extension at 68 ^{o}C for 1min with a final extension at 68 ^{o}C for 5min. Finally, the products were analyzed on a 1.2% agarose gel. Gene expression was quantified based on the band intensity measured by imageJ software and the housekeeping gene β-actin was used as an internal control and its expression was considered 100% for the reference.

3.2.10: Confocal Microscopy : Dual staining of nuclei by using AO/EB was observed by confocal microscopy (LSM 510 Meta, Carl Zeiss, Germany). Green

fluorescence was detected at 488nm excitation with a band pass filter ranging between 505-530nm. Simultaneously, red fluorescence was detected using the long pass filter at 585nm, and superimposition of both green and red fluorescence generated the final images.

3.2.10: Cytotoxicity assay :[19,*] Cytotoxicity due to Ag NPs, 5-FU or in combinations was assayed by measuring the activity of lactate dehydrogenase (LDH) enzyme in culture media using CytoTox 96 Non-Radioactive Cytotoxicity Assay Kit (Roche Applied Science). LDH leakage (%) related to control wells containing cell culture medium without Ag NPs was calculated by $[A]_{test}/[A]_{control}$ X 100, where $[A]_{test}$ is the absorbance of the test sample and $[A]_{control}$ is the absorbance of the untreated control sample at 490 nm. For this 50.0 µL aliquots of culture media were collected at different time points, diluted at 1: 1 ratio with fresh medium and incubated with 50.0 µL of tetrazolium salt (INT) solution (substrate) for 30 min at room temperature. LDH converted INT to the red formazon product which absorbs at 490 nm and detected with a microplate reader BIO-RAD, USA (Model 680).

3.2.11: DNA laddering: [19,*] The confluent cells were treated with Ag NPs or 5-FU or in combination for 12 h and then lysed with buffer containing 5mM Tris-Cl, pH 8.0, 20mM EDTA, and 0.5% Triton X-100 on ice for 20 min. Chromosomal DNA was recovered by gentle phenol/chloroform/isoamyl alcohol (25:24:1, v/v) extraction and alcohol precipitation. DNA was resuspended in TE (20mMTris-Cl, 1mMEDTA pH 8.0) buffer containing RNAs (100 µg mL^{-1}) and incubated at 37 °C for 1 h to remove cellular RNAs. Finally, the DNA fragments were resolved by 1.2% agarose gel electrophoresis.

3.2.12: Cellular DNA fragmentation ELISA : [19,*] Cellular DNA fragmentation ELISA kit (Roche Diagnostics GmbH, Germany) was used to determine release of fragmented DNA into cytoplasm due to apoptosis after Ag NPs (11.0 μg.mL^{-1}), 5-FU or the combine treatment. First, cellular DNA was metabolically labeled with 10μM BrdU labeling solution for 20 h at 37ºC. The labeled cells were electroporated with pORF-UPRT plasmid, seeded in 96well microplates. The BrdU-labeled 2x 10^4 cells per well were incubated with Ag NPs (11.0 μgmL^{-1}) and 5-FU for 2, 4 and 6 h, respectively. After incubation, the supernatant was removed, the cells were lysed and the amount of BrdU labeled DNA in cytoplasm was detected by ELISA. The amount of fragmented DNA, as measured by absorbance at 450nm, increases with time of incubation.

3.2.13: Atomic force microscopic analysis : BHK21 and HT29 cells seeded on poly-l-lysine-coated cover slips were treated with Ag NPs for 6 h. The cover slips were gently rinsed with phosphate buffer and air-dried. Images were taken by AFM (PicoScanTM 2500, Molecular imaging corporation-USA) in a non-contact mode and measurement was done using silicon cantilevers with a spring constant of 21N/m at a resonance frequency of 160 kHz. The images were acquired at a scan field of 10μm×10μm. The three-dimensional images were generated using the Picoscan 5.3.3 software.

3.3: Results and Discussion

Ag NPs synthesized in DME media were characterized by TEM microscopy and also the stability of the NPs throughout the experiment was confirmed. TEM images of Ag NPs before treatment with the cells (at 0 h) in **Figure. 3.1(A)** confirmed the formation

of well dispersed NPs with the particle size between 10-15 nm. TEM images recorded after 16 h of Ag NP exposure to the cells also show the NPs, a representative image being provided in **Figure. 3.1(B)**. This confirmed the stability of the NPs throughout the cytotoxicity experiments. Accompanying SAED patterns also verify

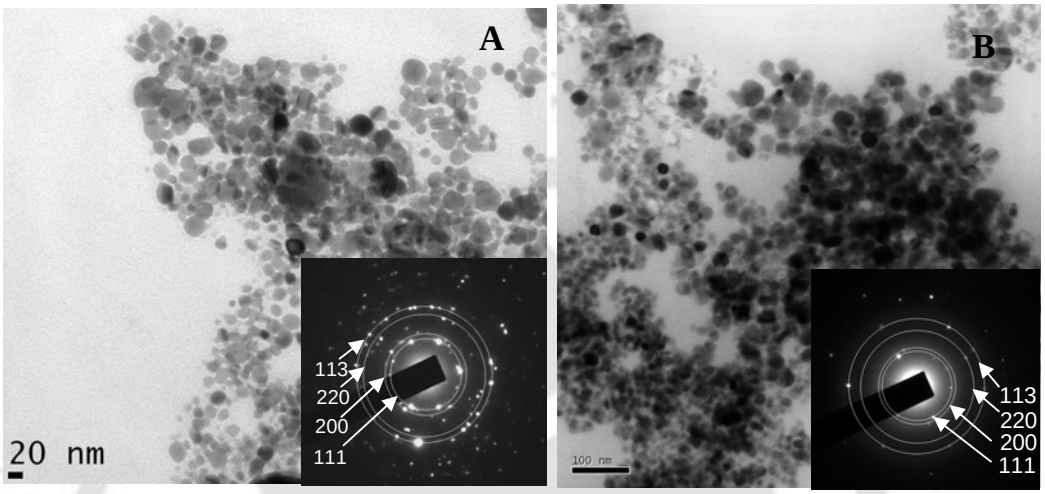

Figure 3.1: TEM images of Ag NPs**, (A)** as synthesized in DME medium; **(B)** at 16 h with the cells. The average particle size is around 10-15nm. Selected area diffraction pattern (SAED) in inset shows the hexagonal pattern of Ag NPs.

the presence Ag NPs in the respective cases. This was further substantiated by XRD measurements (**Figure 3.2**) indicating the formation of Ag NPs which were stable in the medium at least up to the 12th hour of measurements. In the XRD measurements we observed the characteristic peaks for Ag as mentioned in each spectrum with the lattice planes mentioned in bracket. For the Ag NPs synthesized in DME medium, for which XRD is represented in **Figure 3.2(A),** peaks at 2θ values 38^{o}, 44.39^{o} and 64.46^{o} matched with the literature values corresponding to (111), (200) and (220) planes respectively [21]. In **Figure 3.2 (B)**, XRD of the Ag NPs recorded with the BHK21 cells at the 12 h of Ag NPs treatment of the cells, is shown with the presence of peaks at

37.94^{o} and 64.49^{o} corresponding to (111) and (220) planes, confirming the presence of Ag NPs. Similar results were obtained from the XRD of the Ag NPs with HT29 cells at 12 h showing the peak at 38.02^{o} corresponding to (111) plane of Ag.

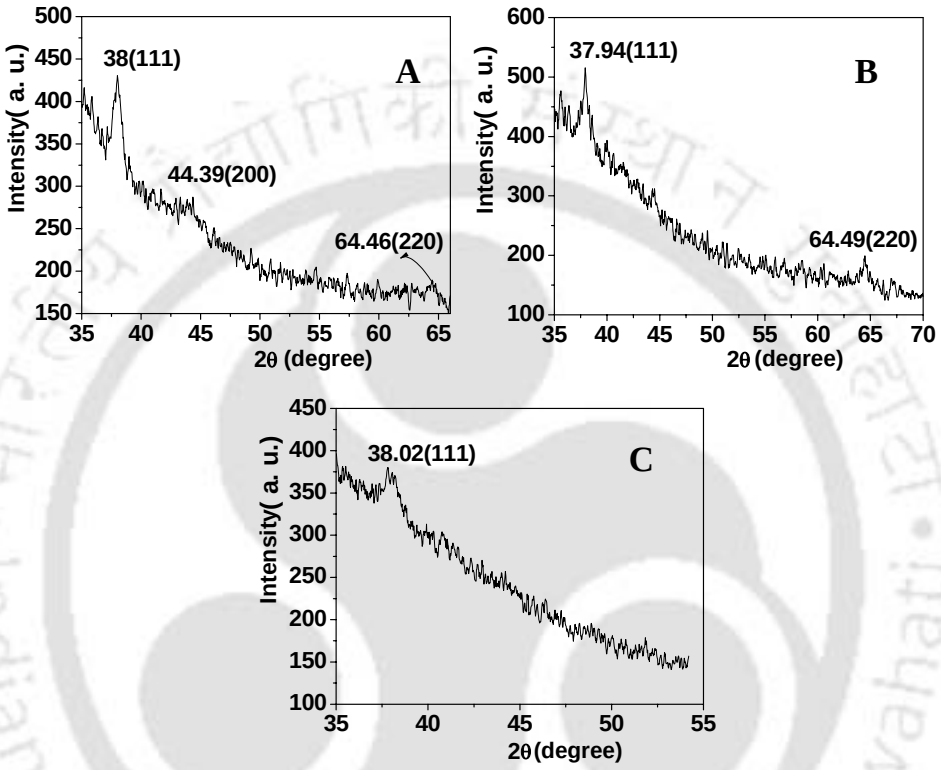

Figure 3.2 : X-Ray diffraction pattern of Ag NPs **(A)** in DME media, **(B)** at 12 h with BHK21 and **(C)** at 12 h with HT 29 cells.

The effect of Ag NP induced cytotoxicity on BHK21 (non-cancer) and HT29 (cancer) cells were studied *in vitro*. Ag NPs were synthesized in DME medium by reduction of $AgNO_3$, at various concentrations, using $NaBH_4$ as the reducing agent [22]. The effect of Ag NPs, over a wide range of concentrations, on cells was tested by the morphological changes of cells, progressive nuclear staining with ethidium bromide

(EB) *, lactate dehydrogenase enzyme (LDH) * release to the media and mitochondrial activity measurement by cell proliferation assay[23]. Ag^+ ions at 10^{-4} M (in the absence of $NaBH_4$) were observed to be highly cytotoxic, whereas Ag^+ concentrations at 10^{-6} M and 10^{-8} M were found to be non-toxic to the cells. Further, $NaBH_4$ alone in the 10^{-4} M concentration used for reduction was found to be non-toxic to the cells. Higher concentrations of Ag NPs (> 44.0 $\mu g mL^{-1}$) became necrotic to cells, leading to rapid cell membrane rupture, which was reflected in quick nuclear uptake of EB. IC_{50} (the concentration of Ag NPs required to inhibit cell growth by 50% compared to the control) was determined from cell proliferation assay and was found to be 27.0 $\mu g\ mL^{-1}$; but coagulation of Ag NPs in the culture medium was observed at this concentration.* On the other hand, at an Ag NPs concentration of 11.0 $\mu g\ mL^{-1}$, which is well below the IC_{50} value; cell death was also observed and the NPs were stable in the medium. Therefore this concentration of Ag NPs was taken as the standard NPs concentration for further investigations.

Time dependent SEM images of Ag NPs treated (11.0 $\mu g\ mL^{-1}$) cells of both BHK21 (**Figure 3.3 (A), (B)** and **(C)**) and HT29 types (**Figure 3.3 (D), (E)** and **(F)**) show the morphological changes in the cells. At an initial time point of 2 h the cells have their normal shape and remain attached to the culture plate (**Figure 3.3 (A)** and **(D)**). However as the time progresses cells treated with Ag NPs became rounded off with progressive membrane shrinkage, widening of cell to cell gaps as seen in (**Figure 3.3. (B)** and **(E)**) **for** BHK21 and HT29 cells respectively. It is followed by eventual detachment of the cells from culture dish (**Figure 3.3. (C)** and **(F)**). These morphological changes indicate possible onset of apoptosis at 4-6 h after Ag NPs

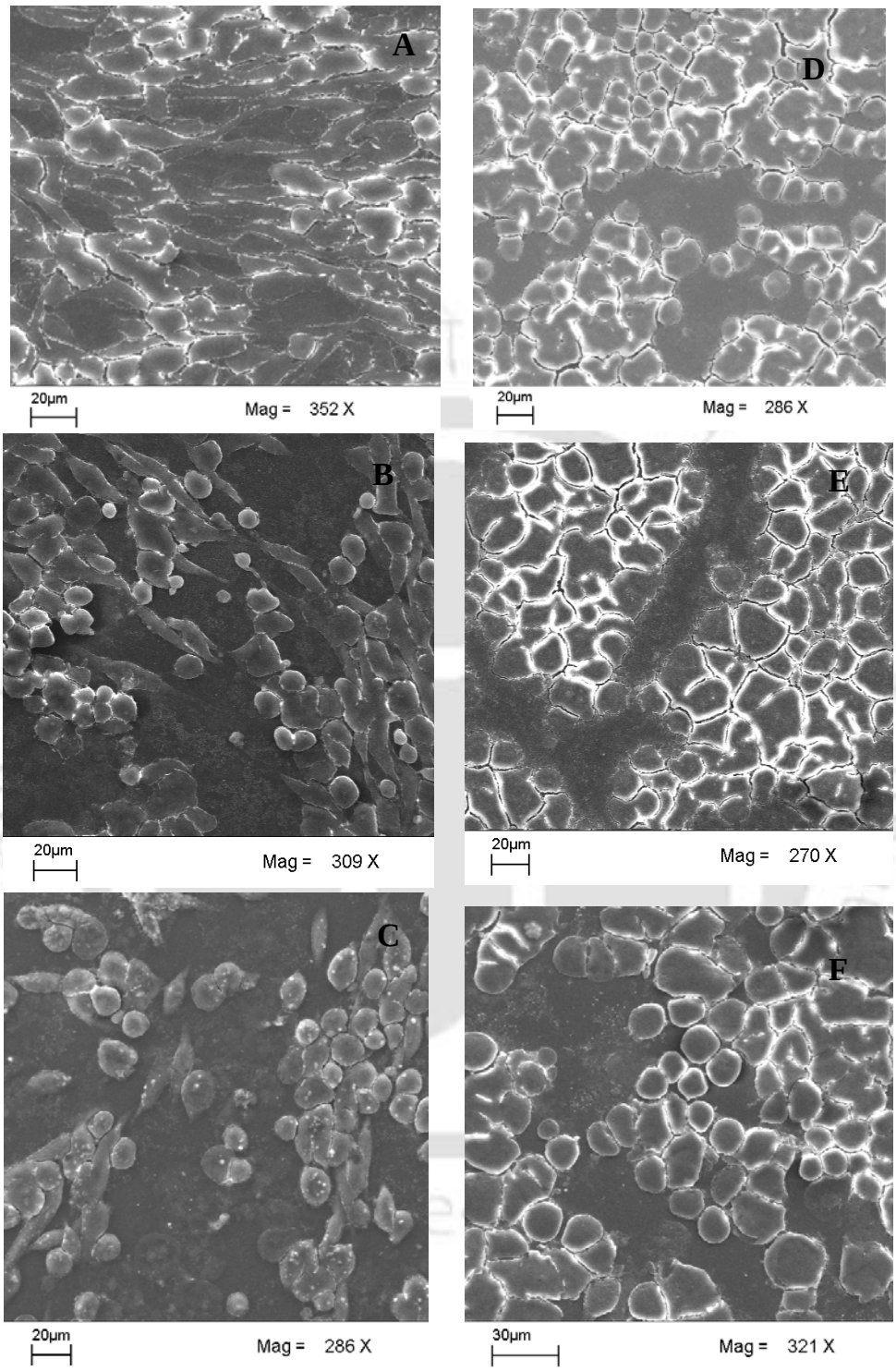

Figure 3.3: Representative Scanning electron micrographs of Ag NPs treated cells, (**A**)-(**C**) BHK21and (**D**)-(**F**) HT29 cells treated with Ag NPs (11.0 µg mL^{-1}) for 2, 4 and 6 h, respectively.

Treatment [24,25]. Furthermore, the appearance of apoptotic bodies and characteristic cell membrane blebbing [26] due to apoptosis, of cells at 6h after treatment, is seen in **Figure 3.4 (A)** and **(B)** for BHK21 and HT29 respectively.

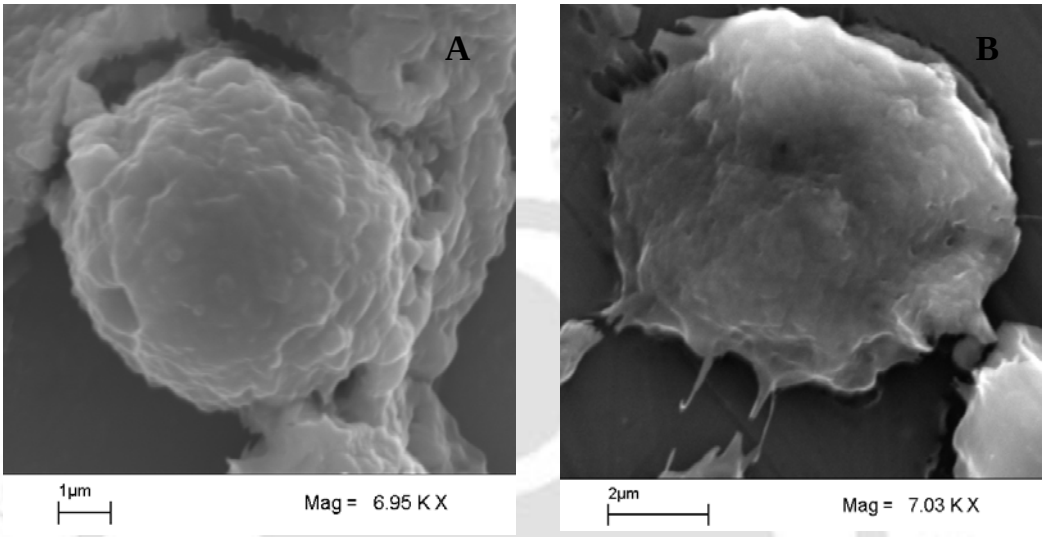

Figure 3.4: Cell membrane blebbing are shown in **(A)** and **(B)** for BHK21 and HT29 cells, respectively, at 6h of treatment with 11.0 μgmL^{-1} Ag NPs.

The induction of Ag NP mediated cell apoptosis was further observed by acridine orange (AO) and ethidium bromide (EB) double staining of treated cell nuclei at different time points [27]. Confocal microscopic images of the dual stained cells, presented in **Figure 3.5**, show that the live cells nuclei stained green due to AO uptake (green colour) and their numbers gradually decreased with time owing to more cell death, which correlates with the SEM data. In the same figure, one could observe progressive nuclear uptake of EB (orange colour) due to cell membrane perforation during apoptosis, which stained nuclei red and such effect was prominent from 4 h onwards. A closer look at the treated as well as untreated cells at 6 h, shown in high magnification images in **Figure 3.5 (I)-(L)**, indicates that live untreated cells have

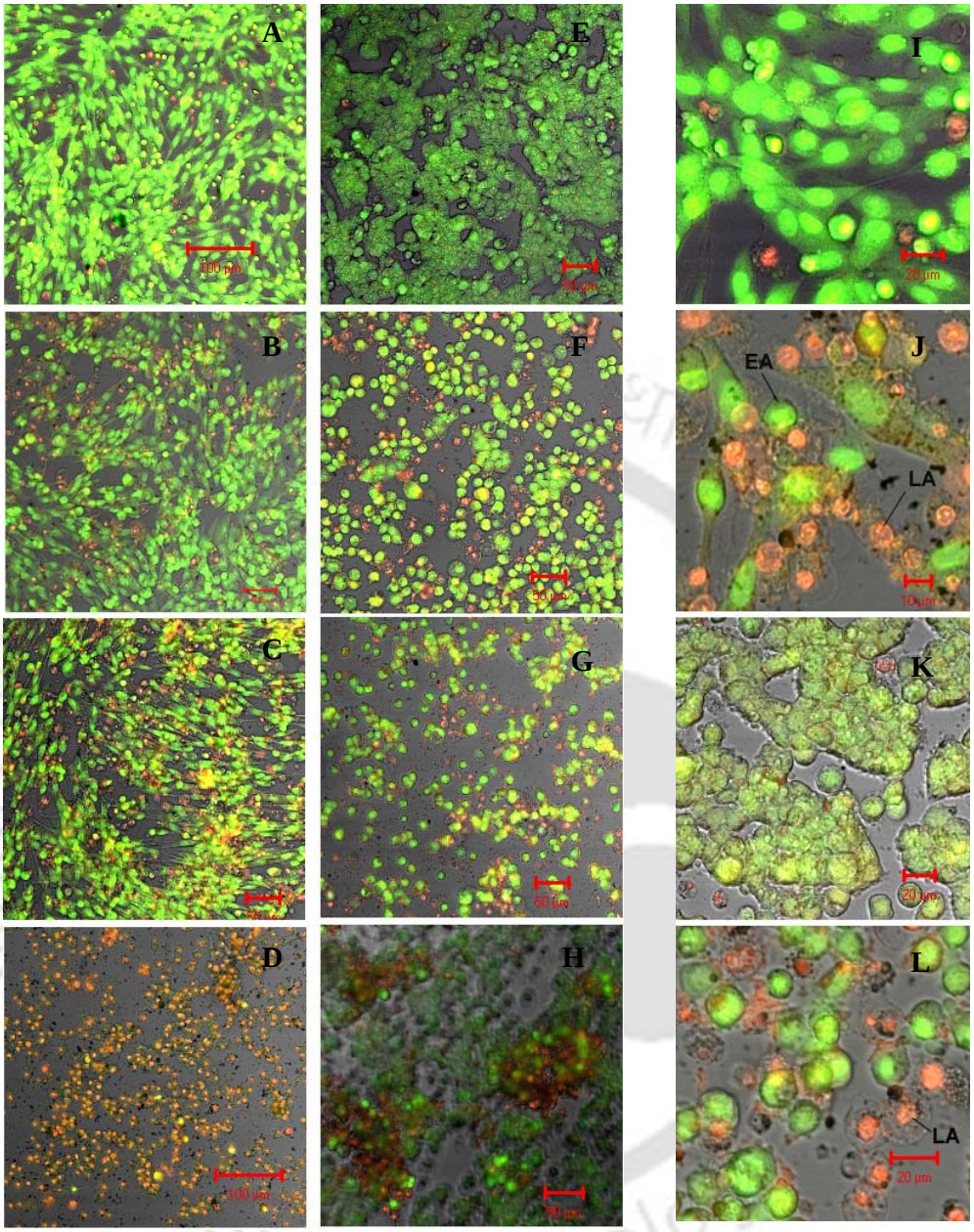

Figure 3.5: Representative time dependent confocal micrographs of AO/EB stained cells **(A)-(D)** BHK21 and **(E)-(H)** HT 29, at 0, 4, 8 and 24h of Ag NPs (11.0 μgmL^{-1}) treatment. High magnification micrographs (**I**) & (**J**), of BHK21 and (**K**) & (**L**), of HT 29 cells.

well organized chromatin structures, whereas the treated cells have fragmented or condensed chromatin consisting of apoptotic nuclei. **Figure 3.5(I)** (for BHK21)and

Figure 3.5(K) (for HT29) shows the untreated nuclei stained green whereas treated nuclei in **Figure 3.5(J)** (for BHK21) and **Figure 3.5 (L)** (for HT29) shows the early apoptotic (EA) nuclei that stained green and late apoptotic (LA) nuclei that stained orange. Therefore, the nuclear staining experiment shows that apoptosis started between 4-6 h after Ag NPs addition to the culture medium.

Molecular analysis of cellular DNA fragmentation by 5'-bromo-2'-deoxyuridine (BrdU) labeling ELISA confirmed Ag NPs induced apoptosis. In this assay, the release of BrdU labeled DNA to cytoplasm of Ag NPs treated cells was monitored up to 6 h. As shown in **Figure. 3.6(A)**, the BrdU labeled DNA increased significantly at 4 and 6 h in the cytoplasm of the treated cells as compared to the untreated control cells, which confirmed cell apoptosis by the nucleolytic cleavage of genomic DNA.

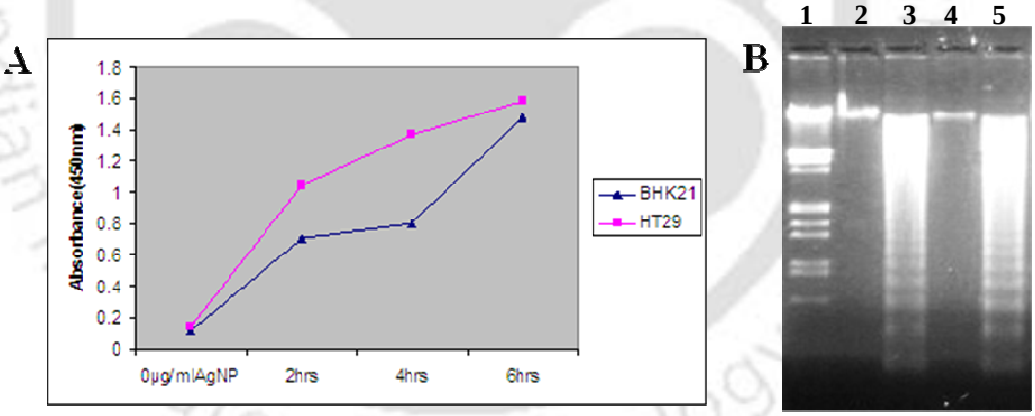

Figure 3.6: Detection of Ag NPs induced apoptosis by cellular DNA fragmentation ELISA (**A**) and DNA laddering **(B)**, In laddering Lane 1: λ/*Eco*R I+ *Hind* III marker; lane 2: untreated control BHK21cells; lane 3: 11.0µg mL^{-1} of Ag NPs treated BHK21 cells; lane 4: untreated control HT29 cells; lane 5: 11.0µg mL^{-1} of Ag NPs treated HT29 cells.

Finally, occurrence of DNA laddering, the widely regarded biochemical hallmark of late apoptosis due to DNA fragmentation [28] was observed in agarose gel

electrophoresis of cellular DNA obtained at 12 h after Ag NPs treatment, **Figure 3.6(B)**.

Atomic force microscopy (AFM) studies indicated that the presence of NPs changed the morphology of the cell membrane. For example, AFM images of the Ag NP treated BHK21 and HT29 cells (recorded after 6 h of treatment) showed higher degrees of surface roughness with pit like structures spread over cell surfaces, **Figure. 3.7(C)** and **(D)**, as compared to the relatively smoother surface of untreated cells **Figure. 3.7(A)** and **(B)**. The particle-like protrusions present in the membranes of treated cells are possibly due to clusters of membrane proteins with the underlying gaps owing to lipid layers [29,30] . The changes in the NP treated cell membrane structure could be attributed to the aggregation of membrane proteins and accompanying randomization of membrane lipids. Taken together, these topographic AFM images provided a direct evidence of toxic effects of Ag NPs on the cell membrane.

Further studies involving a semi-quantitative RT-PCR analysis indicated the involvement of various apoptotic signaling genes in Ag NP mediated cell death. The Ag NP treated cells were analyzed at 6 h, at which time it is known to have high cellular DNA fragmentation due to apoptosis. Expression profiles of apoptotic genes, such as, bak, bax, bad, C-myc, caspase-3 were analyzed. The results are shown in **Figure. 3.8**. Interestingly, it was observed that the apoptotic genes were up- regulated. On the other hand, the anti-apoptotic genes, such as bcl-2 and bcl-XL expression were down-regulated in the process. Additionally, the housekeeping gene β-actin which acts as an internal control remained unaltered.

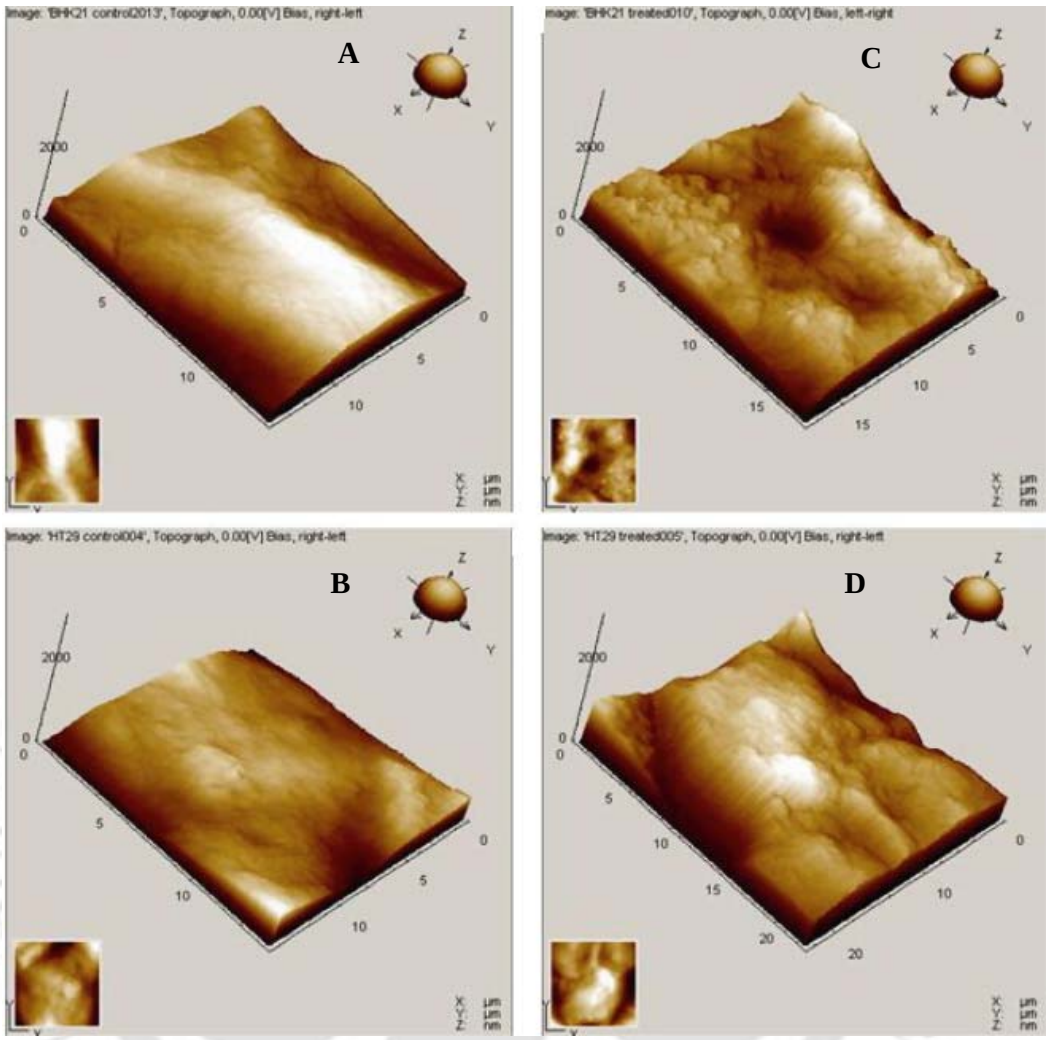

Figure 3.7: AFM images showing three-dimensional surface topography of untreated **(A)** BHK21 and (**B)** HT29 cell membrane under 10μm×10μm fields of view and **(C)** and **(D)** Ag NPs treated BHK21 and HT29 cells respectively.

It is known that most of the chemotherapeutic agents trigger apoptosis through p53 pathway. It is also well-established that destabilization of the mitochondrial integrity by genotoxic as well as cytotoxic agents precedes activation of caspases leading to apoptosis. bcl-2 (B-cell lymphoma 2) family controls the mitochondrial outer membrane permeabilization(MOMP) and can exert their pro-apoptotic (bax, bad, bak)

or anti-apoptotic (bcl-2, bcl-XL) effect by activation or inactivation of an inner mitochondrial permeability transition pore [31]

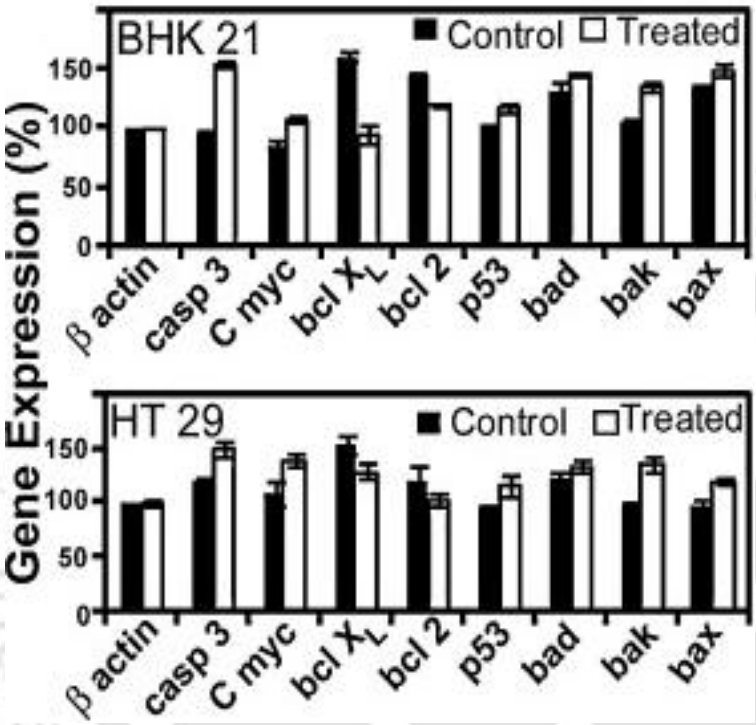

Figure 3.8: Quantitative expression of apoptotic signaling genes in control as well as Ag NP treated BHK 21 and HT 29 cells. Data are shown here as mean ±SD of three individual experiments. . *(Colloids and Surfaces B: Biointerfaces,* **2010**, *77*, 240-245.)

We have observed an up-regulation of p53 gene in the Ag NP treated cells. It has been reported that bax is up-regulated by p53 protein [32]. Since an increase in bax expression was observed, the role of p53 in the up-regulation of bax upon Ag NP treatment (of cells) can be postulated. The insertion of bax into the mitochondrial membrane possibly leads to p53-mediated apoptosis [32]. Similar results have been shown, by Hsin et al. [33], to play important roles in Ag NP induced apoptosis. bcl-XL

(basal cell lymphoma-extra large) is an anti-apoptotic protein, which protects cells from entering into p53-mediated apoptosis and also enables resistance to chemotherapeutic drugs. bad (bcl-2-associated death promoter), bak (bcl-2 homologous antagonist/killer) and bax (bcl-2-associated X protein) play key roles in the inhibition of anti-apoptotic function of bcl-2 and bcl-XL [34,35]. These molecules form oligomeric pores in outer membrane of mitochondria, which subsequently releases cytochrome-c into the cytosol [36]. Cytochrome-c activates caspase-3 mediated apoptosis [37,38]. We have observed an increase in expression of bax, bad and bak, which confirmed the role of these genes in the downregulation of anti-apoptotic genes bcl-2 and bcl-XL in the present study. The role of c-myc in down-regulating bcl-XL was also evident with an increase in expression of c-myc and a decrease in expression of bcl-XL gene. Most of the recent reports indicated oxidative stress (reactive oxygen species, ROS) to be involved directly in DNA damage and/or inducing intrinsic (mitochondria-dependent) apoptosis pathway [33, 39-41]. The up and down-regulation of pro- and anti-apoptotic members of bcl-2 family of genes in the present study strongly correlate with previous findings.

Caspases (cysteine-aspartic acid proteases) are activated during apoptosis in many cells and are known to play a vital role in both initiation and execution of apoptosis. It was reported that caspase-3 is essential for cellular DNA fragmentation [42].We observed that caspase-3 gene expression was up-regulated in Ag NP treated cells, which suggested its role in Ag NP induced apoptosis. Therefore, based on the gene expression profiles as mentioned above, it is proposed that Ag NP treatment of both the BHK21 and HT29 cells leads to programmed cell death, i.e. apoptosis. A schematic representation of apoptotic pathway involved in the death of Ag NP treated cells is shown in **Schematic 3.2.** The NPs once attached to the cell membrane,

damages the integrity of the membrane and triggers activation of p53 protein. In turn p53, a known activator of pro-apoptotic genes, activates bax, bad and bak. These proteins are known to cause mitochondrial membrane leakage and release Cyt c, which in a cascade reaction activates caspase-3. Finally, caspase-3 cleaves nuclear membrane to induce DNA fragmentation. At the same time, up-regulation of C-myc, a known inducer of apoptosis, contributes further amplification of the apoptotic signals and down-regulation of anti-apoptotic genes, bcl-2 and bcl-XL corroborating manifestation of apoptosis and consequent cell blebbing.

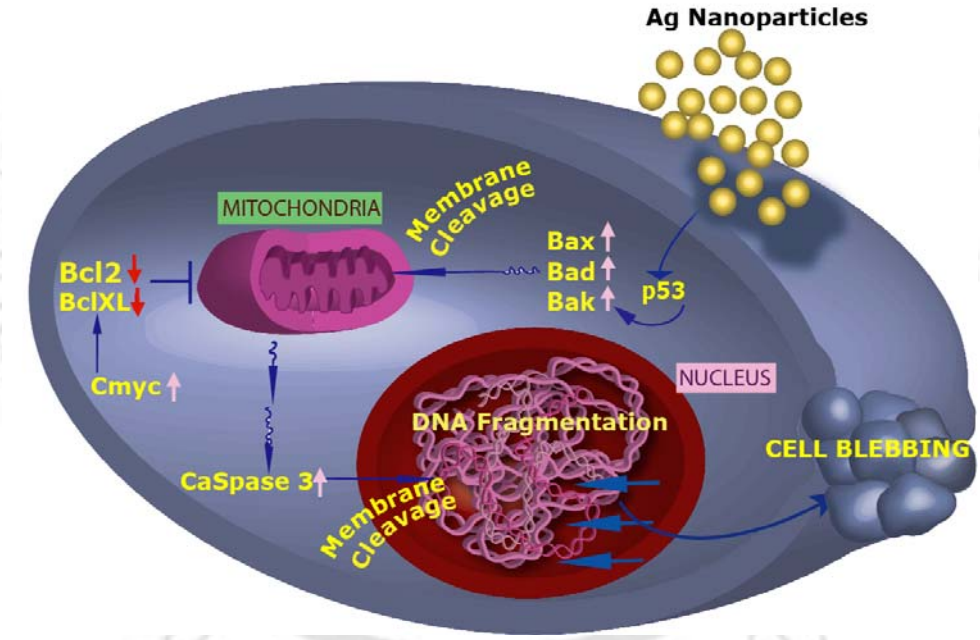

Schematic 2: Schematic representation of the Ag NP induced apoptotic pathway

We further evaluated the effect of Ag NPs on conventional gene therapy. The chemosensitization effect of Ag NPs on cells either treated with 5-FU alone or transduced with *E. coli* uracil phosphoribosyltransferase (UPRT) gene followed by 5-FU treatment was studied. In this context, cloned *E. coli* UPRT gene expressed in to

BHK21 and HT29 cells were used. Subsequently, we found that UPRT transduced cells were more sensitized towards 5-FU treatment as compared to non-transduced 5-FU treated cells, 5-FU alone or transduced with *E. coli* UPRT gene which was monitored by their reduced mitochondrial activity in MTT assay and AO/EB double staining *. The apoptosis pathway for both conditions was detected by DNA laddering pattern in agarose gel electrophoresis *.

Combined effect of Ag NPs on UPRT transduced cells and non-transduced cells, separately, after 5-FU treatment was evaluated. The release of lactate dehydrogenase (LDH) enzyme to the culture media was monitored during apoptosis induction phase at 6 h of treatment [43,44]. The results in **Figure. 3.9 (A)** showed only a slight increase in LDH leakage at 6 h samples due to combination therapy as compared to that of 5-FU and Ag NPs alone, which is indicative of the fact that abrupt cell membrane lysis did not occur to induce discernible necrosis in the combined therapy; rather metabolic alteration had induced apoptotic cell death and the membrane leakage was an effect of the apoptosis. The possible apoptosis pathway in the combination therapy was supported by cellular DNA fragmentation ELISA **Figure 3.9(B)**. **Figure 3.9(B)** depicts that higher number of cells undergo apoptosis when Ag NPs were used in combination with 5-FU as compared to Ag NPs or 5-FU used alone. The results shown in **Figure. 3.9(B)** confirmed that the BrdU DNA release, an index of apoptosis, greatly increased in combination treatment on UPRT transduced cells. Therefore, the effect of Ag NPs can be considered as synergistic to the conventional gene therapy and such treatment worked even in the presence of UPRT expression, which sensitized cells more efficiently towards apoptotic death.

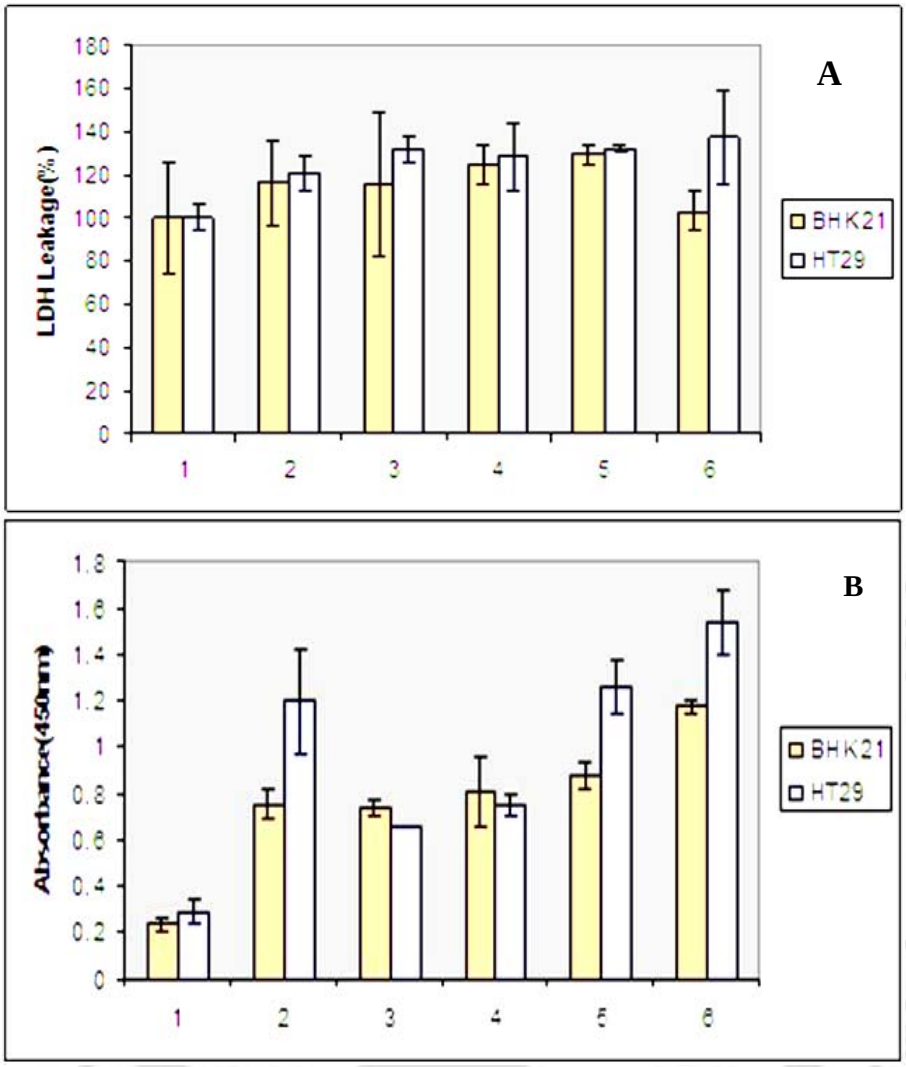

Figure 3.9: Quantitative representation of (**A)** LDH release from cells that were treated with different combinations of Ag NPs and drug 5FU for 6h and (**B)** synergistic apoptosis by cellular DNA fragmentation ELISA of BrdU labeled BHK21 and HT29 cells with a portion of the labeled cells transfected with UPRT vector. Nos. **1**: untreated controls, **2**: 11.0μgmL^{-1} of Ag NPs; **3**: 20mM 5-FU, **4**: 11.0μgmL^{-1} of Ag NPs with 20mM 5-FU; **5**: 20mM 5-FU on UPRT transduced cells; **6**: combine treatment of 11.0 μgmL^{-1} Ag NPs with 20mM 5-FU on UPRT transduced cells. The data are expressed as mean ± SD of three experiments.*

3.4: Conclusion

Apoptosis, a genetically controlled programmed cell death, has been the key criterion in the development of successful drug or gene therapy in anti-cancer treatments. On the other hand, induction of necrosis, a random event of cell lysis under extreme physiological conditions, is not favored owing to its unregulated toxic effects[45,46] In the search for newer drugs, the nanoscale particles and nanovehicles are increasingly being tested for their therapeutic efficacies on cancer cells[47]. Herein we have discovered that Ag NPs, known to be cytotoxic on live cells, induced apoptosis on cancer HT29 as well as non-cancer BHK21 cells. Our experimental observations also suggest that the effect of Ag NPs on UPRT expressing systems, in presence of drug 5FU, was synergistic in terms of enhanced apoptosis. Thus our results suggest that Ag NPs can be combined with traditional gene therapy for cancer treatment with enhanced performance. That the Ag NPs could be synthesized in the cell culture medium and remained stable for extended periods of time in the presence of cells signifies the importance of the present approach in studying the interaction of cells with metal NPs without having to resort to *ex situ* preparation and stabilization with another reagent. Morphological changes of treated cells, progression of floating dead cells from the surface and sprouted multiple small and white buds around the surface of the cells suggested apoptosis of the cells. The possible apoptotic pathway was further substantiated by a time dependent AO/EB dual staining of nuclei monitored by confocal microscopy. AO permeates the cells and makes the nuclei appear green, but EB, a known early apoptosis detection marker stains nuclei red only after cell membrane perforation[48]. Fragmented apoptotic nuclei stained green were observed, which progressively stained with EB (red) due to cell membrane perforation. Our

observations indicate that apoptosis began at 4 – 6 h past Ag NPs addition. The mitochondrial activity measurement of Ag NP treated cells also infers index of mitochondrial membrane damage during cell apoptosis. Further, fragmentation of BrdU- labeled cellular DNA was quantified by ELISA on[49,50]. Moreover, biochemical changes during apoptosis activate endonucleases, which cleave DNA at inter-nucleosomal linker sites to produce 180–200 bp mono- and oligo-nucleosomal fragments that gives a characteristic laddering pattern in agarose gel electrophoresis. Such results were observed in Ag NPs treated cells at 16h, which confirmed apoptosis as the primary mechanism of cell death.

It has been proposed that the treatment of BHK21 and HT29 cells by Ag NPs (at 11.0μg mL^{-1}) leads to apoptosis for both the cells. Surface morphology exhibited alteration of membrane structure, which further indicated that Ag NPs trigger extracellular cytotoxic stress on membrane. Such stress, up-regulates p53, which in turn acts on other apoptotic molecules and involves mitochondria to induce apoptosis. The results indicate that Ag NP induced apoptosis involves complex interplay of classical signaling molecules in p53 dependent pathway. Such, understanding of gene regulation in apoptotic process would primarily establish Ag NP as a potent drug for future therapeutic applications. Further, in order to use Ag NPs in targeted delivery for cancer cells appropriate delivery vehicles need to be developed.

The chemotherapeutic drug 5-FU is cytotoxic to a large numbers of cells, but its activity is quite low in many cancer cells. This problem is typically avoided by using UPRT transduction in the cells to convert 5-FU to more lethal 5-UMP which is known to have significant toxic effects. The present observations of induction of apoptosis in the presence of Ag NPs in addition to 5-FU, in the UPRT non-transduced

and transduced cells, makes the study more appealing. In all cases, slightly higher cytotoxicity was observed by LDH assay, where the stable cytosolic enzyme LDH release was measured in cell culture media upon membrane perforation. Cellular DNA fragmentation ELISA and the laddering experiment on the combined treatment indicated that even though cytotoxicity was enhanced, the affected cells still followed regulated apoptosis pathway. Any potential anti-cancer agent that induces apoptosis is likely to have high clinical efficacy compared to the majority of the reports, related to cytotoxic effect of NPs causing cell death due to necrosis. We were first to report the concentration and time dependent apoptosis in cancer cells by Ag NPs treatment. The concentration dependent induction of Ag NPs mediated apoptotic pathway has immense potential application in gene therapy especially when the cells and tumors are resistant to conventional gene and drug treatments but susceptible towards combined treatment with Ag NPs. Additionally, it is important to note that the concentration of Ag NPs used herein for induction of programmed cell death is much less than the IC50 values of conventional anticancer drugs [51,52]. That the high cytotoxicity of the combined effect of Ag NPs on conventional gene therapy also follows regulated pathway of cell death, could be associated with minimal side effects. Experimental results presented here indicate that the apoptosis induced by Ag NPs follows the same pathway as that by 5-FU and UPRT expressed cells in the presence of 5 FU. In other words, the apoptosis initiated by mitochondrial membrane damage by Ag NPs is similar to the mechanism induced by other drugs or gene therapy treatments. The present findings suggest that Ag NPs may assume significance in the development of a suitable anticancer drug and the approach described here may lead to novel nanomedicines with strong potential in therapeutic use for treatment of cancers in conjunction with conventional gene therapy.

References

1. Catalina Marambio-Jones, C.; Hoek, E. M. V. *J. Nanopart. Res.* 2010**,** *12*, pp1531-1551.
2. Borm, P. J.; Kreyling, W. J. *J. Nanosci. Nanotechnol*. **2004**, *4*, pp 521–531.
3. Magrez, A.; Kasas, S.; Salicio, V.; Pasquier, N.; Seo, J. W.; Celio, M.; Catsicas, S.; Schwaller, B.; Forro, L. *Nano Lett.***2006**, *6*, pp 1121-1125.
4. Baker, C., Pradhan, A., Pakstis, L., Pochan, D. J.& Shah, S. I. *J. Nanosci. Nanotechnol*. **2005**, *5*, pp 244-249.
5. Gogoi, S. K.; Gopinath, P.; Paul, A.; Ramesh, A.; Ghosh, S. S.; Chattopadhyay, A. *Langmuir* **2006**, *22*, pp 9322-9328.
6. Newmeyer, D. D.; Ferguson-Miller, S. *Cell*, **2003**, *112*, pp 481–490.
7. Thompson, C. B. *Science*, **1995**, *267*, 1456–1462.
8. Gopinath, P.; Ghosh, S. S. *Mol. Biotechnol.*, **2008**, *39*, 39–48.
9. Williams, D. R.; Ko, S.; Park, S.; Lee, M.; Shin, I. *Angew. Chem. Int. Ed.* **2008**, *47*, pp 7466–7469.
10. Leist, M.; Jaattela, M. *Nat. Rev. Mol. Cell Biol.* **2001**, *2*, pp 589-98.
11. Renehan, A. G.; Booth, C.; Potten, C. S. *BMJ* **2001**, *322*, pp 1536–1538.
12. Oguri, T.; Bessho, Y.; Achiwa, H.; Ozasa, H.; Maeno, K.; Maeda, H.; Sato, S.; Ueda, R. *Mol. Cancer Ther.* **2007**, *6*, pp 122-127.
13. Pratt, S.; Shepard, R. L.; Kandaswamy, R. A.; Johnston, P. A.; Perry, W.; Dantzig, A. H. *Mol. Cancer Ther.* **2005**, *4*, pp 855-863.
14. Seo, E.; Abei, M.; Wakayama, M.; Fukuda, K.; Ugai, H,; Murata, T.; Todoroki, T.; Matsuzaki, Y.; Tanaka, N.; Hamada, H.; Yokoyama, K. K.; *Cancer Res*. **2005**, *65*, 546-552.
15. Taomoto. J.; Yoshida, K.; Wada, Y.; Tanabe, K.; Konishi, K.; Tahara, H.; Fukushima, M. *Oncology* **2006**, *70* , 458-464.
16. Roy, I.; Ohulchanskyy, T.Y.; Bharali, D.J.; Pudavar, H.E.; Mistretta, R.A.; Kaur, N.; Prasad, P. N. *Proc. Natl. Acad. Sci. U.S.A.* **2005**, *102*, 279–284.
17. Salem, A. K.; Searson, P. C.; Leong, K. W.; *Nat. Mater*. **2003**, *2*, 668–671.
18. Sanpui, P.; Murugadoss, A.; Prasad, P.V.; Ghosh, S.S.; Chattopadhyay, A. *Int. J. Food Microbiol.* **2008**, *24*, 142–146.

19. Gopinath, P.; Gogoi, S. K.; Chattopadhyay, A.; Ghosh, S. S. *Nanotechnology* **2008**, doi:10.1088/0957-4484/19/7/075104.
20. Gopinath, P.; Ghosh, S. S.; *Mol. Cell Biochem.* **2009**, 324, pp 21–29.
21. Chen, D. H.; Chen, C. J. *J. Mater. Chem.*, **2002**, *12*, pp1557–1562.
22. Mandal, S.; Arumugam, S. K.; Pasricha, R.; Sastry, M. *Bull. Mater Sci.* **2005**, *28*, pp 503-510.
23. Fishel, M. L.; He, Y.; Smith, M. L.; Kelley, M. R. *Clin. Cancer Res*. **2007**,13, pp 260-267.
24. Dini, L. *Tissue and Cell.* **2005**, *37*, pp 379–384.
25. Okada, H.; Mak, T. W. *Nat Rev Cancer* **2004**, *4*, pp 592-603.
26. Cohen, E.; Ophir, I.; Shaul, Y. B. *Journal of Cell Science* **1999**, *112*, pp 2657-2666.
27. Ribble, D.; Goldstein, N. B.; Norris, D. A.; Shellman, Y. G. *BMC Biotechnology* **2005**, *5*, p 12.
28. Wolf, B. B.; Schuler, M.; Echeverri, F.; Green, D. R. *J. Biol. Chem*. **1999**, *274*, pp 30651-30656.
29. Grimellec, C. L.; Lesniewska, E.; Cachia, C. J. P.; Schreiber, J. P.; Fornel, F. D.; Goudonnet, J. P. *Biophys. J.* **1994**, *67*, pp 36–41.
30. Parpura, V.; Fernandez, J. M. *Biophys. J.* **1996**, *71*, pp 2356–2366.
31. Chao, D. T.; Korsmeyer, S. J. *Annu. Rev. Immunol.* **1998**, *16*, pp 395–419.
32. Wolter, K.G.; Hsu, Y.; Smith, C.L.; Nechushtan, A.; Xi, X.; Youle, R. J. J. *Cell Biol.* **1997**, *139*, pp 1281–1292.
33. Hsin, Y. H.; Chen, C. F.; Huang, S.; Shih, T. S.; Lai, P. S.; Chueh, P. J. *Toxicol. Lett.* **2008**, 179, pp 130–139.
34. Yang, E. H.; Zha, J.; Jockel, J.; Boise, L. B.; Thompson, C. B.; Korsmeyer, S. J.; *Cell* **1995**, *80*, 285–291.
35. Boise, L. H.; Gonzalez-Garcia, M.; Postema, C. E.; Ding, L.; Lindsten, T.; Turka, L. A.; Mao, X.; Nunez, G.; Thompson, C. B. *Cell* **1993**, *74*, 597–608.
36. Liu, X.; Kim, C. N.; Yang, J.; Jemmerson, R.; Wang, X. *Cell* **1996**, *86*, 147–157.
37. Yang, J.; Liu, X.; Bhalla, K.; Kim, C. N.; Ibrado, A. M.; Cai, J.; Peng, T. I.; Jones, D. P.; Wang, X. *Science* **1997**, *275*,1129–1132.

38. Kluck, R. M.; Wetzel-Bossy, E.; Green, D. R.; Newmeyer, D. D. *Science* **1997**, *275*,1132–1136.
39. Hussain, S. M.;. Hess, K. L; Gearhart, J. M.; Geiss, K. T.; Schlager, J. J. *Toxicol. In Vitro* **2005**, *19*, 975–983.
40. AshaRani, P. V.; Mun, G. L. K.; Hande, M. P.; Valiyaveettil, S. *ACS Nano* **2009**, *3*, 279–290.
41. Arora, S.; Jain, J.; Rajwade, J. M.; Paknikar, K. M. *Toxicol. Lett.* **2008**, *179*, 93–100.
42. Janicke, R. U.; Sprengart, M. L.; Wati, M. R.; Porter, A. G. *J. Biol. Chem.* **1998**, *273*, 9357–9360.
43. Kolber, M. A.; Quinones, R. R.; Gress, R. F.; Henkart, P. A. *J. Immunol Methods.* **1988**, *108*, 255-264.
44. Rhodes, J. D.; Monckton, D. G.; McAbney, J. P.; Prescott, A. R.; Duncan, G. *Hum. Mol. Genet*. **2006**, *15*, 3559-3568.
45. Kanduc, D.; Mittelman, A.; Serpico, R.; Sinigaglia. E.; Sinha, A. A.; Natale, C.; Santacroce, R.; Di Corcia, M. G.; Lucchese, A.; Dini, L.; Pani, P.; Santacroce, S.; Simone, S.; Bucci, R.; Farber, E. *International Journal of Oncology* **2002**, *21*, pp 165-170.
46. Fortunato, F.; Deng, X.; Gates, L. K.; McClain, C. J.; Bimmler, D.; Graf, R.; Whitcomb, D. C. *Am. J. Physiol. Gastrointest. Liver Physiol.* **2006**, *290*, pp 232–241.
47. Verma, S. K.; Mani, P.; Sharma, N. R.; Krishna, A.; Kumar, V. V.; Reddy, B. S.; Chaudhuri, A.; Roy, R. P.; Sarkar D. P. *J Biol Chem*. **2005**, *280*, pp 35399-35409.
48. Tsangaris, G. T.; Tzortzatou-Stathopoulou, F. *In Vivo* **1996**, *10*, pp 435-43.
49. Muir, D.; Varon, S.; Manthorpe, M. *Anal. Biochem*. **1990**, *185*, pp 377-82.
50. Nakamura, N.; Wada, Y. *Cell Death and Differentiation* **2000**,*7*, pp 477 – 484.
51. Kusunoki, N.; Yamazaki, R.; Kitasato, H.; Beppu, M.; Aoki, H.; Kawai, S. *BMC Pharmacology* **2004**, *4*, p 2.
52. Lu, D. Y.; Huang, M.; Xu, C. H.; Yang, W. Y.; Hu, C. X.; Lin, L. P.; Tong, L. J.; Li, M. H.; Lu, W.; Zhang, X. W.; Ding, J. *BMC Pharmacology* **2005**, *5*, p 11.

* *Prodrug Gene Therapy Vectors in Combination Therapies,* Ph D Thesis, Gopinath, P., Department of Biotechnology, Indian Institute of Technology Guwahati, 2008.

Chapter IV

Generation of AgAu Bimetallic Nanoparticle Patterns on a Templated Surface by Chemical Reaction

4.1: Introduction

There has been a growing interest in nanoparticle (NP) constituted patterned surfaces with micron and nanometer scale resolutions from the points of view of both scientific investigations and technological applications [1-10]. Advances in understanding of the surface reaction mechanisms [11] as well as in nanofabrication techniques have led to a considerable surge in attempts to control the structure, shape, and composition of surfaces at the nanoscale[12]. Ability to control the surface structure is crucial for their applications in biomedical implants,[13] increased efficiency of electrodes for sensors and actuators, [14,15] enhanced catalytic properties,[16] maximization of hydrophobicity and hydrophilicity [17-19] etc. On the front of optical properties, interesting outcomes of controlling the surface structure, especially those consisting of noble metals, constitute the possibility to affect the spectral properties of certain molecules/fluorophores positioned in its vicinity, thanks to the phenomenon of plasmonic coupling [20, 21]. One such technique is metal-enhanced fluorescence (MEF),[22, 23] where a remarkable increase of fluorophore emission intensity is observed when a fluorophore is placed at a certain distance from nanostructured metal particles and has applications ranging from biodiagnostics to imaging, sensing and photovoltaic cells[24,25]. Another application involves taking advantage of the surface enhanced raman spectroscopy (SERS) [26, 27].

As can be anticipated, growing interest in nanostructured surfaces has led to the development of various methods to generate such metallic surfaces. Some of these methods include photoinduced deposition[28, 29] physical vapour deposition,[30] electrochemical roughening of metal surfaces [31] chemical deposition of metals [30] nanosphere lithography [32], adsorption of metal colloids on substrates [33],

dealloying[34,35] and various lithographic techniques [2,36-39]. In spite of these developments, there is still the possibility of new methods to come up with simpler, cost effective and based on versatile synthetic approaches. In this respect, the precise control over the patterns and the composition are the prime criteria to be met with. A chemical approach when combined with physically imprinted structures to generate appropriately patterned surface may provide the ideal solution in this regard.

On the other hand, it is known that competition between reaction and diffusion in many cases lead to emergence of elaborate spatial and temporal structures, which have been studied for a long period for their aesthetic appeal and the scientific challenges they pose [40, 41]. In their seminal review [40], Bartosz A. Grzybowski et. al. have very nicely documented various processes generating spatio-temporal patterns and structures created in natural and artificial reaction diffusion processes. Well known examples of pattern formation found in nature are finger prints, skin patterns in animals like zebra, tiger etc., cave stalactite, rock patterns etc. On the other hand, among the artificial chemical systems the pattern formation is observed in Turing patterns, Belusov-Zhabotinsky reaction, microstructured foils, discharge filaments etc. Grzybowski et. al. have also demonstrated the possibility of these reaction diffusion systems to be used to fabricate micro and nanostructured surfaces [40,42].

Noble metal NPs are of special importance for their interesting optical [12, 43-45] and chemical properties [46, 47]. Bimetallic NPs, consisting of two different metal elements, are of greater interest than monometallic ones, from both scientific and technological views [48-56], for the improvement of the catalytic properties[49-51] as well as optical properties [56]. This is because bimetallization can improve catalytic properties of the original single-metal catalysts and create a new property, which may not be achieved by monometallic catalysts[49-51]. On the other hand bimetallization helps in tuning the

plasmon resonance [55, 56] of the NPs by variation of composition without the change in particle size [48, 54]. Galvanic replacement reaction is one of the common approaches to synthesize bimetallic NPs [54, 57, 58] where NPs of the metal with lower reduction potential are synthesized first and then reacted with a metal ion with higher reduction potential for the spontaneous replacement of the former by the later to occur. Interestingly, in a recent report, Pier Paolo Pompa and coworkers have combined photolithography with galvanic replacement reaction to obtain micro and nanostructured metal substrates for plasmonic application [35].

We have tried to use a combination of conventional 'top down' and 'bottom up' approach for NP synthesis [59-61], in order to generate a NP patterned surface where reaction diffusion process also governs the pattern formation. Based on that herein we report the formation of patterned arrays of Ag and Au composite particles on a polymer film. The patterned particle arrays were the results of galvanic replacement reaction of $HAuCl_4$ with metallic Ag present in the foils of commercially available compact discs (CDs) and digital versatile discs (DVDs). Initially, arrays of crystals of AgCl, Ag and Au were formed on the surfaces of the substrate, which consisted of lacquer supporting the Ag film. The dimension of the particles varied from tens of nanometers to several microns. The AgCl so formed could be removed upon treatment with saturated aqueous solution of NaCl or dilute aqueous ammonia, leaving arrays of particles consisting of Ag and Au only. Interestingly, the pattern of the so-formed particles followed the lines of the CD or DVD which were present in the original foil. Further, in the arrays of particles formed on CD, cross patterns could be observed. The cross patterns consisted of particles which seemed to have been formed in perpendicular linear arrays, ones along the lines of the CD, while the others

perpendicular to them. These patterns indicated the role of reaction diffusion waves in the formation of patterns. On the other hand, such cross patterns were elusive in the case of DVDs while at times their formation could be observed. It was observed that the presence of the dye covering the metallic film was necessary for the formation of the patterns, without which a few random particles were deposited on the substrate surface. Finally, there was a distinct difference in patterns observed in the written (burned with some data) part of a CD from the unwritten (without burning). This may make it possible for arbitrary pattern generation by imprinting (burning) patterns on a CD followed by chemical reactions. Compared to the currently available lithographic techniques [2, 36-39], the method reported herein may be useful for mass production of metal NP patterned surfaces as it takes advantage of chemical synthetic processes, which are useful for large scale production of materials.

4.2: Experimental section

4.2.1: Materials and Substrates: 17% Chloroauric acid was purchased from Sigma-Aldrich (Germany). Compact discs (CDs) and digital versatile disks (DVDs) were purchased from the local market. NaCl and NH_3 were procured from Merck India Ltd. Deionised water from Milli-Q water purification system is used for making all the solutions and washing purposes.

4.2.2: Structure of a CD and a DVD and getting the reflecting silver layer exposed: The basic structure of a commercially available CD is shown in the ***Schematic 4.1***[62-64]. It consists of different layers, namely polycarbonate, photoactive dye, reflective silver, protective layer, and the CD label. It is the polycarbonate layer

that gives the hard physical support to a CD. It is possible to remove the rest of the layers

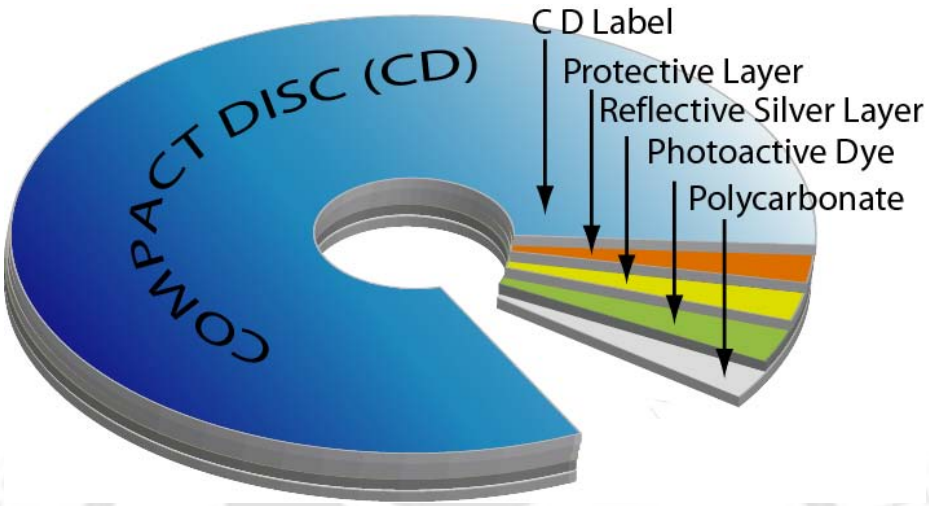

Schematic 4.1: Cartoon of layered structure of a commercially available CD-R

from the polycarbonate layer in such a way that the silver layer is exposed with the photoactive dye covering it. We have removed the reflective layer from a CD by putting cellotape (adhesive tape) on the non reflective side and pulling it up. This separates the polycarbonate base of the CD from the reflective layer leaving the photoactive dye on both polycarbonate and the reflective layer as shown in the **Schematic 4.2**. The part which gets stuck to the cellotape having the reflective layer of the CD with a coating of the photoactive dye is now exposed. This exposed surface stuck on the cellotape consists of metallic silver, which we have characterised by energy dispersive X-ray (EDX) spectroscopy and X-ray diffractometry. The literature reports also indicate the presence of silver layer in the commercial CDs [63, 64]. It is worth mentioning here that some other metals with high reflectivity like aluminium, gold or some alloys are also used. But the CDs we have used have a silver reflective

layer, which is the most common metal used. We will call the removed film as CD Ag foil.

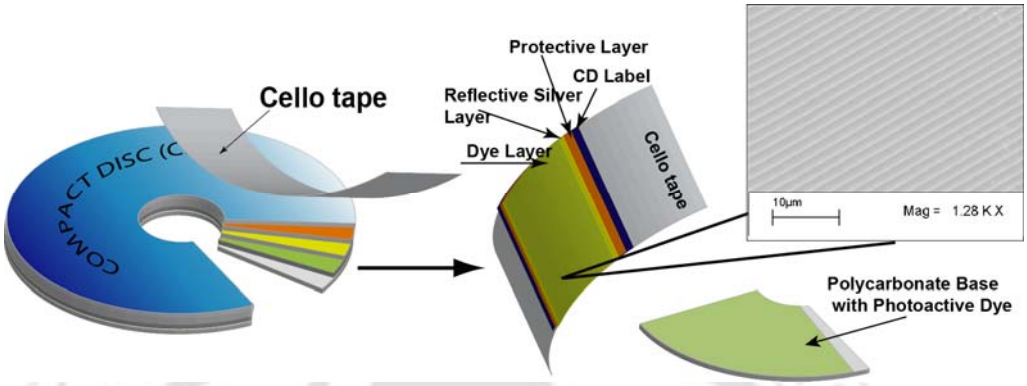

Schematic 4.2 Cartoon of removal procedure of the silver layer from the polycarbonate base of a commercially available CD-R

DVDs also have a similar physical structure as the CDs except that, in DVDs the protective layer is also some sort of hard plastic and the silver layer can be easily exposed by simply cutting the DVD with a scissor and then peeling off the polycarbonate layer. All the DVDs we have used have a silver reflective layer.

4.2.3: Initial galvanic replacement reaction leading to formation of silver chloride (AgCl) patterned surfaces : Approximately 1.55 cm x 2.6 cm cut pieces of Ag foils from CDs and DVDs were reacted with different concentrations of $HAuCl_4$ solutions given in **Table 4.1** to observe the patterns formed on the silver foils. Observations were made at different time points, concentrations and temperatures. The same sizes of the silver foils were used to keep the amount of silver reacting constant. Except for the time dependent experiments all the reactions are carried out for 5 hours to generate the desired patterns.

Table 4.1. Concentrations of $HAuCl_4$ used for galvanic replacement reaction with Ag.

Sl. No.	Amount of Ag (mol) per CD piece ($X10^{-6}$)	Concentration of $HAuCl_4$ (M)
1	2.8469	$3.46x10^{-6}$
2	2.8469	$8.65x10^{-6}$
3	2.8469	$1.73x10^{-5}$
4	2.8469	$3.45x10^{-5}$
5	2.8469	$8.60x10^{-5}$
6	2.8469	$1.28x10^{-4}$
7	2.8469	$1.71x10^{-4}$
8	2.8469	$2.14x10^{-4}$
9	2.8469	$2.56x10^{-4}$
10	2.8469	$2.98x10^{-4}$
11	2.8469	$3.39x10^{-4}$
12	2.8469	$4.22x10^{-4}$

4.2.4: Generation of AgAu bimetallic nanoparticle patterns: After the patterns were generated on the surface we have treated some patterned samples with a saturated solution of NaCl [65] and others with dilute aqueous NH_3 solution. This is to remove the AgCl (if formed) on the surface in the process. It is well known that in both the solutions AgCl is soluble by formation of complex species such as $[AgCl_2]^-$ and $[Ag(NH_3)_2]^+$ respectively with saturated NaCl and dilute aqueous NH_3 solutions. [66, 67] It was observed that after treatment with NaCl or aqueous NH_3 the patterns on the CD were retained with higher percentage of Au than Ag. Also, the AgCl if present on the surface could be reduced to Ag electrochemically. In the electrochemical reduction process the film was used as the cathode and a silver foil from a CD (or DVD) was used as the anode placed 1cm apart and ~15V potential applied till the gray colour of the AgCl on patterns turned yellow.

4.2.5: Scanning Electron Microscopy: A Leo-VP 1430 scanning electron microscope (SEM) equipped with Oxford-INCA energy dispersive X-ray (EDX) analyzer was used to characterize all the samples. Samples were analysed with 20 kV electron beam from a tungsten filament gun. Approximately 5.0 mm x 5.0 mm pieces from different samples were taken for analysis. All the samples were coated with a thin layer of gold in a sputtercoater to make the sample conducting in order to avoid charging during imaging.

4.2.6: X-Ray Diffraction: A Bruker D8 Advanced powder X-ray diffraction spectrometer with copper anode and Kα radiation was used to characterize the samples. Approximately 3.0 cm x 2.5 cm samples were analysed here.

4.2.7: UV-Visible Spectroscopy: For UV-Visible studies of the samples a Perkin Elmer Lambda 25 instrument was used in the solid state sample analysis mode. Samples as prepared were fixed onto the diffuse reflectance sample holders with double sided cellotape and the spectra were then recorded.

4.3: Results and Discussion

We have developed an easy and economic method to generate NPs bound to a flexible surface. Since the standard reduction potential of $AuCl_4^-$ /Au (1.0 V versus standard hydrogen electrode, or SHE)[68] is higher than that of the Ag^+/Ag (0.80 V versus SHE)[68], the Ag from the CDs are easily oxidized to Ag^+ by aqueous $HAuCl_4$ solution according to the following galvanic replacement reaction [54,69].

$$3Ag(s) + AuCl_4^-(aq) \longrightarrow 3AgCl(s) + Au(s) + Cl^-(aq)$$

Contrary to the common practice of immobilizing presynthesized NPs onto a surface, our method is of direct synthesis of bimetallic NPs forming nanostructures on to a flexible surface, which is a combination of top down and bottom up approaches for NP synthesis, along with their organization in two-dimensional surface. For this we have taken shiny silver layer of a commercially available CD as templates and one of the precursors, reacting with $HAuCl_4$ to give patterned surface of AgCl microcrystals. Along with AgCl, also formed were Au NPs by reduction of $AuCl_4^-$ and Ag NPs by the partial removal of Ag by oxidation to AgCl. We have used different concentrations of $HAuCl_4$ (**Table 4.1**) to react with Ag foils of the same size i.e. 1.55 cm X 2.6 cm (4.03 cm^2), so that the amount of silver (~0.3071 mg) reacting is constant.

SEM images and EDX spectra are shown in **Figure 4.1**. **Figure 4.1(A)** shows the SEM image of a CD silver foil whereas **Figure 4.1(B)** is that of a foil from DVD. The spiral tracks in CDs and DVDs appear as parallel troughs and crests. The width of the troughs and crests are approximately 1μm and 400 nm for CDs and DVDs respectively as seen in **Figure 4.1(A)** and **Figure 4.1(B)**. EDX spectra of the respective CD and DVD samples are shown in **Figure 4.1(C)** and **Figure 4.1(D)**. The EDX spectra confirm the presence of silver in the films for both the samples. The peaks due to carbon and oxygen are from cello tape and the protective layer.

At a very low concentration ($3.45x10^{-6}$M) of $HAuCl_4$ we have observed AgCl crystal (white particles) formation at the hills of the CD tracks (**Figure 4.2(A)**). At this stage the $HAuCl_4$ added was not sufficient to react with all the silver in the foil, hence the un-reacted silver is observed at the valley regions of the CD, where there are no crystals, as clear from the SEM image (**Figure 4.2(A)**). In **Figure 4.2(A)** ~200 nm

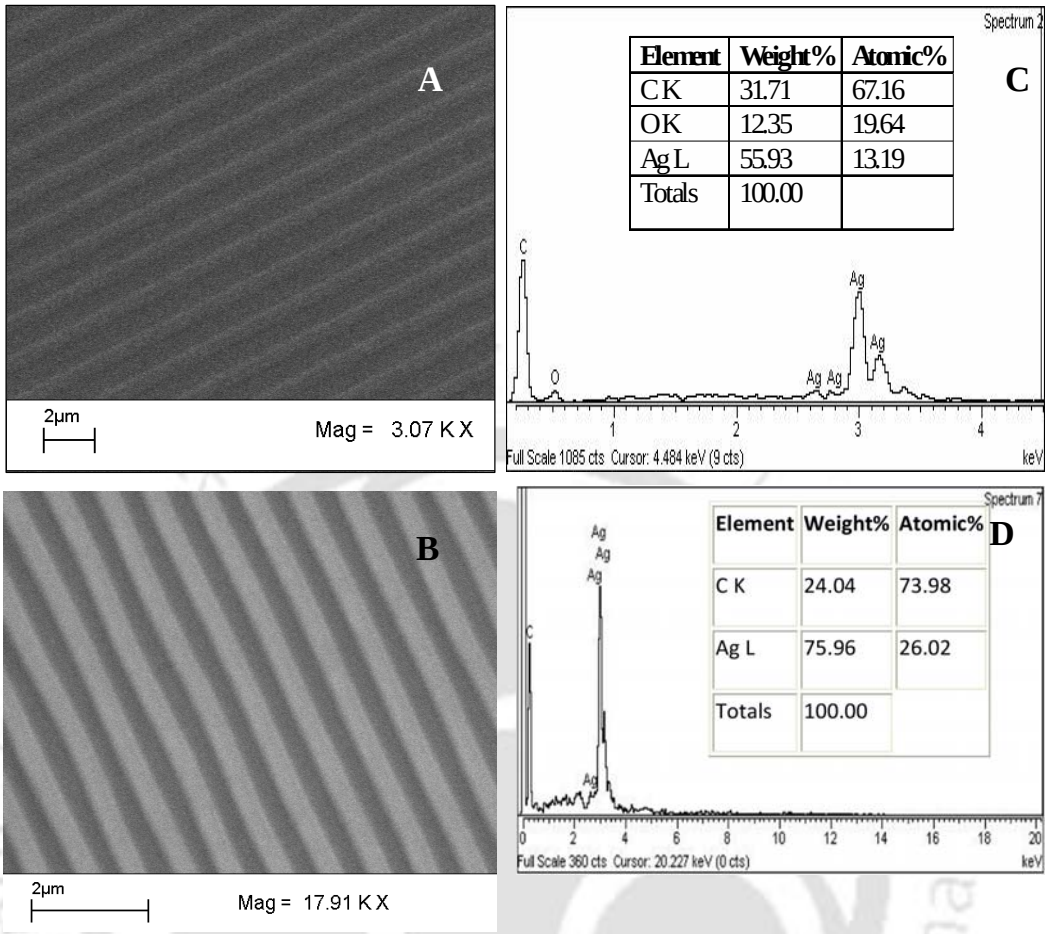

Figure 4.1: SEM image of **(A)** compact disc (CD), **(B)** digital versatile disc (DVD) and EDX spectra of **(C)** CD and (**D)** DVD.

diameter particles present along the CD track hills are possibly AgCl crystals as indicated by the presence of Cl and Ag in the EDX spectrum (**Figure 4.2(B)**). On the other hand EDX spectrum recorded in the parts of the CD where there were no crystals indicated the presence of Ag only (**Figure 4.2(D)**) and the absence of Cl possibly indicated the absence of any AgCl crystal. Interestingly, the crystals were aligned on the CD track hills in the forms of parallel arrays and the arrays were separated by a distance of 1.5µm indicating that the arrays were formed along the CD tracks.

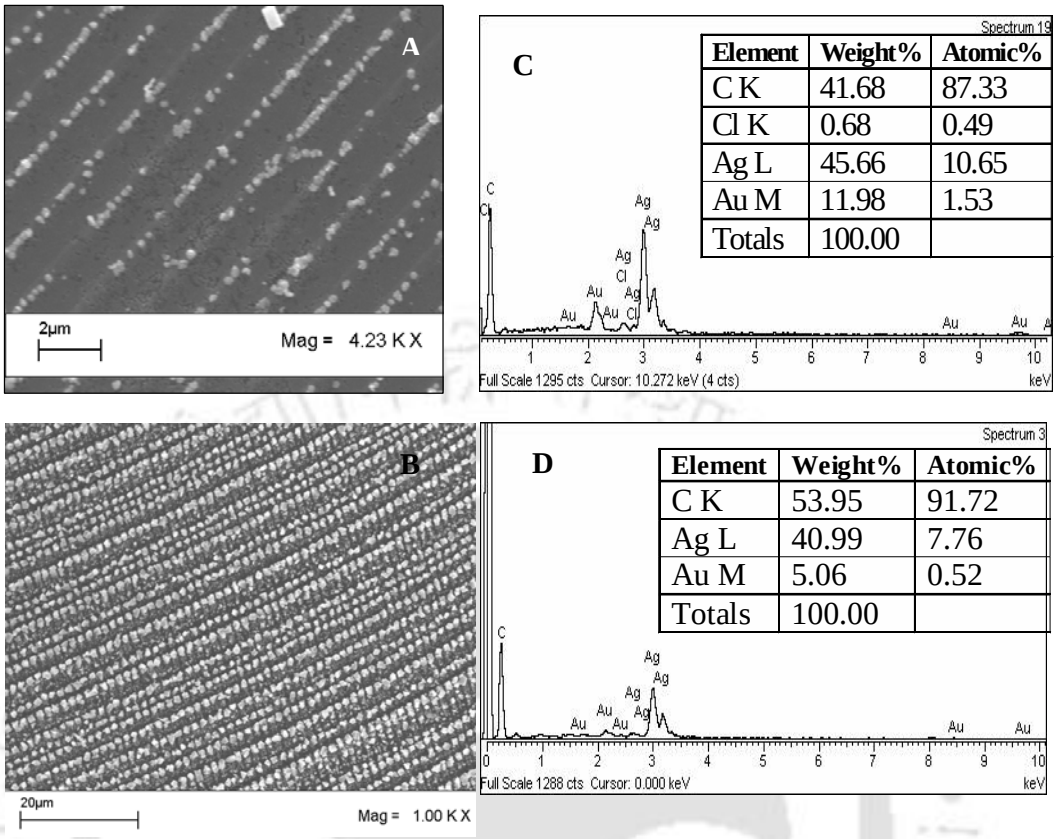

Figure 4.2: SEM image patterns of AgCl crystal generated by reacting **(A)** 3.45×10^{-6} M and **(B)** 8.60×10^{-5} M $HAuCl_4$ for 5 h with CD Ag foil and **(C)** & **(D)** are the EXD spectra of the white spots on the CD tracks and the dark regions in between respectively for image **(A)**.

When the concentration of $HAuCl_4$ was increased to 8.60×10^{-5} M, more dense distribution of particles formed on the surface. A low magnification view of a pattern generated by a higher concentration (8.60×10^{-5} M) of $HAuCl_4$ is shown in **Figure 4.2(C),** where the long range pattern of the AgCl microcrystals formed is observed. Interestingly, there is a two way pattern of arrays of particles, one along the CD tracks and the other making an approximate 70^0 angle to the CD tracks creating the appearance of a cross pattern. At low concentrations of $HAuCl_4$, the region between the AgCl microcrystals contain metallic Ag without any chloride as shown by the EDX spectra shown in **Figure: 4.2(D)** while at higher concentrations of $HAuCl_4$ we

observed higher percentage of carbon in the EDX spectra of in between regions indicating more consumption of Ag in the galvanic replacement reaction exposing the background lacquer layer.

The variation of pattern as a function of concentration of $HAuCl_4$ reacting with the same amount of Ag in the foil (as determined by the size used) is shown in **Figure 4.3(A)-(K)**. At the lowest concentration of $HAuCl_4$ (3.46 x 10^{-6} M) used, the AgCl crystals formed are observed to be aligned on the CD tracks as seen in **Figure 4.3 (A)** and the crystals are of approximate size 200 nm. Then at a little higher concentration of $HAuCl_4$ (8.65 x 10^{-6} M) assembling processes of the crystals is

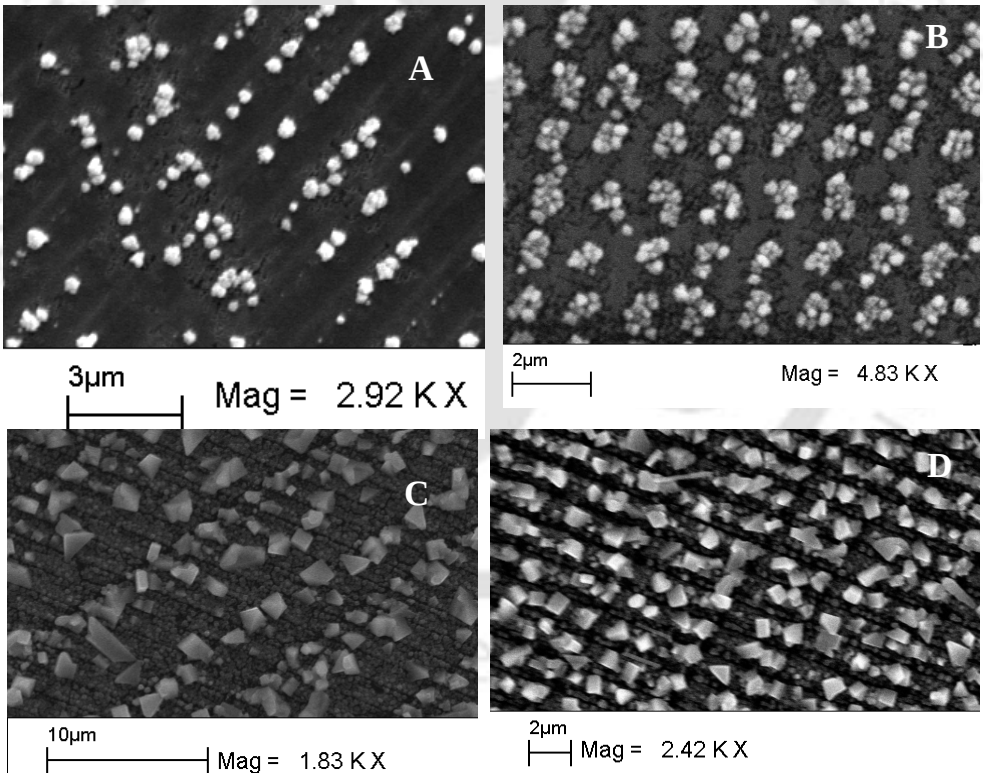

Figure 4.3: (A)-(K) SEM images of patterns obtained by reacting CD Ag foil at different concentrations of $HAuCl_4$. (**A)** 3.46x10^{-6}M, (**B)** 8.65x10^{-6}M, (**C)** 1.73x10^{-5}M , (**D)** 3.45x10^{-5}M for 5 h.

Continued to next page..

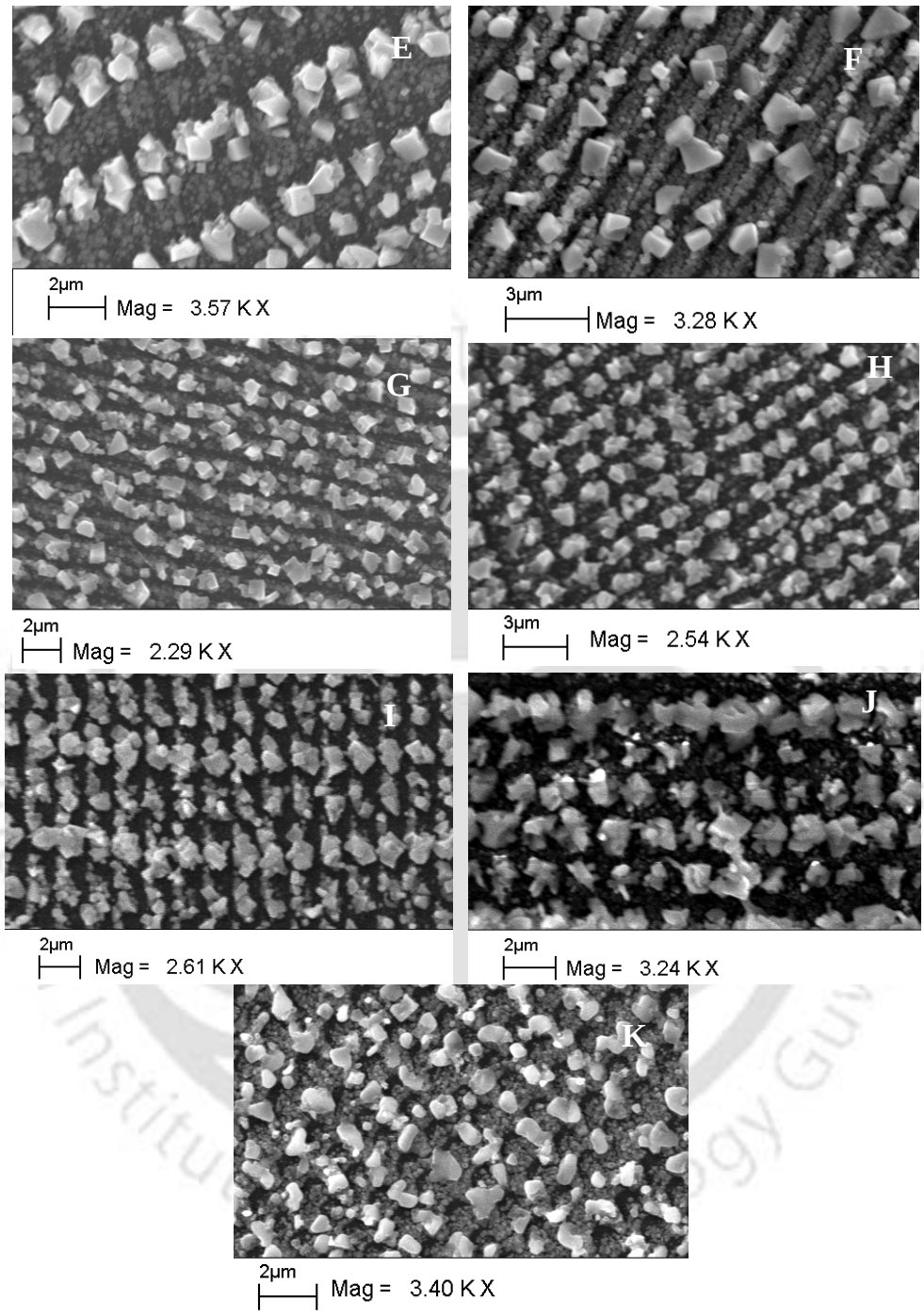

Figure 4.3: (A)-(K) SEM images of pattern obtained by reacting CD Ag foil at different concentrations of $HAuCl_4$. **(E)** $8.60x10^{-5}$M, **(F)** $1.28x10^{-4}$M, **(G)** $1.71x10^{-4}$M, **(H)** $2.14x10^{-4}$M, **(I)** $2.56x10^{-4}$M, **(J)** $2.98x10^{-4}$ M, **(K)** $3.39x10^{-4}$M for 5 h.

.

observed i.e. clusters of crystal were formed as could be seen in **Figure 4.3(B)**. Here it is observed that 6-7 of small (~200nm) crystals are grouped together and they follow a long range two dimensional (2D) pattern along and across the CD tracks. As the concentration of $HAuCl_4$ was increased further, we observed a blanket deposition of smaller crystals maintaining the pattern of the CD tracks and also some larger (~1.0 μm) crystals appeared on top of the smaller crystals. These larger crystals followed a wave-like pattern for certain concentrations of $HAuCl_4$, especially between 1.71×10^{-4} M to 2.98×10^{-4} M as could be viewed in **Figures 4.3 (G) - 4.3(J)**. This wave-like pattern led to the formation of a cross pattern of (~1μm) AgCl microcrystals, one along the CD tracks and the other across it, separately shown in **Figure 4.4**. Although it is not that the cross patterns were not formed beyond this concentration range of $HAuCl_4$, certain degree of cross patterning was observed even at 8.60×10^{-5} M $HAuCl_4$ as shown in **Figure 4.3(E).** However, it is worth mentioning here that the cross patterns were not always observed at concentrations beyond this range. We must acknowledge the fact that the complete reaction dynamics involved in the process of pattern generation is a complex one for multiple factors like distribution of the photoactive dye, concentration of the Cl^- ions (from the $HAuCl_4$ solution), temperature, local concentrations of the reactants and the mobility of the ionic species like Ag^+, Cl^- etc. may play important roles. It may be mentioned here that the photoactive dye is some kind of cyanine or pthalocyanine dye [63,64]. The presence of the dye is indeed essential for the generation of the patterns, not only those formed along the CD tracks but also for the cross patterns.

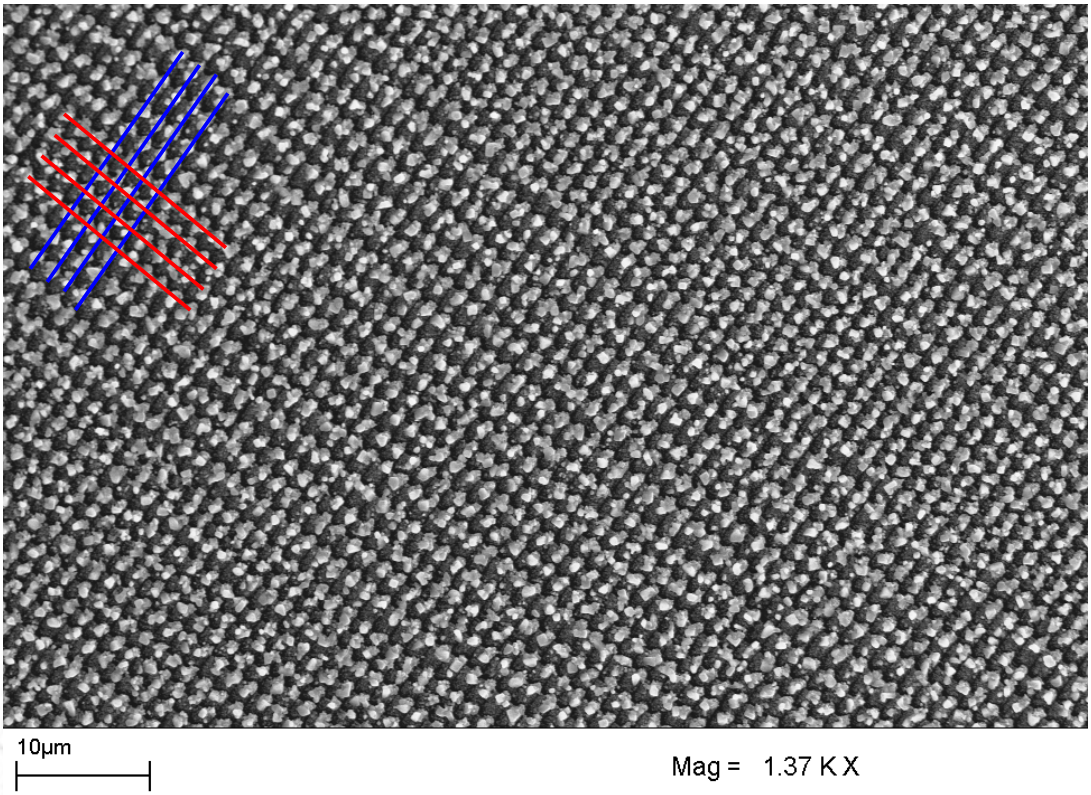

Figure 4.4: Representative SEM image of AgCl microcystals formed by reaction of Ag layer and $2.98x10^{-4}$ M $HAuCl_4$ for 5 h showing the cross pattern. Blue lines indicate the direction of the CD tracks and the red lines indicate the direction of a part of the wave.

A set of control experiments with the photoactive dye removed from the silver foil by washing with ethanol was carried out to confirm this. We have treated the photoactive dye removed silver foils with the entire concentration range of $HAuCl_4$ (from 3.46 x 10^{-6} M to 3.39 x 10^{-4}M) under study. **Figure 4.5 (A) and 4.5(B)** are the representative SEM images for two samples generated by 2.56 x 10^{-4} M and 2.98 x 10^{-4} M $HAuCl_4$ (within the range for cross pattern generation) reaction on Ag layer respectively, showing the absence of any clear long range pattern of microcrystals.

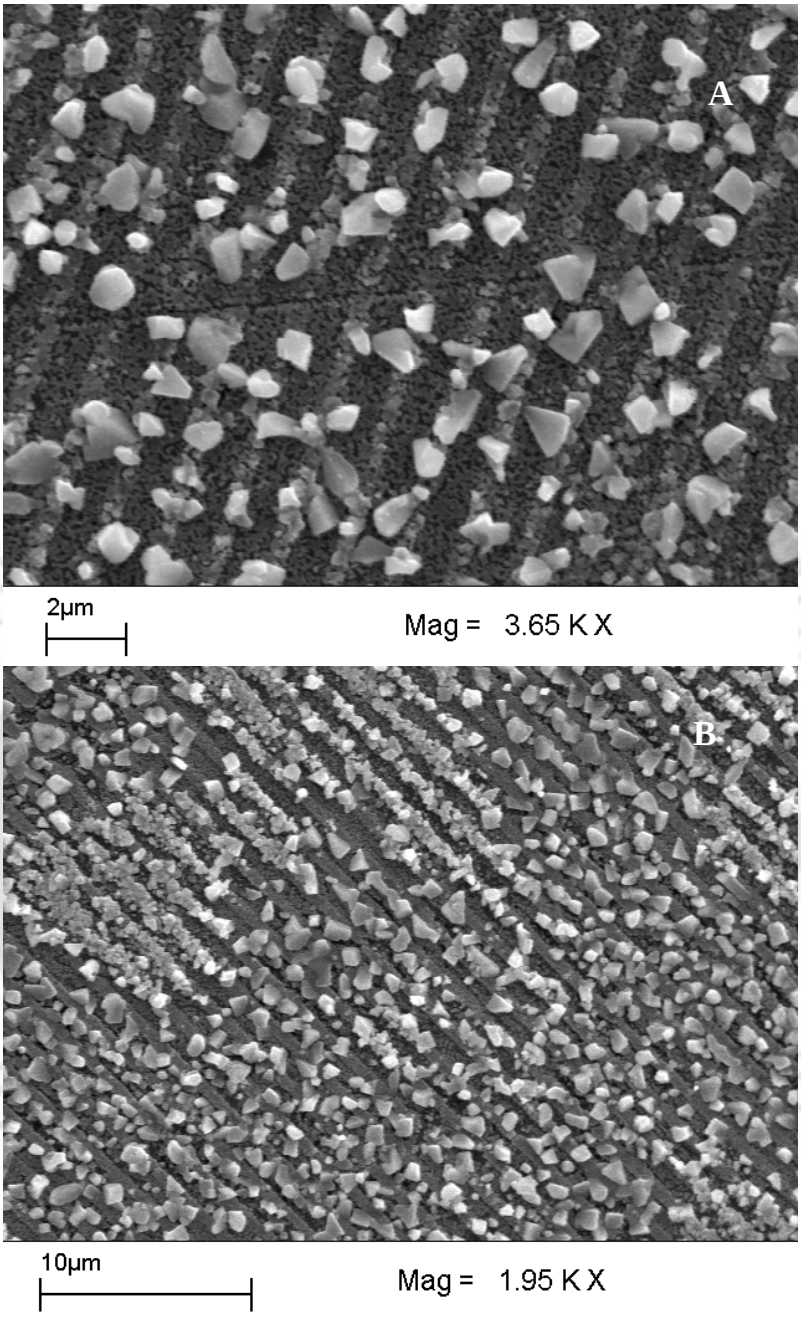

Figure 4.5: Representative SEM image of microcystals formed by reaction of Ag layer and **(A)** $2.56x10^{-4}$M and **(B)** $2.98x10^{-4}$M $HAuCl_4$ for 5 h, after removing the photoactive dye layer.

In order to follow the growth process of the patterns we have studied the SEM images of the silver foil from CD reacting with $HAuCl_4$ ($2.98x10^{-4}$M, within the range for cross pattern generation) at different time points starting from 5 s after dipping the

silver foil into $HAuCl_4$ for a maximum period of 8 h. Initially at 5 s, AgCl crystals of approximate size 100 nm and below were formed. The pattern appeared like a series of comets separated by a distance of 1µm from each other as shown in **Figure 4.6(A)**.

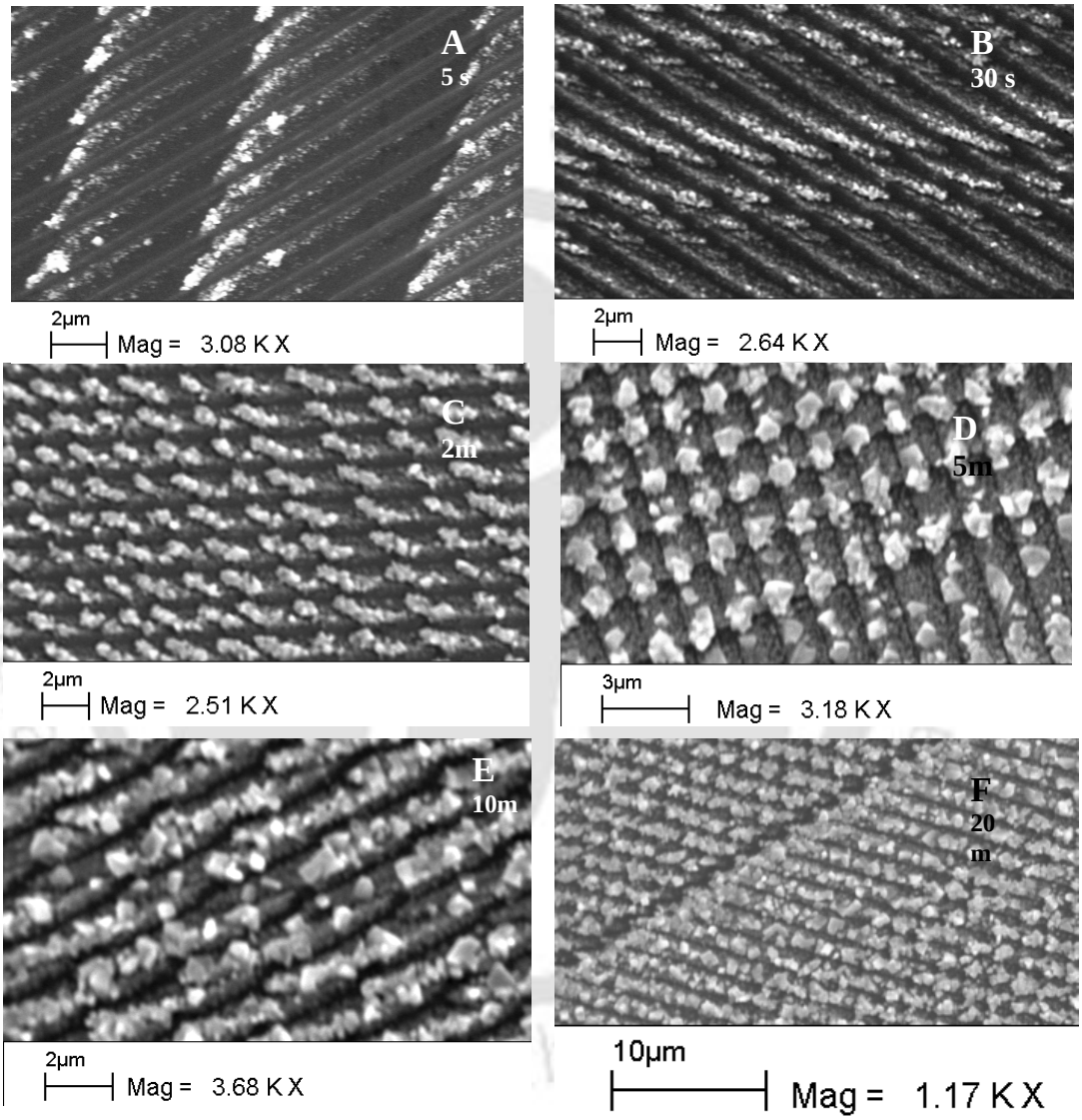

Figure 4.6: (A)-(F) SEM images of AgCl pattern obtained by etching CD silver foil at $2.98X10^{-4}$M of $HAuCl_4$ at different time points. **(A)** 5s, **(B)** 30 s, **(C)** 2 min, **(D)** 5 min, **(E)** 10 min, **(F)** 20 min. Continued to the next page.

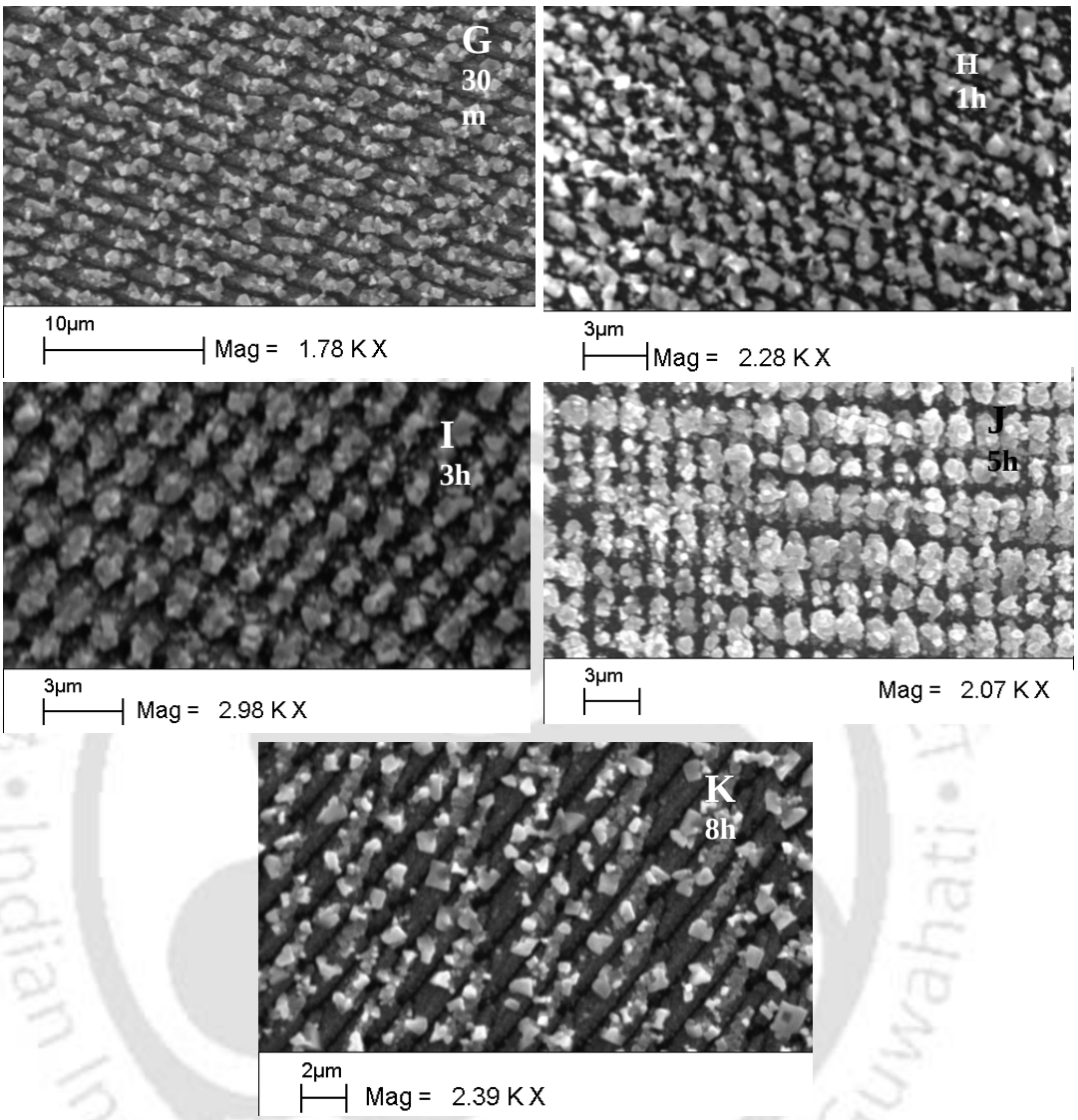

Figure 4.6: (G)-(K) SEM images of AgCl pattern obtained by etching CD silver foil at 2.98X10^{-4}M of $HAuCl_4$ at different time points. **(G)** 30min, **(H)** 1 h, **(I)** 3 h, **(J)** 5 h and **(K)** 8 h.

The same pattern persisted till 5 min but with more crystals being formed as shown in **Figures 4.6(B)** and **4.6(C)**. Beyond this time point the comet like pattern was superseded by appearance of a new pattern formed by little larger (~1µm) AgCl crystals separated from each other by uniform distances (1.5 µm). This new pattern formed by the larger crystals looks like arrays of square-like blocks as seen in **Figures**

4.6(D) – 4.6(J). At 8 h i.e. beyond the time for generation and development of cross patterns, the larger 1μm crystals were somewhat broken into smaller crystals and little of the cross pattern was retained. Based on our observations of the time dependent experiments, with 2.98 x 10^{-4} M of $HAuCl_4$, we propose that the reaction proceeds at a considerable rate at 5s, the initial pattern (**Figure 4.6(A))** is formed by possible deposition of AgCl formed from Ag^+ ions being oxidized from silver foil and Cl^- from $HAuCl_4$ solution. The formation of AgCl crystals was also confirmed by XRD studies as discussed later in this chapter. We believe that as the AgCl crystals are formed there is a process of dissolution and recrystallization which occur simultaneously (because of high Cl^- concentration) [65,67]. During recrystallization process the initially formed small AgCl crystals act as seeds for relatively larger AgCl crystals to generate a new pattern (**Figure 4.6(D) – 4.6(J))**. It is worth mentioning here that the cross patterns generated here are results of a wave of AgCl crystal deposition perpendicular (although at places at angles different from 90^0) to the CD tracks. For the waves to be generated the photoactive dye on the CD (used for the writing purpose) is important, as we did not observe any pattern generated for samples where the dye was removed by washing it with ethanol. The samples without the dye can be considered as the simple silver films with corrugation. The importance of the dye was also tested by carrying out the reaction with $HAuCl_4$ using CD foils where a part of it was 'written' using an ordinary data file. The patterns of the crystals formed in the written and unwritten part of the CD were distinctly different from each other, which will be discussed little later in this chapter.

The patterns thus generated on the CDs can be converted to either AgAu bimetallic NPs with higher percentage of silver or AgAu bimetallic NPs with higher percentage

of Au depending upon the treatment of the AgCl structures following the formation of the patterns. When the patterns, formed from the CD foil, was treated with a saturated solution of NaCl, the AgCl was washed off and there remained the structures

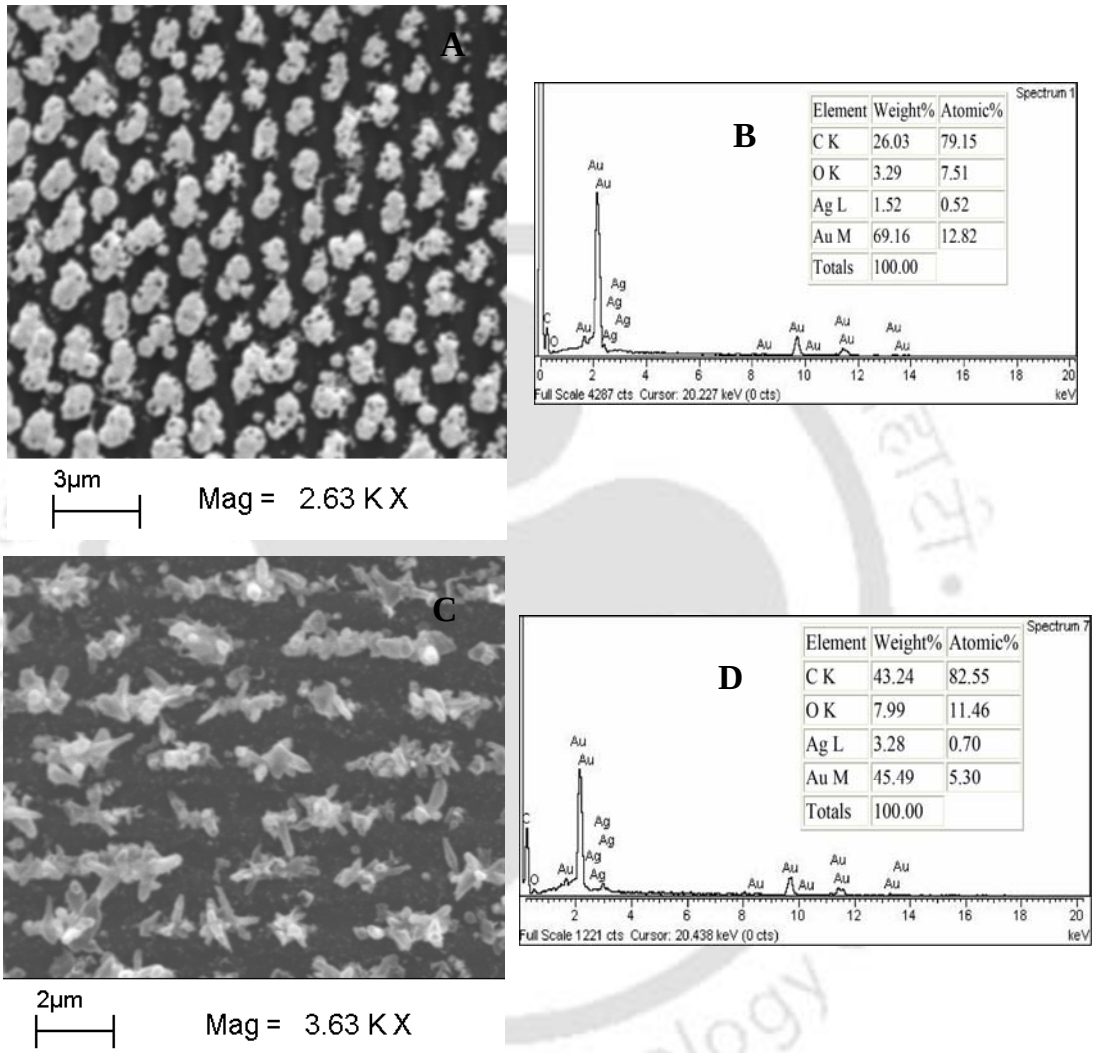

Figure 4.7: **(A)** SEM image of AgCl patterns after treatment with saturated solution of NaCl **(B)** spot EDX on the bright particles in **(A)**, **(C)** SEM image of AgCl patterns after dilute aqueous NH_3 solution, **(D)** spot EDX on the bright particles in **(C)**.

containing only AgAu bimetallic NPs with a higher percentage of Au (69.16% weight) compared to Ag(1.52% weight), as seen from the EDX spectra in **Figure**

4.7(A) and **Figure 4.7(B).** The absence of any Cl indicates the bimetallic nature of the patterns. Similar results were also observed for the samples after being washed with dilute NH_3 solution in place of saturated NaCl solution as shown in **Figure 4.7(C)** and **Figure 4.7(D)**. In the aqueous NH_3 treated samples also the pattern was retained (**Figure 4.7(C))** and AgCl was completely removed as EDX spectrum did not show any presence of Cl (**Figure 4.7(D)**); while there was Ag and Au present in considerable amount i.e. Ag (3.28% weight) and Au (45.48% weight).

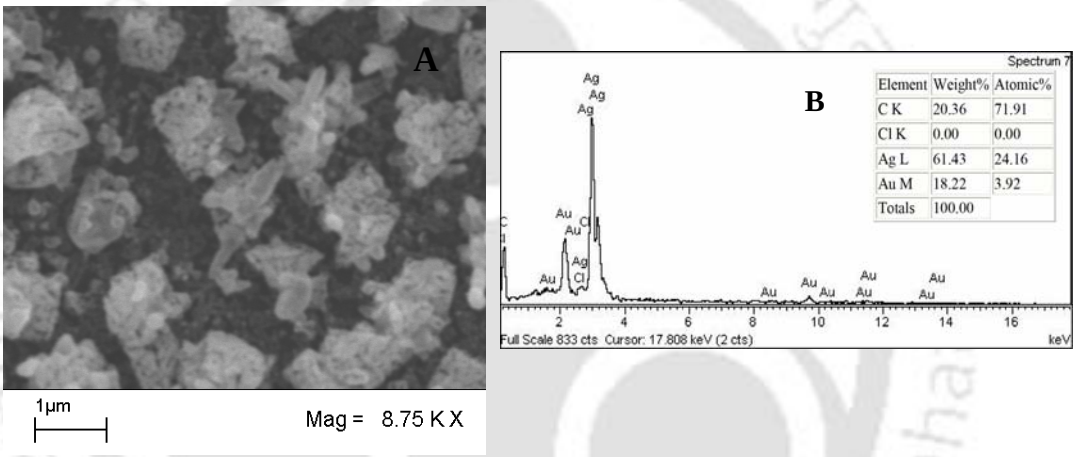

Figure 4.8: (A) SEM image of an electrochemically reduced AgAu NP pattern **(B)** Spot EDX taken on one of the bright particles.

On the other hand, the AgCl bound to the surface can be converted to Ag NP aggregates by reducing it with either ascorbic acid or via electrochemical reduction. The electrochemical reduction resulted into conversion of AgAu bimetallic (Ag 61.43% by weight and Au 18.22% by weight) NP aggregates (**Figure 4.8 (A) and (B)**) with possibly Ag NPs exposed on the surface following generation by reduction of AgCl.

It is difficult to comment on the composition of the AgAu bimetallic NPs on the basis of UV-visible spectrum only. Nonetheless combination of SEM imaging with EDX spectroscopy as shown in **Figure 4.7** and **Figure 4.8** and the UV–visible spectra in **Figures 4.9(A), (B)** and**(C)** point toward an important observation on the basis of which the composition of the Ag-Au bimetallic NPs could possibly be guessed. In the UV-visible spectrum of **Figure 4.9(A)**, two peaks at 469 nm and 564 nm could be observed. It may be recalled that the sample was prepared by reaction of $HAuCl_4$ with the silver foil thus Au and Ag may be present in addition to the formation of AgCl. The peaks may be assigned to the surface plasmon resonance (SPR) of AgAu alloy NP and monometallic Au NPs respectively[70]. Further, after removal of the AgCl by washing the sample with saturated solution of NaCl the peaks were present with slight shifts in their positions occurring at 461 nm and 571 nm respectively. This means that the components constituting the patterns and which are responsible for the SPR peaks around 469 nm and 564 nm did not change significantly following treatment with saturated NaCl solution. It could be that after AgCl being removed during washing with NaCl the surface was left with Ag and Au constituting the patterns remained on the CD substrate, as indicated by the EDX spectra in **Figure 4.7(A)** and **Figure 4.7 (B)**. An important observation that should be noted here is that the Au deposited after the reduction of Au^{3+} from $HAuCl_4$ by Ag follows the same pattern of the AgCl deposition as indicated by the spot EDX taken at the bright spots shown in **Figure 4.7 (A)** and **Figure 4.7 (B)**. Thus after the treatment with NaCl, AgCl patterned CDs exhibited that most of the Au was present where AgCl crystals were there and the darker regions between these spots contained little, if any, of Au.

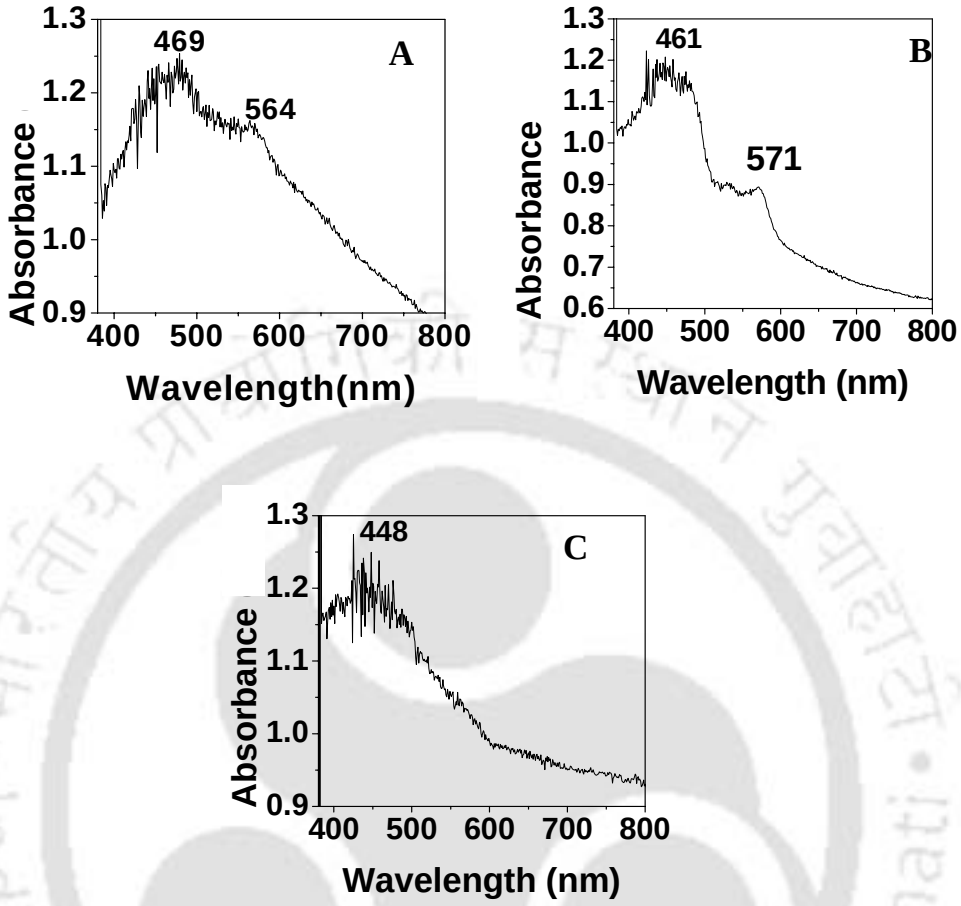

Figure 4. 9: UV-Visible sperum of silver CD, after etching **(A)** without any further treatment **(B)** after NaCl treatment **(C)** Electrochemically reduced.

Interestingly, after electrochemical reduction of AgCl, larger (~1 μm) porous particles were formed with the plasmon peak occurring at 448 nm (**Figure 4.9A**). The particles appear to be porous and conglomeration of smaller particles. Also, the peak at 564 nm disappeared indicating possible deposition of Ag on the Au NPs in the form of shells (**Figure 4.9(C)**). It is known that even if a thin layer of metal is deposited on Au NPs the SPR peak vanishes [70]. This is plausible because SPR in nanoparticles is a surface phenomena hence a monolayer of Ag nanoparticles over Au is good enough to mask the plasmon peak of Au[71]. The presence of Au in the arrays was ascertained by EDX

spectrum as shown in **Figure 4.8(B).** Thus AgCl originally formed in the arrays were reduced to Ag, which could have been present on the film as independent particles or deposited onto already formed Au NPs as shells.

The XRD patterns of CD and DVD Ag foils in **Figure 4.10** showed peaks corresponding to Ag as the peaks occurred around 2θ values of 38^0, 44^0 and 64^0 corresponding to lattice planes (111), (200) and (220) respectively.[70] For the CD sample (**Figure 4.10 (A)**) there is a peak at 2θ of 42.7 ^{0} which is unassigned; however, it possibly corresponds to the CD substrate attached to Ag foil. It is worth mentioning that it does not change in any of our reaction conditions (**Figure 4.11(A)-(C)**), hence the background CD substrate does not has any effect on the reactions carried out on the silver foils. Therefore for us the reactive component wise, i.e. silver, CDs and DVDs are not different except for the type of the dye present.

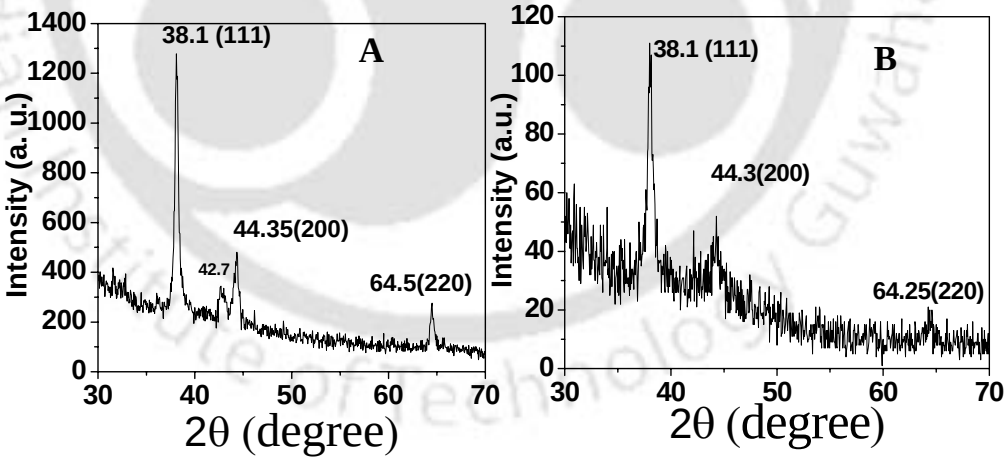

Figure 4.10: XRD patterns of the silver foils from **(A)**, CD and **(B)** DVD without any further treatment. Peak positions are mentioned in the spectra and the corresponding lattice plane are mentioned within the brackets.

The $HAuCl_4$ treated Ag foil samples were further studied using powder XRD. Powder XRD results concur with the UV-Visible spectroscopic results for the samples which

we have studied. For example, pattern (**Figure 4.11(A)**) for the treated film of CD consisted peaks occurring at 2θ values of 27.82^0 (111), 32.24^0 (200), 46.22^0 (220), 54.78^0 (311), 57.46^0 (222) corresponding to AgCl[72] with planes mentioned in the parentheses. On the other hand, the additional peaks (**Figure 4.11A)** observed at 2θ values of 38.18^0(111), 44.42^0 (200) and 64.7^0(220) correspond to the planes (mentioned in the parentheses) of Ag or Au metal [70,73]. The results confirm the formation of AgCl upon the reaction of silver foil from CD with $HAuCl_4$. On further

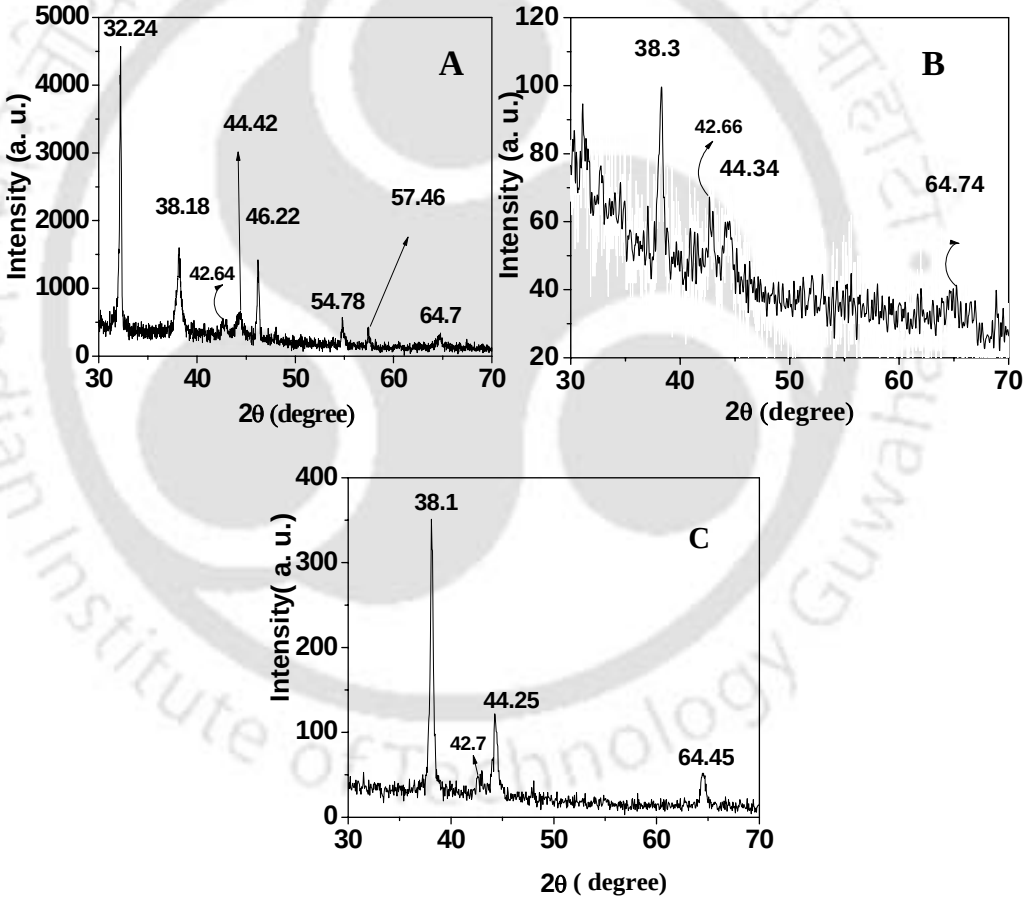

Figure 4.11: X-ray diffraction patterns of **(A)** AgCl patterns on CD substrate as it is, **(B)** after the treatment with saturated NaCl solution, **(C)** after the electrochemical reduction.

treatment of the etched silver foil with saturated solution of NaCl to remove AgCl crystals the Ag/Au peaks remained while occurring at 38.3^0, 44.34^0 and 64.74^0. On the other hand, the peaks corresponding to AgCl disappeared, which is consistent with the fact that in the presence of excess chloride ions AgCl is dissolved. From the XRD patterns it is not possible to conclusively say whether the peaks occurring at 2θ values of 38.3^0, 44.34^0 and 64.74^0 in the etched Ag foil and the NaCl solution treated samples are from elemental Ag or Au or both as Ag and Au have similar lattice constants [73]. It may be mentioned here that the lattice constant of Au is 4.078 Å and that for Ag is 4.086 Å. There is the possibility for both elemental Ag and Au to be present for the reaction between Ag and $HACl_4$ may leave behind some unreacted Ag and also same reaction will form Au, after reduction of the parent salt $HAuCl_4$. The presence of both Au and Ag in the arrays is supported by EDX spectra as mentioned before. However, UV-Visible observations indicated the formation of AgAu composite NPs along with the presence of Au NPs after the galvanic reaction. It may be that separate Ag and Au NPs were not present in the final structures (as oppose to composite particles). Further, literature reports indicate that partial galvanic replacement of Ag by $AuCl_4^-$ leads to the formation of composite particles [69]. Finally, as shown in **Figure 4.11(C),** the XRD pattern on CD after electrochemical reduction consisted of peaks corresponding to Ag/Au occurring at 38.1^0(111), 44.25^0(200) and 64.25 (220) respectively. Overall, considering the observations in EDX spectroscopy, UV-visible spectroscopy and X-ray diffractometry it could be said that final arrays in the film consisted of AgAu bimetallic NPs.

We were also interested in reducing the dimensions of the particles formed on the patterned surface. An obvious and easy choice was to use commercially available

DVD Ag foil for this purpose. As the DVD tracks are of approximately 400 nm widths contrary to the 1 μm tracks of CDs, therefore the patterns generated are expected to be smaller in dimensions than those in CDs. Upon reaction with $HAuCl_4$ the Ag foils under same reaction conditions as used for CD Ag foils, generated patterned structures with the formation of particles. SEM images (along with EDX spectrum) of typical patterns are shown in **Figure 4.12**. As is clear from the figures particles were formed along the lines of the DVD. The average particle sizes were

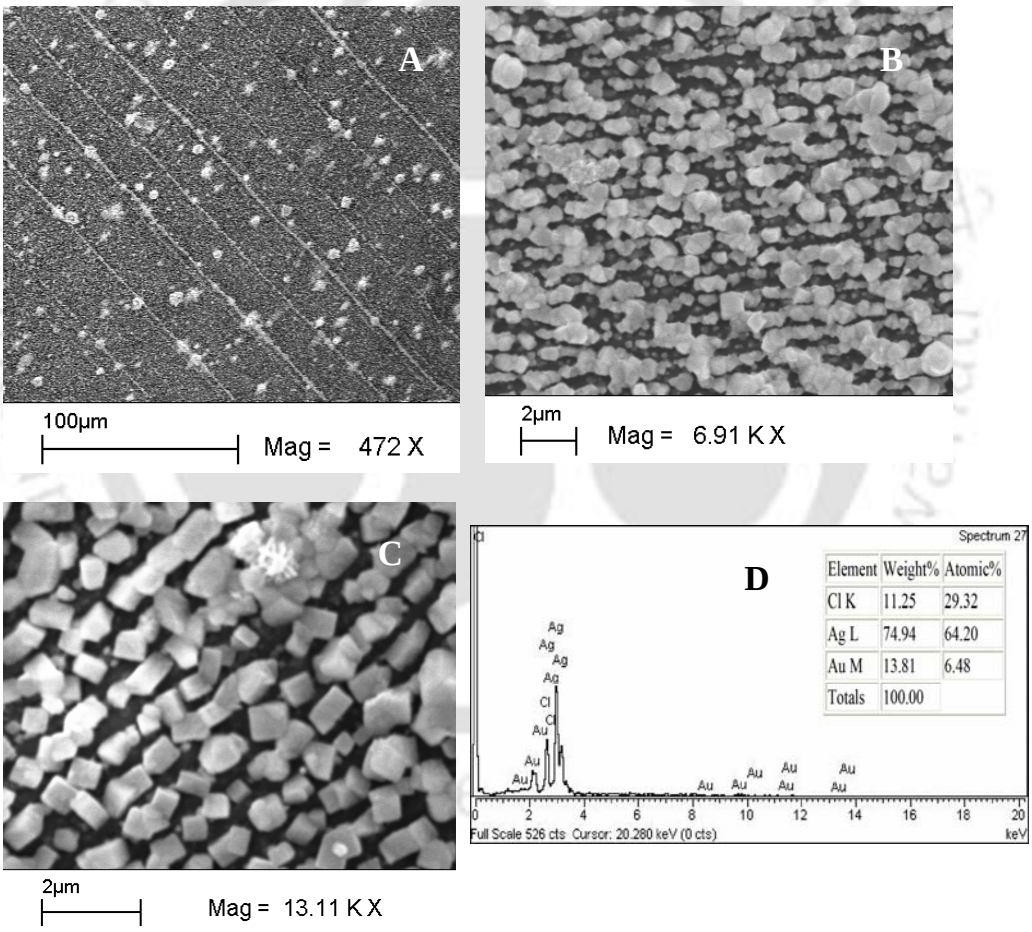

Figure 4.12: (A), (B) and **(C)** AgCl patterns generated on DVD Ag foil at different magnifications. **(D)** Spot EDX on the cubic particles.

smaller than those generated in CD (for example, 400 nm as opposed to 1 μm). EDX spectrum (**Figure 4.12(D)**) indicated the formation of AgCl in the process, being present along the DVD hill tracks. However, cross patterns of particles were not observed always (in comparison to those present in films from CD Ag foils). However

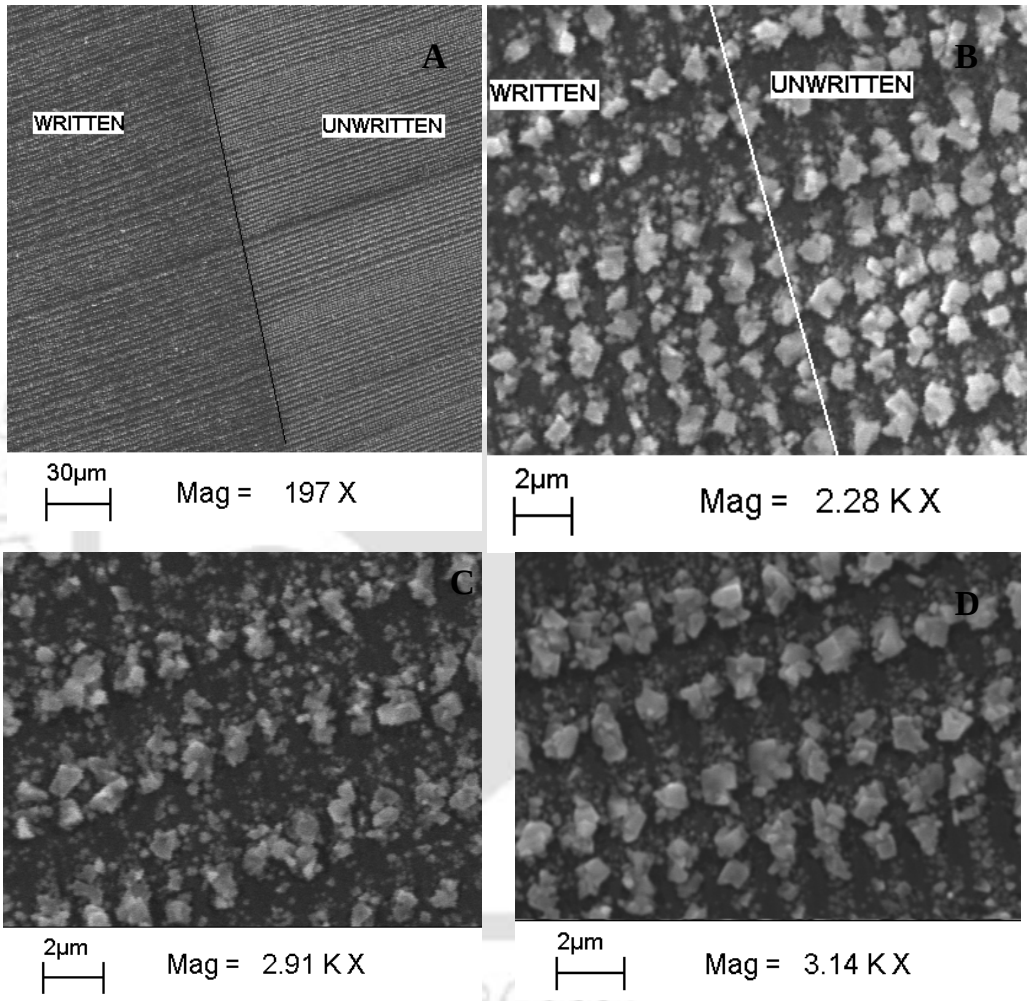

Figure 4.13 : SEM image of AgCl crystals deposited along the CD tracks **(A)**, **(B)** of written and unwritten parts at different magnifications; **(C)** written part, **(D)** unwritten part.

Figure 4.12 (B) has a certain degree of cross patterning. It is possible that the key role played by the cross pattern generation is the presence of the dye. The nature of the dye would be crucial in that respect, hence the difference in the observations. Since

the reaction diffusion waves contributed in the formation of the cross patterns in the CD foils, their absence in the DVD films may be speculated to be the cause of absence of such patterns under the present reaction conditions. On the other hand, the formation of particles along the track was possible as reaction occurred and the rates may be different depending on the heights. The hills of the DVD (CD as well) may have easier access to the reagents in comparison to the valleys due to the narrowness of the structures.

A natural extension of the work would be the ability to have control over the pattern formation with an additional handle such as light. In these cases (with CD) it can be easily achieved by 'burning' the CD before dismantling and etching. In order to achieve this, we have written (burned) data on a CD, followed by removing the Ag foil using the previously described method. This was followed by reaction with $HAuCl_4$ following the same procedure. The reaction was carried out with the same film contained both the written and unwritten parts of the same CD Ag foil. To our amusement we did observe difference in the type of patterns generated on the written and unwritten parts of the CD silver foils. Typical patterns observed in CD films are shown in **Figure 4.13**. The SEM images shown in the figure correspond to Ag foils reacted with 3.46 X 10^{-4} M $HAuCl_4$. As is clear from the **Figure 4.13 (A)** and **Figure 4.13 (A)**, the AgCl crystals were deposited over the CD tracks at both the written and unwritten parts. However, the density of particles and sizes were different as seen in **Figure 4.13 (C)** for the written part and **Figure 4.13 (D)** for the unwritten part. The crystals formed in the written part were typically smaller (~800nm) in comparison to those formed in the unwritten parts (~1μm). Also when we observed the patterns at shorter times it appeared that the reactivity at the written part is less than the

unwritten parts therefore smaller crystals are observed in the written part compared to the unwritten part **Figure 4.14**.

The difference in the distribution of AgCl crystals in the written part and the unwritten part again indicated the importance of the photoactive dye. During the burning process of a CD-R the photoactive dye which is a transparent substance is converted to an opaque substance by an infra red Laser [62-63]. This implies that the chemical composition of the photoactive dye changes upon burning, which affects the distribution of the AgCl crystals possibly due to difference in the rates of the reaction of the reflective silver foil with $HAuCl_4$ as seen in **Figure 4.13** .

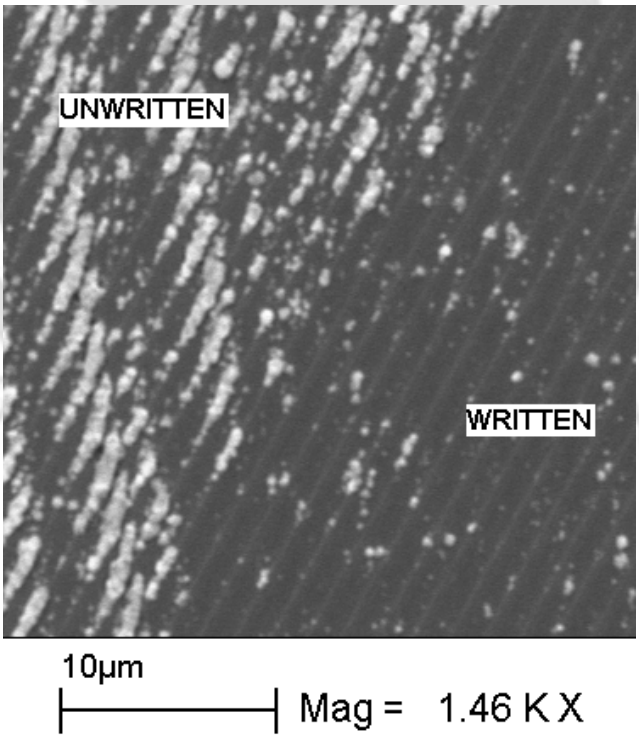

Figure 4.14: SEM image of AgCl crystals deposited on CD tracks at 5 min.

4.5: Conclusion

In the midst of ever increasing number of methods for NP synthesis we have tried to integrate the conventional "top down" and the "bottom up" approaches to directly synthesise surface immobilised NPs of Au and Ag along with the formation of AgCl microcrystals. The marked difference of the reported process with the currently available methods is that we have synthesized AgAu composite NPs immobilised onto a flexible plastic surface in a well-defined pattern. In doing so, we have utilised an easily available and economic templated Ag film to carry out a galvanic replacement reaction with $HAuCl_4$. Galvanic replacement reactions are commonly applied to generate monometallic porous films from a bimetallic precursor, but here we use a monometallic template to generate bimetallic NP patterns. Also the scientific importance of this work from the point of view of surface chemistry cannot be overemphasized. We have demonstrated the generation of AgCl microcrystals aligned according to the tracks of a CD by reacting the CD silver foils with $HAuCl_4$. The line patterns generated were separated by micrometers. We were also able to generate patterns separated from each other by approximately 400 nm distances by taking the Ag foils from DVDs. These patterns have been converted to AgAu bimetallic NP patterns by either electrochemical reduction or treatment with saturated NaCl solution or with dilute aqueous NH_3 solution. The optical properties of the patterned substrates could be changed following reduction of the incipient AgCl crystals. These patterns can have important applications in metal enhanced fluorescence, plasmonics, surface enhanced raman spectroscopy (SERS), recoverable catalysis etc. With a greater degree of control over the patterns and the composition of the NPs this may be a good lithographic technique. The work presented here is of preliminary in nature.

Mechanistic understanding of the process involved in the pattern generation and the role of the photoactive dye would be scientifically very important for future studies. Also, this opens up a new area of galvanic replacement in surface driven patterning of metal NPs and might lead to exploration of more of the possible metal pairs.

References

1. Porter, L. A. Jr.; Choi, H. C.; Schmeltzer, J. M.; Ribbe, A. E.; Elliott, L. C. C.; Buriak, J. M. *Nano Lett.*, **2002**, *2*, pp 1369-1372.
2. Xia, Y.; Rogers, J. A.; Paul, K. E.; Whitesides, G. M. *Chem. Rev.* **1999,** *99*, pp 1823-1848.
3. Gur, I.; Fromer, N. A.; Geier, M. L.; Alivisatos, A. P. *Science* **2005**, *310*, pp 462–465.
4. Cheng, M. M.-C.; Cuda, G.; Bunimovich, Y. L.; Gaspari, M.; Heath, J. R.; Hill, H. D.; Mirkin, C. A.; Nijdam, A. J.; Terracciano, R.; Thundat, T.; Ferrari, M. *Curr. Opin. Chem. Biol.* **2006**, *10*, pp11–19.
5. Zhang, G.; Sun, S.; Ionescu, M. I.;Liu, H.;Zhong, Y.; Li, R.; Sun, X. *Langmuir*, **2010**, *26*, pp 4346–4350.
6. Ma, Y., Wong, C. P., Zeng, X. T., Yu, T., Zhu, Y. and Shen, Z. X. *J. Phys. D: Appl. Phys.* **2009**, *42*, 065417.
7. Lee, E. P., Chen, J., Yin, Y. Y., Campbell, C. T. and Xia, Y. *Adv. Mater.* **2006**, *18*, pp 3271– 3274.
8. Zhang, B., Weng, Y., Huang, X., Wang, M., Peng, R., Ming, N., Yang, B., Lu, N. and Chi, L. *Adv. Mater.* **2009**, *21*, pp 3576–3580
9. Duan, X.; Zhao, Y.; Berenschot, E.; Tas, N. R.; Reinhoudt, D. N.; Huskens, J. *Adv. Funct. Mater.* **2010**, *20*, pp 2519–2526.

10. *Unconventional Nanopatterning Techniques and Applications;* John A. Rogers, J. A.; Lee, H. H., Eds.; John Wiley & Sons, Inc.: Hoboken, New Jersey. 2009.
11. Ertl, G. *Angew. Chem. Int. Ed.* **2008**, *47*, pp 3524 – 3535.
12. Stewart, M. E.; Anderton, C. R.; Thompson, L. B.; Maria, J.; Gray, S. K.; Rogers, J. A.; Nuzzo, R. G. *Chem. Rev.* **2008,** *108*, pp 494-521.
13. Khang, D.; Lu, J.; Yao, C.; Haberstroh, K. M.; Webster, T. J. *Biomaterials* **2008**, *29*, pp 970-983.
14. Bonroy, K.; Friedt, J.-M.; Frederix, F.; Laureyn, W.; Langerock, S.; Campitelli, A.; Sara, M.; Borghs, G.; Goddeeris, B.; Declerck, P. *Anal. Chem.* **2004**, *76*, pp 4299-4306.
15. Kramer, D.; Viswanath, R. N.; Weissmuller, J. *Nano Lett.* **2004**, *4*, pp 793-796.
16. Bansal, V.; Jani, H.; Plessis, J. D.; Coloe, P. J.; Bhargava, S. K. *Adv. Mater.* **2008**, *20*, pp 717-723.
17. Namavar, F.; Cheung, C. L.; Sabirianov, R. F.; Mei, W.-N.; Zeng, X. C.; Wang, G.; Haider, H.; Garvin, K. L.. *Nano Lett.* **2008**, *8*, pp 988-996.
18. Shi, F.; Song, Y.; Niu, J.; Xia, X.; Wang, Z.; Zhang, X. *Chem. Mater.* **2006**, *18*, pp 1365-1368.
19. Li, X. M.; Reinhoudt, D.; Crego-Calama, M. *Chem. Soc. Rev.* **2007**, *36*, pp 1350–1368.
20. Stewart, M. E.; Anderton, C. R.; Thompson, L. B.; Maria, J.; Gray, S. K.; Rogers, J. A.; Nuzzo, R. G. *Chem. Rev.* **2008**, *108*, pp 494-521.
21. Haes, A. J.;Haynes, C. L.;McFarland, A. D.; Schatz, G. C.; Van Duyne, R. P.; Zou, S. *MRS Bull.* **2005**, *30*, pp 368-375.

22. Lakowicz, J. R.; Geddes, C. D.; Gryczynski, I.; Malicka, J.; Gryczynski, Z.; Aslan, K.; Lukomska, J.; Matveeva, E.; Zhang, J. A.; Badugu, R.; Huang, J. *J. Fluoresc.* **2004**, *14*, pp425−441.

23. Pompa, P. P.; Martiradonna, L.; Torre, A. D.; Sala, F. D.; L. Manna,; De Vittorio, M.;Calabi, F.; Cingolani , R.; Rinaldi, R. *Nat. Nanotech.* **2006**, *1*, pp 126-130.

24. Aslan, K.; Gryczynski, I.; Malicka, J.; Matveeva, E.; Lakowicz, J. R.; Geddes, C. D. *Curr. Opin. Biotechnol.* **2005**, *16*, pp 55-62.

25. Tvingstedt, K.; Persson, N. K.; Ingana¨s, O.; Rahachou, A.; Zozoulenko, I. V. *Appl. Phys. Lett.* **2007**, *91*, 113514.

26. Michaels, A. M.; Nirmal, M.; Brus, L. E. *J. Am. Chem. Soc.* **1999**, *121*, pp 9932-9939.

27. Caldwell, W. B.; Chen, K.; Herr, B. R.; Mirkin, C. A.; Hulteen, J. C.; Van Duyne, R. P. *Langmuir* **1994**, *10*, pp 4109-4115.

28. Geddes, C. D.; Parfenov, A.; Lakowicz, J. R. *Appl. Spectrosc.* **2003**, *57*, pp526-531.

29. Geddes, C. D.; Parfenov, A.; Roll, D.; Fang, J.; Lakowicz, J. R. *Langmuir* **2003**, *19*, pp6236-6241.

30. Cao, G. *Nanostructures and Nanomaterials;* Imperial College Press: London, 2004, pp 173-228.

31. Geddes, C. D.; Parfenov, A.; Roll, D.; Gryczynski, I.; Malicka, J.; Lakowicz, J. R. *Spectrochim. Acta, A* **2004**, *60*, pp 1977-1983.

32. Jensen, T. R.; Malinsky, M. D.; Haynes, C. L.; Van Duyne, R. P. *J. Phys. Chem. B* **2000,** *104*, pp10549-10556.

33. Xie, F.; Baker, M. S.; Goldys, E. M. *Chem. Mater*. **2008**, *20*, pp1788-1797.

34. Ahl, S.; Cameron, P. J.; Liu, J.; Knoll, W.; Erlebacher, J.; Yu, F. *Plasmonics* **2008**, *3*, pp 13-20.

35. Shankar, S. S., Rizzello, L., Cingolani, R., Rinaldi, R. and Pompa, P. P. *ACS Nano* **2009**, *3*, pp 893–900**.**

36. Wouters, D.; Schubert, U. S. *Angew. Chem. Int. Ed.* **2004**, *43*, pp2480 – 2495.

37. Gates, B. D.; Xu, Q.; Stewart, M.; Ryan, D.; Willson,C. G.; Whitesides, G. M. *Chem. Rev*. **2005,** *105*, pp 1171-1196.

38. Rogers , J. A.; Paik, U. *Nat. Nanotech.***2010**, *5*, pp 385–386.

39. Aizawa, M. and Buriak, J. M. *J. Am. Chem. Soc.* **2006**, *128*, pp 5877-5886.

40. Grzybowski, B. A.; Bishop, K. J. M.; Campbell, C. J.; Fialkowski, M.; Smoukov, S. K. *Soft Matter* **2005**, *1*, pp 114-128.

41. Imbihl, R.; Ertl, G. *Chem. Rev.* **1995,** *95*, pp 697-733.

42. Bensemann, I. T.; Fialkowski, M.; Grzybowski, B. A. *J. Phys. Chem. B* **2005**, *109*, pp2774-2778.

43. Kelly, K. L.; Coronado, E.; Zhao, L. L.; Schatz, G. C. *J. Phys. Chem. B* **2003**, *107*, pp 668–677.

44. Eustis, S.; El-Sayed, M. A. *Chem. Soc. Rev.* **2006**, *35*, pp 209-217.

45. Ozbay, E. *Science* **2006**, *311*, pp189-193.

46. Burda, C.; Chen, X.; Narayanan, R.; El-Sayed, M. A. *Chem. Rev.* **2005,** 105, 1025-1102.

47. Ramachandra Rao, C. N.; Kulkarni, G. U.; Thomas, J.; Edwards, P. P. *Chem. Soc. Rev.* **2000**, *29*, pp 27−35.

48. Kariuki, N. N.; Luo, J.; Maye, M. M.; Hassan, S. A.; Menard, T.; Naslund, H. R.; Lin, Y.; Wang, C.; Engelhard, M. H.; Zhong, C.-J. *Langmuir* **2004**, *20*, 11240−11246.

49. Sun, S. H.; Murray, C. B.; Weller, D.; Folks, L.; Moser, A. *Science* **2000**,*287*, pp1989-1992.

50. Toshima, N.; Harada, M.; Yamazaki,Y. Asakura, K. *J. Phys. Chem.* **1992**, *96*, pp 9927-9933.

51. Tokonami, S.; Morita, N.; Takasaki, K.; Toshima, N. *Phys. Chem. C* **2010**, *114*, pp 10336–10341.

52. Toshima, N.; Yonezawa, T. *New J. Chem.* **1998**, *22*, pp 1179-1201.

53. Ferrando, R.; Jellinek, J.; Johnston, R. L. *Chem. Rev.* **2008**, *108*, pp 845-910.

54. Zhang, Q.; Lee, J. L.; Yang, J.; Boothroyd, C. Zhang, J. *Nanotechnology* **2007**, *18*, 245605 (8pp) doi:10.1088/0957-4484/18/24/245605

55. Murray-Methot, M. P.; Ratel, M.; Masson, J. F. *J. Phys. Chem. C* **2010,** *114*, pp 8268–8275.

56. Major, K. J.; De, C.; Obare, S. O. *Plasmonics* **2009**, *4*, pp 61– 78.

57. Chen, J.; Wiley, B.; McLellan, J.; Xiong, Y.; Li, Z.-Y.; Xia, Y. *Nano Lett.* **2005**, *5*, pp2058– 2062.

58. Zhang, Q. B.; Xie, J. P.; Lee, J. Y.; Zhang, J. X.; Boothroyd, C. *Small* **2008**, *4*, pp 1067-1071.

59. Mazzola, L. *Nat. Biotechnol.* **2003**, *21*, pp 1137-1143.

60. Wang, Y.; Xia, Y. *Nano Lett.* **2004**, *4*, pp2047-2050**.**

61. Li, F.; Wang, Z. Y.; Stein, A. *Angew. Chem., Int. Ed.* **2007**, *46*, pp 1885-1888.

62. Pohlmann, K. C. *The Compact Disc Handbook*; Oxford University Press Inc.: New York, 2001, pp47-102.

63. CD-R - Compact Disk-Recordable. http://www.pctechguide.com/33CDR-RW_CD-R.htm. Accessed on 3rd December, 2010.

64. How is CD/ Compact Disk Made. http://realitypod.com/2010/07/how-is-cd-compact-disk-made/ . Accessed on 3rd December 2010

65. Sun, Y.; Wiley, B.; Li, Z. Y.; Xia, Y. *J. Am. Chem. Soc.* **2004**, *126*, pp 9399-9406.

66. Zumdahl , S. S. *Chemical principles,5th Edition*; Houghton Mifflin Company : New York, 2005, pp 276-346.

67. Caley, E. R.; Shank, L. W. *The Ohio J. of Science*, **1968**, *68*, pp 100-104.

68. Electrochemical Series. In *CRC Handbook of Chemistry and Physics, 85th Edition;* Lide, D. R. Ed., CRC Press, Boca Raton, FL: 2005.

69. Sun, Y.; Xia, S. *J. Am. Chem. Soc.*, 2004, *126*, pp 3892–3901.

70. Chen, D. H.; Chen, C. J. *J. Mater. Chem.*, **2002**, *12*, pp1557–1562.

71. P. Mulvaney, M. Giersig and A. Henglein, *J. Phys. Chem.*, 1993, *97*, pp 7061-7064.

72. Zayat, M.; Einot, D.; Reisfeld, R. *J. Sol -Gel Sci. Tech.* **1997**, *10*, pp64-74.

73. Srnova´-Sÿloufova, I.; Lednicky, F.; Gemperle, A. Gemperlova, J. *Langmuir* **2000,** *16*, pp 9928-9935.

Chapter V

Application of Surface Synthesized Silver Chloride Crystals in Photo Degradation of an Organic Dye and as an Antibacterial Agent

5.1: Introduction

According to the world health report-2005 published by World Health Organization, the health consequences associated with the microbial contamination of water supplies remain a pressing global issue facing the human society in the new millennium [1,2]. Approximately 1.8 million people die per year from waterborne infections around the world [3]. Apart from the older chemical disinfectants, newer methods are like ozonation, ultraviolet light treatment etc. are common at present. Still, ever increasing number of health problems caused by microbial contaminated water suggests the need for more intense research in this direction.

On the other hand, there are requirements of cleaning of water polluted by chemical contaminants like the dyes used in textile, ink, paper, ceramic, food processing, leather industries etc. [4, 5] These also pose threat to human health and the environment [6-8]. Commonly used methods for the removal of the chemical contaminants in water are chlorination, ozonation, ultrasonication, reverse osmosis, membrane filtration and adsorption on activated charcoal.[9-11]. However, the phenomenal growth in nanotechnology research has opened the doors to new strategies using nanomaterials for more effective disinfection and decontamination. The excellent antimicrobial properties of the nanoparticles (NPs) qualify for their use as viable alternatives for water disinfection while the photocatalytic semiconductor nanoparticles offer better alternatives for decontamination. [1]

Among the metallic particles, silver is known for its antimicrobial properties for centuries [12-15]. With the recent development in nanotechnology there has been a renewed interest in exploring the potential of Ag as potent antimicrobial agent [16]. Ag NPs could be used in the form of stable dispersion or in the form of solid-state device

where the NPs would be embedded in the solid and at the same time be accessible for interaction with microbes present in the liquid (especially water) medium. On the other hand for cleaning the organic dyes from water, scientists are exploring the use of photocatalytic pathways especially by using sunlight as the primary source of light, which is considered as an environment friendly approach [17-20]. Special emphasis is given on the development of visible light photocatalysts in order to utilize the sunlight, which reaches the earth surface, more effectively [21-24]. AgCl is known to be a photosensitive semiconductor material with an indirect band gap of 3.3 eV, which accordingly has its intrinsic light sensitivity situated in the ultra-violet region [24]. However, through a process of self sensitization it can be tuned to be photoactive in the visible region [24-26]. This has boosted renewed interest in the material [26-30].

For use in water purification systems, it would be of great assistance if the same material serves the dual purpose of acting as an antimicrobial agent as well as a photodegradation catalyst for organic dyes. In this regard nanoscale materials may be of great help for providing both the activities by the same material. Moreover, if the active NPs are bound to a macro surface it also makes the recovery of the active material easier. For this purpose nanomaterials embedded in polymer matrices have been widely used [31-33]. Herein we report the development of a new material consisting of micron size AgCl crystals and Ag and Au NPs bound to a flexible polymer surface. The development and characterizations of the material have been discussed in **Chapter IV**. In this chapter we demonstrate, as a proof of principle, the antimicrobial activity as well as the photochemical activity of AgCl and the AgAu composite NPs generated by reacting $HAuCl_4$ with the silver layer of a commercially available CD (compact disc) or DVD (digital versatile disc). From this point onwards we will refer to the composite as AgClAgAu (CD) or AgClAgAu (DVD) depending upon the

precursor CD or DVD respectively. We have tested the photocatalytic activity of the composite towards the degradation of a common azo dye, methyl orange (MO) and antimicrobial activity of the same on *Escheria Coli (E. Coli)* bacteria. Photochemical degradation of methyl orange was carried out under direct sunlight with the amount AgCl in AgClAgAu (DVD) 0.40mg for 10.55 mg L^{-1} of dye, while the antimicrobial activity was demonstrated by a zone of inhibition test. For complete degradation of the dye it took about 300 min and there was no observable degradation of the dye without the composite. Photodegradation activities of the composites prepared from the Ag layer of a CD and DVD tested were found to be similar (within 5 hours of reaction). The photodegradation activity of the composite in presence of UV light was found to be similar in rate in comparison to that in presence of sunlight indicating that the origin of activity may lie with the UV content of the sunlight and that is sufficient to photodegrade a dye. Interestingly this is possibly the first report on the use of UV-light of sun reaching the earth surface for inducing a photochemical activity such as the degradation of the dye.

5.2: Experimental Section

5.2.1: Materials and Substrates: Chloroauric acid (17%) was purchased from Sigma-Aldrich Chemical Company. Commercially available CDs and DVDs were used. The procedure for exposing the Ag surface for reaction was described in Chapter IV. Milli-Q grade water was used for making all the solutions and washing purposes. Methyl orange (MO) dye was procured from Merck India Ltd. and was used without purification.

5.2.2: Generation of AgClAgAu Composites on Surfaces: Details of the process is discussed in Chapter IV. In brief, approximately 1.55 cm x 2.6 cm cut pieces of silver foils from CDs and DVDs were reacted with different concentrations of $HAuCl_4$ solutions to obtain the AgClAgAu (CD/DVD) composite formed from the silver foils. Observations were made at different time points, concentrations and temperatures. Thus the obtained composites bound to plastic surface were further cut into approximately 1.0 cm X 2.6 cm ($2.6cm^2$) pieces in order to fit them into a quartz cuvette which was used for the photochemical studies.

5.2.3: Photochemical Degradation Experiment: Photochemical degradation of MO in presence of the AgClAgAu composite from CDs and DVDs were carried out in presence of sunlight by placing the composite in 3.0 mL solutions containing 3.3 X 10^{-5} M MO in a quartz cuvette and then placing the cuvette in the sunlight (September-October 2009, IITG longitude $91^o44'$ east and latitude $26^o10'$ north). Photodegradation was monitored by recording the UV-Visible spectrum of the sample at 15 min intervals using a Hitachi U-2800 UV-Visible spectrophotometer. Photodegradation of MO under UV light was carried out in a Delta Scientific UV chamber with the same amount of MO and the AgClAgAu composite. Control experiments were carried out without AgClAgAu.

5.2.4: Antimicrobial Activity Test: The antimicrobial activity of the AgNPs was studied by standard disk diffusion method. Overnight culture of ampicillin resistant GFP expressing recombinant *E. coli* bacteria was taken, suitably diluted and spread (approximately 10^6 CFU) on previously prepared 1.5 % Luria Bertani-agar plate containing 100 μg mL^{-1} ampicillin. These plates were observed for colony formation after 24 h of incubation at 37 ^{0}C. Sample photographs and colony counting was

primarily used to evaluate the antimicrobial activities. After 24 h incubation with chips of CD and DVD containing AgNPs a clear zone (Zone of Inhibition) around 8 mm and 7.5 mm were observed. But, control plates with nano-silver free chips did not produce any inhibition zones. The inhibitions of bacterial growth around the chips were due to the release of diffusible inhibitory compounds from chips containing AgNPs into the surrounding medium. The antimicrobial activity of the composite AgClAgAu was also tested on ampicillin resistant GFP expressing recombinant *E. coli* in aqueous LB medium containing 100 μg mL^{-1} of ampicilin.

5.2.5: Scanning Electron Microscopy (SEM): Leo-VP 1430 scanning electron microscope (SEM) equipped with an Oxford-INCA energy dispersive X-ray (EDX) analyzer was used to image and characterize composite AgClAgAu in order to compare the morphological and compositional changes before and after the photocatalysis.

5.2.6: X-Ray Diffraction (XRD): A Bruker D8 Advanced powder X-ray diffraction (XRD) instrument was used to characterize the composite before and after photodegradation experiment.

5.3: Results and Discussion

Herein we try to demonstrate as a proof of principle the possibility of the AgCl microcrystals and the AgAu nanoparticles bound to the CD/DVD plastic as a potential water purifying agent (AgClAgAu (CD)/ AgClAgAu (DVD)). The composition of the films was established in Chapter IV. Representative SEM image (**Figure 5.1(A)**) and the EDX spectra of the as prepared AgClAgAu (DVD) sample showed the presence of AgCl along with Ag and Au (**Figures 5.1(B) and (C)**). X-ray diffraction (XRD)

pattern shown in **Figure 5.1(D)** for the AgClAgAu (DVD) sample confirmed the presence of AgCl as indicated by the peaks at 2θ values of 27.8°{111}, 32.25°{200}, 46.25°{220}, 54.85°{311} and 57.65°{222} [34]. On the other hand, the peaks at 38.2°{111}, 44.4°{200} and 64.75°{220} indicated the presence of Ag and/or Au.

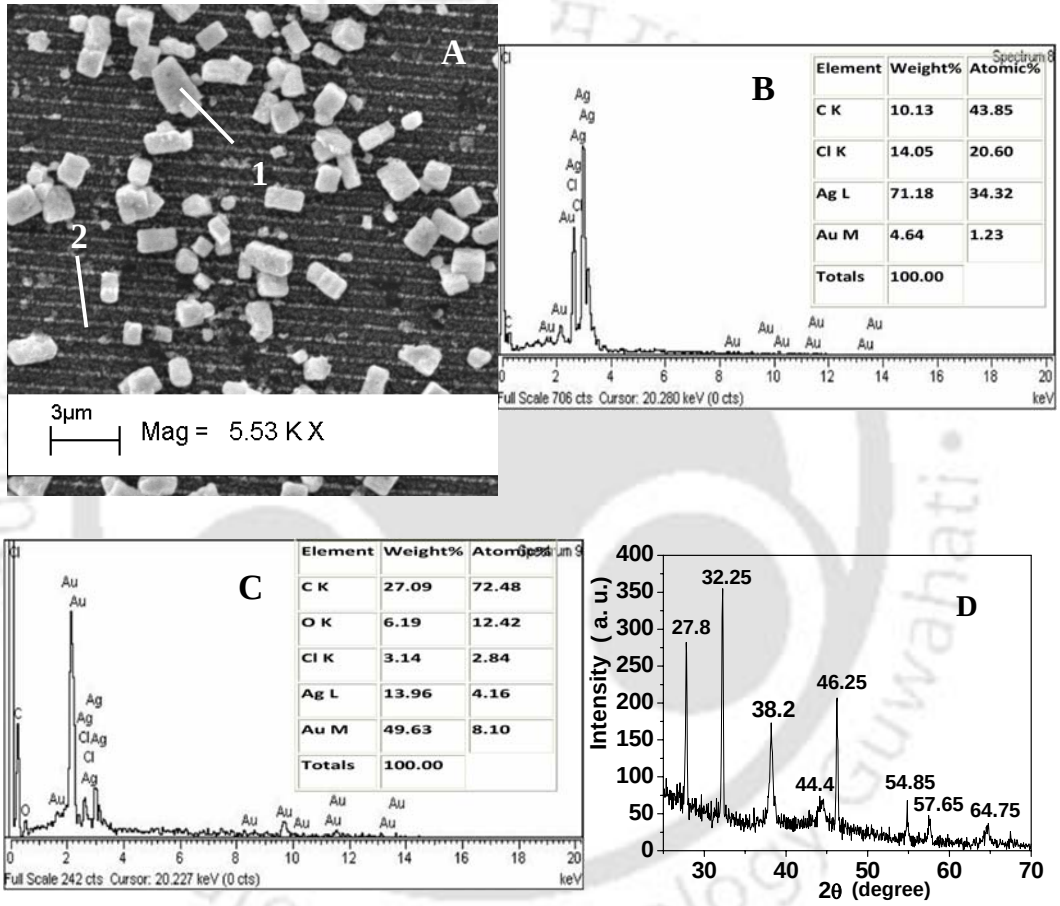

Figure 5.1 (A) Representative SEM image of a as prepared AgClAgAu (DVD), **(B)** and **(C)** EDX spectra at spots 1 and 2 respectively in **(A)**, **(D)** the X-ray diffraction pattern of the same sample.

Presence of Ag or Au cannot be distinguished from the observed XRD pattern for both have nearly identical lattice constants and hence XRD patterns[35, 36]. But comparing EDX and the XRD data it can be said that both Ag and Au were present in

the samples. Further, from the UV-Visible spectrum of the AgClAgAu (DVD) sample shown in **Figure 5.2** it can be seen that there is absorbance in the whole visible range possibly due to the presence of Au and Ag NPs. The broadness of the peak extending beyond the visible region to near infrared region is indicative either of presence of agglomerated particles.

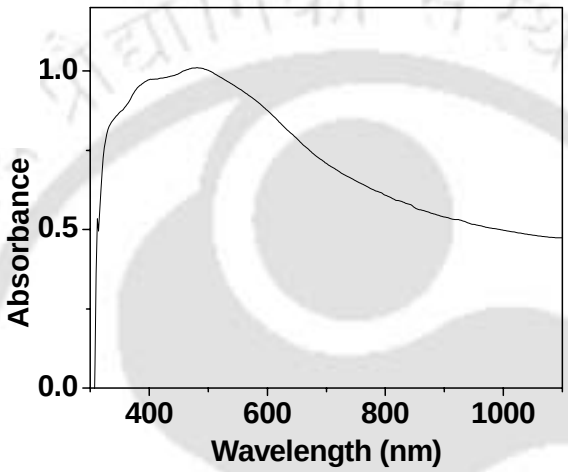

Figure 5.2: UV-Visible spectrum of the AgClAgAu (DVD).

For the photocatalytic activity we have studied the rates of the photodegradation of MO and found it to be low and the activity of the reagent gradually decreases with subsequent batches of experiment. In our study we have observed a photochemical degradation rate of 3 mL of 10.55 mg L^{-1} MO when exposed to sunlight with the photoactive AgClAgAu (DVD) (**Figure 5.3(A)**), while no degradation of MO was observed for the control experiment without AgClAgAu (DVD). The photochemical nature of the degradation of MO rather than chemical degradation is proved by the fact that there was no degradation of MO in with AgClAgAu (DVD) without the sunlight. The rate of photochemical degradation was determined by considering it to be a pseudo first order reaction[5].

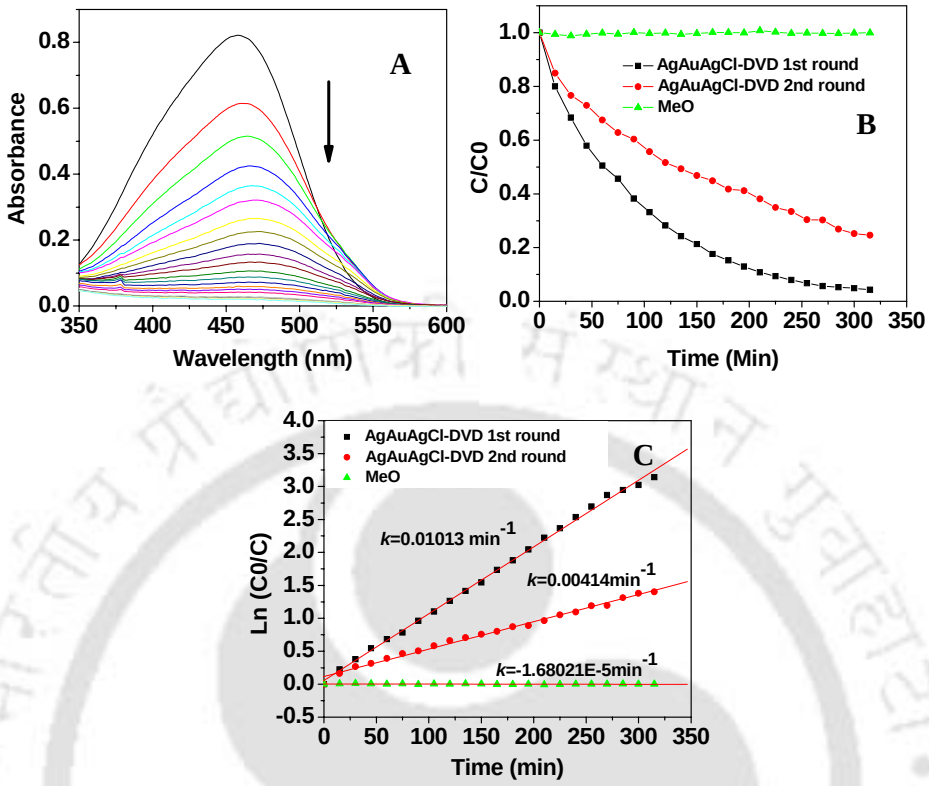

Figure 5.3: (**A)** Photo degradation of curves of methyl orange under sunlight between time points 0 min to 315 min indicated by arrow at the interval of 15 min in presence AgClAgAu (DVD), (**B)** plot of C/C_0 versus time and **(C)** plot of *Ln*(C_0/C) versus time with the line fit and the rate constants given as k near to each plot.

Figures 5.3(B) and **(C)** show the plot of C/C_0 versus time and *Ln*(C_0/C) versus time respectively. Control experiments showed that in absence of the AgCl AgAu (DVD) no degradation of the dye is observed as shown by the representative graph in **Figure 5.3(B)**. On the other hand, in the presence of the AgClAgAu (DVD), there is exponential degradation of the MO dye and at a rather high rate when AgClAgAu (DVD) were used as the photocatalyst for the first time. The rate decreased on a second run with the same AgClAgAu (DVD) sample as is clear from the figure. The rate constant for the photodegradation reaction was determined by considering the

Langmuir-Hinshelwood (L-H) model for heterogeneous photochemical degradation of the MO dye [5, 37] which can be expressed as

$$\frac{dC}{dt} = \frac{k_{L-H}K_{ad}C}{1+K_{ad}C} \qquad \textbf{(5.1)}$$

Here $k_{L\text{-}H}$ is the reaction rate constant, K_{ad} is the adsorption coefficient of the dye on the photocatalyst, and C is the variable concentration at any time t. For a pseudo-first order reaction $K_{ad}C$ is very small as compared to 1 in the denominator of equation (5.1) and thus can be neglected. Integrating equation (5.1) (after neglecting $K_{ad}C$), we obtain

$$Ln\left(\frac{C_0}{C}\right) = k_{L-H}K_{ad}t = kt \qquad \textbf{(5.2)}$$

Here C_0 is the initial concentration and $k=k_{L\text{-}H}K_{ad}$ is the pseudo first order reaction rate constant. **Figure 5.3(C)** shows a plot of *Ln* (C_0/C) versus time in minutes. The slopes of the fitted straight line provided the rate constants for the photo catalytic degradation of MO dye in the presence of AgClAgAu (DVD) and in absence of it. The rate constant for the photodegradation of MO dye in presence of AgClAgAu (DVD) used for the first time was found to be 0.01013 min^{-1}, while the rate constant decreased to 0.00414min^{-1} on the second run of the photocatalyst. As the rate constant indicates the catalyst efficiency, so in our case the catalyst efficiency was reduced to almost half in consecutive runs. This may be caused by adsorption of some of the dye degradation products present on to the catalyst surface, partial dissolution of ions (due to Ksp) from the AgClAgAu-CD substrate and/or photo-reduction of AgCl to Ag. EDX spectrum of the photocatalyst surface after the experiment indicated the presence of AgCl even after the two batches of photodegradation experiments. The lower reaction rate in these cases may be due to the lower amount of AgCl present in

the AgClAgAu (DVD) photocatalysts compared to the literature reports [26], where 0.2 g of Ag@AgCl photocatalyst was used for 2 mg of the dye with the catalyst suspended in water compared to the 0.403mg AgClAgAu (DVD) per 0.032 mg of the dye in our experiments. It is worth mentioning here that the amount of $HAuCl_4$ used to get the AgClAgAu (DVD) was 10 mL^{-1} $2.98x10^{-4}$ M solution reacting with 0.47 mg ($0.44X10^{-6}$ mol) Ag on 1.55 X 2.6 cm^2 (4.03 cm^2) DVD. Therefore the maximum amount of AgCl that could have been generated is approximately 0.624 mg by the reaction given below and that amount of AgCl would be formed if the reaction (1) was complete. So we can consider that approximately 0.15 mg of AgCl was formed per cm^2 of the DVD. As we have taken 2.6 cm^2 pieces of DVD for the photodegradation experiment, so AgCl used per photodegradation experiments is approximately 0.403 mg per 0.032 mg of the dye. Now the reaction between Ag and $HAuCl_4$ does not go to completion as the difference of their standard reduction potentials is only 0.2V [38]. So the actual amount of AgCl used was less than 0.403 mg. Moreover the $HAuCl_4$ solution used in the reaction was highly acidic and has a higher concentration of Cl^- which may dissolve AgCl further reducing the amount of AgCl bound to the DVD surface.

$$3Ag(s) + AuCl_4^-(aq) \longrightarrow 3AgCl(s) + Au(s) + Cl^-(aq) \quad .....(1)$$

It has been reported in the literature that in the successive rounds of photocatalysis (by the same catalyst) the photodegradation rate becomes slower [24]. Also there is a possibility of the difference between the intensity of the sun light we have used and the 300 W Xe-arc lamps used for the experiments reported in literature, thus lowering the catalytic degradation rate in comparison to literature value[24, 26].

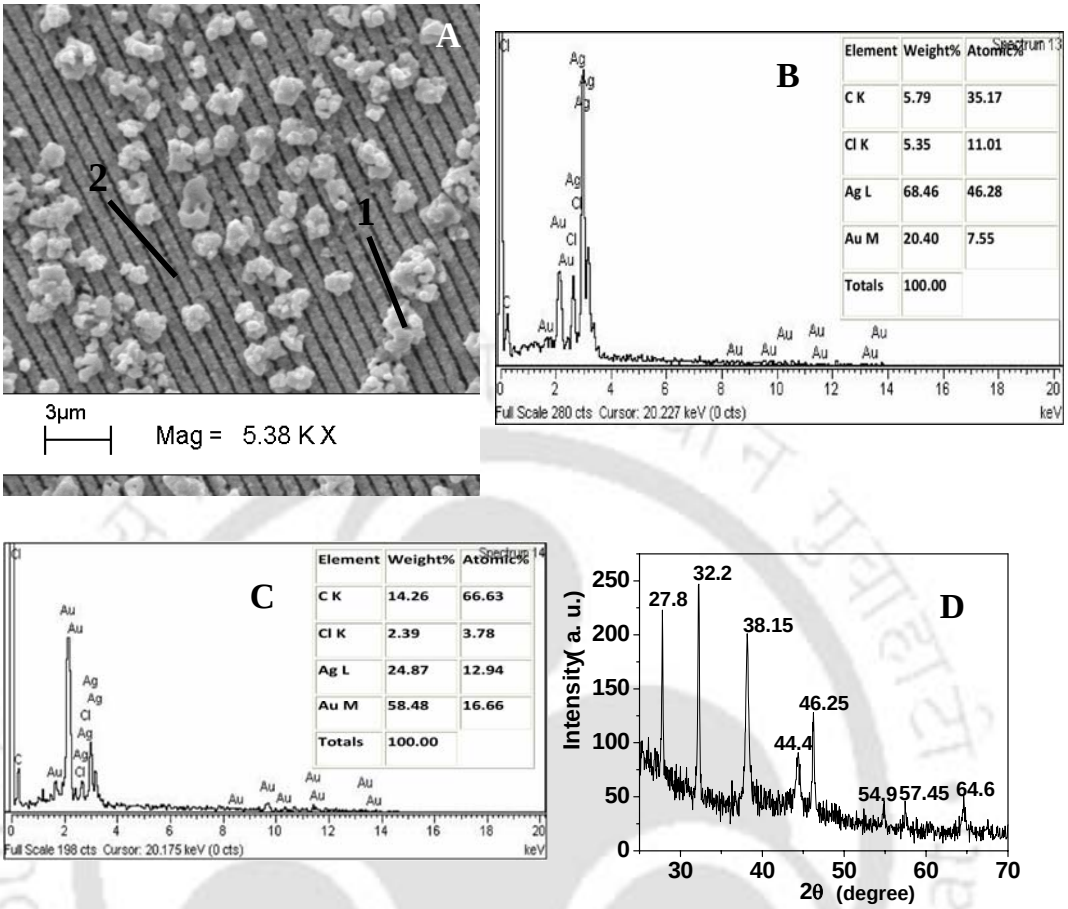

Figure 5.4 Representative SEM image of **(A)** AgClAgAu (DVD) after two consecutive runs photodegradation experiment. **(B)** And **(C)** EDX spectra with the percentage elemental composition table of points 1 and 2 in **(A)**. **(C)** X-ray diffraction pattern of the same sample.

Figure 5.4(A) represents the SEM of the composite AgClAgAu (with the arrays) after the two consecutive cycles of catalysis. It is observed from the SEM image in that the AgCl crystals appeared broken and rounded off after the photodegradation experiment as compared to sharp edged cubic crystals as seen in **Figure 5.1 (A)** of the AgClAgAu (DVD) before photocatalysis. However, the presence of AgCl is indicated by the EDX (**Figure 5.4(B)** and **(C)**). The presence of AgCl in the AgClAgAu (DVD) even after the loss of photocatalytic activity was confirmed by the XRD pattern of the same

sample as shown in **Figure 5.4 (D)**. In the XRD pattern peaks at 2θ values of 27.8^0(111), 32.2^0(200), 46.25^0(220), 54.9^0(311) and 57.45^0(222) confirm the presence of AgCl while peaks at 2θ values 38.15^0(111), 44.4^0(200) and 64.6^0(220) confirm the presence of Ag and /or Au.

According to Wang et. al. [26] possible photocatalytic degradation pathway for MO dye is through an electron hole pair formation mechanism. The surface bound AgCl particles probably has Cl^- as the end groups on the surface of AgCl or there is a possibility of Cl^- adsorbed onto the AgCl surface due to the higher concentration (from $HAuCl_4$ solutions used) of Cl^- ions during synthesis. Hence the AgNPs formed from the Ag^+ ions during the initial stage of MO dye degradation should polarize the electron such as to create positive and negatively charged regions. The surface plasmon resonance of Ag and Au NPs present in AgClAgAu (DVD) lie in the visible region. For the dipolar nature of the surface plasmon the photon adsorbed is likely to be efficiently separated into an electron and a hole such that the hole transferred to AgCl surface corresponds to oxidation of Cl^- to Cl(0) atoms. As chlorine atoms are active radical species they possibly oxidize MO dye and in the process get reduced back to Cl^-. The photogenerated electrons are expected to be trapped by O_2 present in water to produce superoxide ions and other reactive oxygen species. Yu et.al has suggested that these active oxygen species can also take part in photodegradation of MO dye [39].

In another experiment we have determined the rate constant of the photodegradation of MO dye with the same catalyst but in presence of UV light in a chamber and the plot of Ln (C_0/C) versus time in minutes with the linear fits is shown in **Figure 5.5**. The rate constant for the reaction is found to be $0.00657 min^{-1}$. While there was no

degradation observed without the catalyst. This is an interesting observation as this indicates that the UV part of the sunlight may have some crucial role in the photocatalytic degradation by AgClAgAu (DVD) as photocatalytic degradation was not observed in presence of only visible light sources.

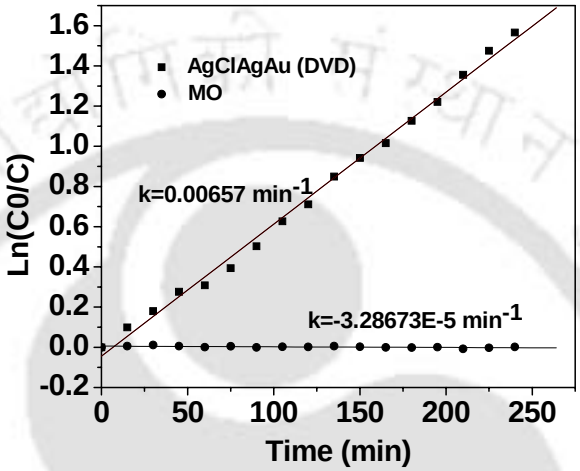

Figure 5.5: Plot of *Ln*(C_0/C) versus time for the photodegradation experiment of MO dye under UV light with the liner fit . Rate constants given near each plot as k.

We have tested the antibacterial activity of the AgClAgAu (DVD) and AgClAgAu (CD) samples towards green fluorescent protein (GFP) expressing *E. coli*. A modified disk diffusion technique was used to probe the bactericidal effect of the composites. Identically sized AgClAgAu (DVD) and AgClAgAu (CD) samples were placed on bacteria-inoculated agar plates and were visualized for antibacterial activity after 12 h and 24 h of incubation. The choice of bacteria spread on agar plates lies with close resemblance with real world situations where pathogenic bacteria are often present on receptive nutrient surfaces in biomedical implants, medical devices, or food packaging surfaces. AgClAgAu (DVD) and AgClAgAu (CD) samples placed on the bacteria-inoculated surfaces killed all the bacteria under and around them. We

observed distinct zones of inhibition (clear areas with no bacterial growth) around the composite samples *E. coli* as shown in **Figure 5.6**. High bacterial growth as indicated by bacterial growth lawn (large indistinguishable collection of colonies) was observed

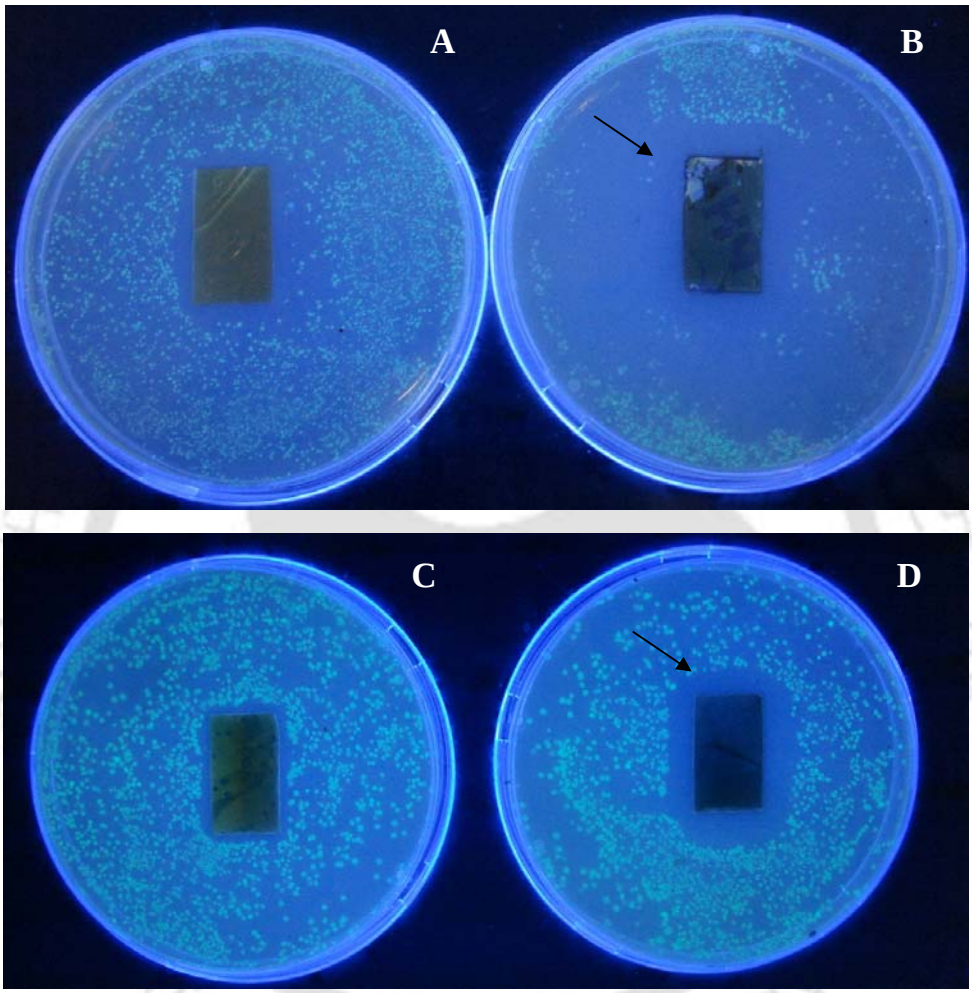

Figure 5.7: Antibacterial activity of **(A)** control Ag foil from CD , **(B)** AgClAgAu (CD) and **(C)** Ag foil from DVD **(D)** AgClAgAu (DVD) samples placed on the LB agar plate inoculated with *E. coli* Zone of inhibition indicated by arrows.

everywhere else. Also, no bacterial growth was observed under or within the composites. Control samples of plain silver foils from CDs and DVDs of similar shape and sizes were kept under identical conditions for observations. As compared to

the samples the control tests showed no zone of inhibition around the CD and DVD foils thus indicating the role of the composite in bacteria annihilation.

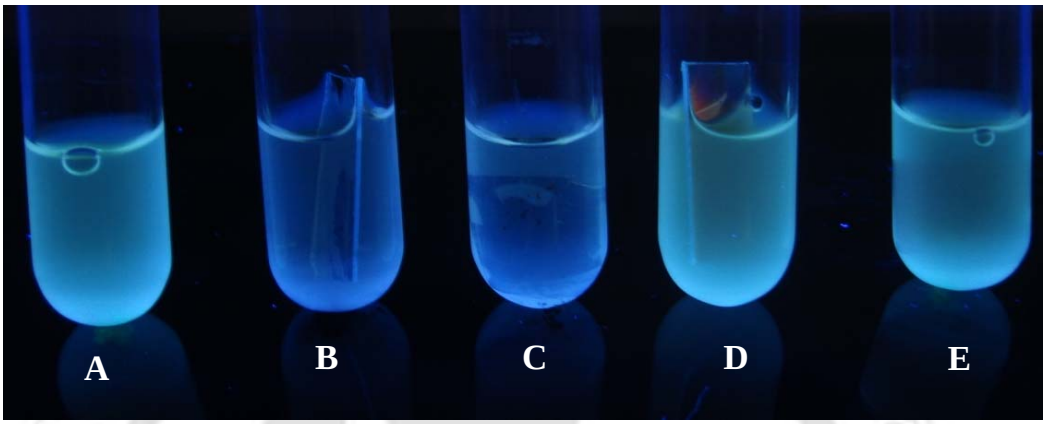

Figure 5.7: Photograph of the samples for bactericidal effect on GFP expressed *E. coli* taken under UV light *(***A)** Control, **(B)** in presence of a 4.03 cm^2 AgClAgAu (DVD) foil, **(C)** in presence of a 2.6 cm^2 AgClAgAu (DVD) foil, **(D)** in presence of a 4.03cm^2 Ag DVD foil, **(E)** in presence of a 2.6 cm^2 Ag foil from DVD.

Moreover, we have also tested the antibacterial ability of these samples against bacterial growth in solution. **Figure 5.7** shows the bactericidal effect of the AgClAgAu (DVD) bacterial growth medium. Here we observed considerable growth of the GFP expressed *E. coli* in the control sample (**Figure 5.7(A)**) as compared to the samples where AgClAgAu (DVD) were present (**Figure 5.7(B),(C)**) in the bacterial growth solutions, indicated by the green fluorescence (from GFP expressing bacteria) in the control sample. Green fluorescence was also observed in other samples (**Figures 5.7(D)** and **(E)**), where bulk Ag thin film from DVD is dipped into the bacterial growth solutions. From this we can infer that AgCl generated on DVD had a prominent bactericidal effect, which was not observed with the DVD silver foil

without the formation of AgCl. One may also argue that the formation of Ag NPs during the process and their presence in the film may also play important role in antibacterial activity.

5.4: Conclusion

In conclusion, we have been able to demonstrate the possible use of surface bound AgCl microcrystals along with Ag and Au NPs in the decontamination of water either via photodegradation of dyes or by their antimicrobial activity. Though in our experiments the rate of photo degradation of MO in presence of light was lower than what has been previously reported by other groups it is worth mentioning that ours is the first case of photocatalyst (AgCl) being synthesized on to a plastic surface, which at the same time has antimicrobial effect. Further, that the photocatalytic activity was tested with direct sunlight rather than Xe-arch lamp used earlier provides a new way of harvesting sunlight for practical applications. This provides the advantages of easy catalyst recovery and less possibility of contamination of the water by the catalyst. With improvement of the dye degradation rate these films have the potential to be used for water purification. Hear we try to reap the benefit of higher reactivity of the micro particles at the same time retaining easy maneuverability of the macro object. The dual role of dye degradation and bacterial annihilation of the film may be of important practical consequences.

References

28. *Nanotechnology Applications for Clean Water;* Savage, N.; Diallo, M.; Duncan, J.; Sustich, R., Eds.; William Andrew Inc: New York, 2009.
29. World Health Organization. *World Health Report*, Geneva, World Health Organization, 2005.
30. Reynolds, K.A. *Water Conditioning and Purification*, **2007**, *39*, pp 66–68.
31. Buitron, C.L.; Quezada, M.; Moreno, G. *Bioresource Technol.* **2004**, *92*, pp143-149.
32. Badr, Y.; Mahmoud, M. A. *J. Phys. Chem. Solids* 2007, *68*, pp 413– 419.
33. Sauer, T.; Nero, G.C.; Jose, H.J.; Moreira, R.F.P.M. *J. Photochem. Photobiol. A: Chem.* **2002**, *149*, pp 147-154.
34. Guyer, G.T.; Ince, N.H. *Ultrasonics Sonochem.* **2003**, *10*, pp 235-240.
35. Sokmen, M.; Allen, D.W.; Akkas, F.; Kartal, N.; Acar, F. *Water Air Soil Pollut.* **2001**,*132*, pp 153-163.
36. Robinson, T.; McMullan, G.; Marchant, R.; Nigam, P. *Bioresour. Technol.* **2001**, *77*, pp247-255.
37. McKay, G.; Porter, J.F.; Prasad, G.R. *Water Air Soil Pollut.* **1999**, *114*, pp 423-438.
38. Kannan, N.; Meenakshisundaram, M. *Water Air Soil Pollut.* **2002**, *138*, pp 289-305.
39. Gogoi, S. K.; Gopinath, P.; Paul, A.; Ramesh, A.; Ghosh, S. S.; Chattopadhyay, A. *Langmuir* **2006**, *22*, pp 9322-9328.
40. Feng, Q. L.; Wu, J.; Chen, G. Q.; Cui, F. Z.; Kim, T. N.; Kim, J. O. *J. Biomed. Mater. Res.* **2000**, *52*, pp 662-668.
41. Batarseh, K. I. *J. Antimicrob. Chemother.* **2004**, *54*, pp 546-548.
42. Baker, C.; Pradhan, A.; Pakstis, L.; Pochan, D. J.; Shah, S. I. *J. Nanosci. Nanotechnol.* **2005**, *5*, pp 244-249.
43. Catalina Marambio-Jones, C.; Hoek, E. M. V. *J. Nanopart. Res.* 2010**,** *12*, pp1531-1551.
44. Tratnyek, P. G.; Johnson, R. L. *NanoToday* **2006**, *1*, pp 44– 48
45. Zhang, H.; Chen, D.; Lv, X.; Wang, Y.; Chang, H.; Li, J. *Environ. Sci. Technol.* **2010**, *44* , pp 1107–1111.

46. Daskalaki, V. M.; Antoniadou, M.; Puma, G. L.; Dimitris, I. K.; Lianos, P. *Environ. Sci. Technol.* **2010**, *44*, pp 7200−7205.
47. Zhao, D.; Chen, C. C.; Wang, Y. F.; Ma, W. H.; Zhao, J. C.; Rajh, T.; Zang, L. *Environ. Sci. Technol.* **2008**, *42*, pp 308– 314.
48. Borgarello, E.; Kiwi, J.; Gratzel, M.; Pelizzetti, E.; Visca, M. *J. Am. Chem. Soc.* **1982**, *104*, pp 2996–3002.
49. Elahifard, M. R.; Rahimnejad, S.; Haghighi, S.; Gholami, M. R. *J. Am. Chem. Soc.* **2007**, *129*, pp 9552–9553.
50. Shang, M.; Wang, W. Z.; Zhang, L.; Sun, S. M.; Wang, Lu.; Zhou, L. *J. Phys. Chem. C* **2009**, *113*, pp 14727–14731.
51. Li , Y.; Ding, Y. *J. Phys. Chem. C* **2010**, *114*, pp3175–3179 .
52. Lanz, M.; Calzaferh, G. *J. Photochem. Photobiol. A* **1997**, *109*, pp87-89.
53. Wang, P.; Huang, B.; Qin, X.; Zhang, X.; Dai, Y.; Wei, J.; Whangbo, M. H. *Angew. Chem. Int. Ed.,* **2008**, *47*, pp7931-7933.
54. Glaus, S.; Calzaferri, G.; Hoffmann, R. *Chem. Eur. J.* **2002**, *8*, **pp**1785–1794.
55. Wang, P.; Huang, B. B.; Zhang, X. Y.; Qin, X. Y.; Dai, Y.; Jin, H.; Wei, J. Y.; Whangbo, M. H. *Chem. Eur. J.* **2008**, *14*, pp 10543–10546.
56. Morimoto, T.; Suzuki, K.; Torikoshi, M.; Kawahara, T.; Tada, H. *Chem. Commun.* **2007**, pp 4291–4293.
57. Currao, A.; Reddy, V. R.; Calzaferri, G. *Chem. Phys. Chem.* **2004**, *5*, pp720–724.
58. Porel, S.; Singh, S.; Harsha, S. S.; Rao, D. N.; Radhakrishnan, T. P. *Chem. Mater.* **2005**, *17*, pp 9-12.
59. Matsui, J.; Akamatsu, K.; Hara, N.; Miyoshi, D.; Nawafune, H.; Tamaki, K.; Sugimoto, N. *Anal. Chem.* **2005**, *77*, pp 4282– 4285.
60. Malynych, S.; Luzinov, I.; Chumanov, G. *J. Phys. Chem. B* **2002**, *106*, pp1280– 1285.
61. Zayat, M.; Einot, D.; Reisfeld, R. *J. Sol -Gel Sci. Tech.* **1997**, *10*, pp64-74.
62. Srnova´-Sÿloufova, I.; Lednicky, F.; Gemperle, A. Gemperlova, J. *Langmuir* **2000,** *16*, pp 9928-9935.
63. Chen, D. H.; Chen, C. J. *J. Mater. Chem.*, **2002**, *12*, pp1557–1562.
64. Houas, A.; Lachheb, H.; Ksibi, M.; Elaloui, E.; Guillard, C.; Herrmann, J. *Appl. Catal. B: Environ.* **2001**, *31*, pp145-157**.**

65. *Vogel's Text Book of quantitative Chemical Analysis, 5th edition;* Jeffery, G. H.; Bassett, J.; Mendham, J.; Denney, R. C. Eds., , Addison Wesley Longman: Essex, 1989, pp 67-70.

66. Yu, J.; Dai, G.; Huang, B. *J. Phys. Chem. C* **2009**, *113*, pp16394–16401.

Chapter VI

Chemical Reaction Based Generation of Electronically Transparent AgAu Thin Films

6.1: Introduction

Transition metal nanoparticles (NPs) occupy a major share in nanotechnology[1,2] research for their special catalytic[1,3-8], optical [1,10-15] and electronic properties[1,13,14]. Among the metal NPs, gold (Au) and silver (Ag) NPs occupy the centre stage for their relatively high stability, excellent optical properties [16-18], promising catalytic activity[6,9,16] and relatively low toxicity [18] (although cytotoxicity of Ag NPs are known at their high concentrations [19]). At the same time bimetallic NPs of silver and gold open up another direction of the properties of NPs [20-28] for bimetallic NPs have distinctly different properties from the individual metallic NPs [22]. This gives dual control to the NP properties in terms of composition leading to varying catalytic and optical activity. However, the best use of the NPs would require construction of devices with tunable properties based on the compositions and the devices need to be portable and workable. One form of the constructions could be films (even better in the form of flexible ones) where the NPs would be deposited on the surface of the films. The stable NPs on the film would provide easily accessible optical, chemical and other properties so desirous in the multitude of applications. Thin films composed of monometallic [30-36] or bimetallic [37-41] NPs are of special importance for their various applications as in biosensing [42, 44] and in the preparation of optoelectronic nanodevices [45-50]. Additionally, intensive research is being pursued in NP based structured films for their potential applications in catalysis [39,51-53], microelectronics [54], photonics [49,55,56], optoelectronics [45-50] , molecular recognition [57,58], and chemical [59,60] and biological sensing [59-61]. The functional properties of NP assemblies are dominated by the NP type (size, shape and composition), surface properties and the spatial distribution of the particles in the film[39]. A prime requirement in the development

and preparation of the films is the ability to controllably assemble NPs in the film with preferably predictable and well defined structural characteristics for desired physical and chemical properties. The development of newer methods to prepare nanostructures with tailored properties (electrical, optical, electrochemical, magnetic, surface etc.) will be crucial to the exploitation of nanostructured thin films [50, 51]. Present technologies for nanostructured thin film generation [51,63,64] include vapor phase based methods like evaporation, molecular beam epitaxy (MBE), sputtering, chemical vapor deposition (CVD), and atomic layer deposition (ALD) and liquid phase deposition methods like electrochemical deposition, chemical solution deposition (CSD), Langmuir-Blodgett technique, self-assembled monolayers (SAMs), layer by layer deposition and polymeric template depositions. Apart from the pure metal films polymer-NP composite films are also known [65]. There have also been attempts to embed ordered structures in thin films for surface enhanced luminescence[40], for antireflective[66-68], superhydrophilic (antifogging) [68, 69], superhydrophobic [69,70] materials and photonics applications[68]. For example, thin films showing photonic activity consist of ordered subwavelength structures that can control the propagation of light by allowing certain wavelengths (or range of wavelengths) to pass through it [55, 56,71]. Use of ultrathin grafted NP film to impart desired chemical and physical properties onto various solid substrates is of great importance in preparing new composite and functional materials[64]. Moreover for commercialisation, simple, economic and rapid manufacture of these thin films is of great significance. Interestingly, chemical reaction based formation of arrays of NPs on films have not been reported so far. This is important as one can use various principle of chemistry to not only form and organize the NPs but also tune the properties of the assemblies formed out of the NPs and their components.

Herein we report the formation of thin corrugated films of AgAu composite NPs starting with commercially available metallic silver deposited compact discs (CDs) and digital versatile discs (DVDs) (structure of CD/DVD and the method of obtaining the silver foils from CDs/DVDs are discussed in **Chapter IV**, hence will not be repeated here). The films were nanoporous, consisting of interconnected networks of fused NPs of Ag and Au. The corrugated films, which could be generated by galvanic replacement reactions of patterned metallic Ag foils by $HAuCl_4$ in the presence of cetyltrimethylammonium bromide (CTAB), were amenable to manipulations such as floating on water and being able to transfer to glass slides. The corrugations present in the films had the motifs of the parent CD or DVD which are engraved on the polycarbonate plates of the discs. The optical properties of the films revealed those of characteristics of AgAu bimetallic nanoparticles. In our method we try to reap the benefits of both "top down" and the "bottom up" [72-74] synthetic strategies along with the template growth of thin films. The top down generated structures were bulk silver foils with corrugated structure present in the CDs or DVDs which were to be galvanically replaced partially by the oxidizing agent $HAuCl_4$; while the ionic $AuCl_4^-$ reacted with bulk Ag and got reduced to be deposited as NPs providing a bimetallic thin films with sub 100 nm thickness thus constituting the bottom-up part of the approach. The presence of the surfactant, CTAB, is critical in not only the formation of the film based on the original template but also in removing the film so formed from the template (CD substrate). The three-dimensional nature of the films provides additional advantages for future generation of thin NP based films with well-defined morphology in terms of surface undulation. This can potentially be an important method for generating thin films consisting of NPs especially for the surfaces where direct deposition is not possible. Interestingly, films generated from previously

'written' CD retained the patterns of the original imprints thus providing a way of generating 'written' films with corrugated structures.

6.2: Experimental Section

6.2.1: Materials and Substrates: Chloroauric acid ($HAuCl_4$, 17% in HCl) and cetyltrimethylammonium bromide (CTAB) were purchased from Sigma-Aldrich (Germany) and were used as received. CDs and DVDs were purchased from the local market. Milli-Q grade water was used for making all the solutions and for washing purposes. Glass cover slips were purchased from Bluestar, India. NaCl was obtained from Merck India Ltd..

6.2.2: Preparation of the AgAu thin films: Before performing any chemical reaction, the silver foils from CDs and DVDs were detached from the polycarbonate layer by using a cello tape after cutting the CDs and DVDs into small pieces. The details were discussed in **Chapter IV**. AgAu thin films were prepared by reacting approximately 1.55 cm x 2.6 cm pieces of silver foils with different concentrations of $HAuCl_4$ present in 10.0 mL solutions, which also contained 0.1M CTAB. The treatment led to change of the color of silver of the CD or DVD into golden in about 10-12 h. The best films were obtained from the reactions of the silver foils with 2.0 x 10^{-4}M - 5.0 X 10^{-4}M $HAuCl_4$ solutions. It is worth mentioning here that the time for appearance of golden color depended on the concentration of $HAuCl_4$, which was early for high concentration of $HAuCl_4$, while it took longer time at low concentrations. On keeping the samples in solution after the appearance of the golden color, the color gradually disappeared leaving behind a blue coloration on the CD or DVD substrate. The samples thus prepared (golden colored ones) were washed

carefully with water and air dried. Dried samples were used for further characterizations.

6.2.3: Scanning Electron Microscopy (SEM): Leo-VP 1430 scanning electron microscope (SEM) equipped with an Oxford-INCA energy dispersive X-ray (EDX) analyzer was used to characterize all the samples. Images were recorded using the secondary electron detector. Approximately 5.0 mm x 5.0 mm pieces from different samples were taken for analysis. For some of the samples, thin films were transferred to aluminum foils or glass substrates before measurements. This was pursued by first putting the film, prepared on the original CD or DVD substrate, in saturated NaCl solution and then suspending the films in water. By carefully placing the aluminium foil or glass cover slip below the floating films they could then be lifted (and thus be transferred). Except for the samples transferred onto aluminum foil all samples were coated with a thin layer of gold prior to SEM imaging, in order to make them conducting so as to avoid charging of the samples. We have used the EDX studies to show the relative elemental abundance in the films and the substrates on which the films were placed like the substrate from the CD or DVD or the glass cover slips.

6.2.4: Transmission electron microscopy (TEM) Characterization: TEM images were recorded for the thin films after transferring the films on to 300 mash copper grids. The transfer was achieved in a way similar to above where aluminium foil or glass cover slip was replaced by the grid. The instrument used was a Jeol JEM-2100 transmission electron microscope operating at a maximum voltage of 200 kV.

6.2.5: Atomic Force Microscopy (AFM): AgAu thin films transferred onto glass cover slips were used for AFM studies. The instrument used was a Vecco Multimode

SPM attached with a Nanoscope IV controller (manufactured in USA). Images were recorded in contact mode with silicon nitride tips.

6.2.6: X-Ray Diffraction (XRD): A Bruker D8 Advanced powder X-ray diffraction (XRD) instrument was used to characterize the samples. Samples of approximately 3.0 cm x 2.5 cm dimensions were then analyzed using XRD. Also, XRD of the thin films after being transferred cover slips were recorded.

6.2.7: UV-Visible spectroscopy: The samples were first transferred onto a cover slip by the same method mentioned earlier. Then the UV visible spectra of the samples were recorded in a Perkin Elmer Lambda25 instrument by vertically placing the sample carrying cover slip in the path of the beam with blank cover slip used as reference.

6.2.8: Infra Red (IR) Spectroscopy: For infrared spectroscopic characterization of the samples a Perkin Elmer Sepctrum One FTIR spectrophotometer was used. The samples here were prepared by scrapping off the AgAu films from the lacquer layer of CD/DVD and then mixed with KBr to make translucent pallet for the measurement. Also the FTIR spectrum of CTAB in KBr pallet was recorded.

6.2.9: Optical Imaging: Images of the films transferred to a glass cover slip is taken in both the reflected light and the transmitted light by a Nikon-D3000 SLR camera. Reflected light photographs were taken in the same way as the regular photography while for the transmitted light image a normal fluorescent lamp was placed behind the sample containing cover slip and the camera focussed at the light.

6.3: Results and Discussion

When the Ag foil parts (being attached to the lacquer) of a CD and DVD were immersed in aqueous solutions of $HAuCl_4$ in the presence of CTAB golden coloration of the surface of the foils could be observed in about 12 h. The foils were then taken out and washed with deionised water followed by placing the same into a petri-dish full of water. Upon gentle shaking the films could be observed to come out and float on the water surface. The films were then ready for transfer. Typically, 1.55 cm x 2.6 cm pieces of Ag foils were immersed in 10 mL water containing 2-5 X 10^{-4} M $HAuCl_4$ and 0.1 M CTAB in order obtain the best of films. **Figure 6.1** shows the representative SEM image of one of the films generated from a CD silver foil. It is interesting to note that the film appear to consist of tracks of parallel lines which could be the original patterns of the foil. Further details in this regard are discussed in the subsequent sections.

Encouraged by the success of formation of corrugated films obtained from the foil of a CD, we were further interested in producing such films from the foils of DVD in the hope to generate films with higher density of lines of corrugation as a DVD consists of tracks of higher density than a CD. Typically, the width of a DVD track is about 400 nm [75]. It was observed that films like those obtained from a CD could also be generated from DVD, the details of which are presented in the subsequent sections.

The films obtained by reaction of Ag foils, obtained from CDs and DVDs, with $HAuCl_4$, appear visibly similar. For example, when photographed ordinarily the film appears golden in colour **Figures 6.2(A)**. On the other hand, when the same film is

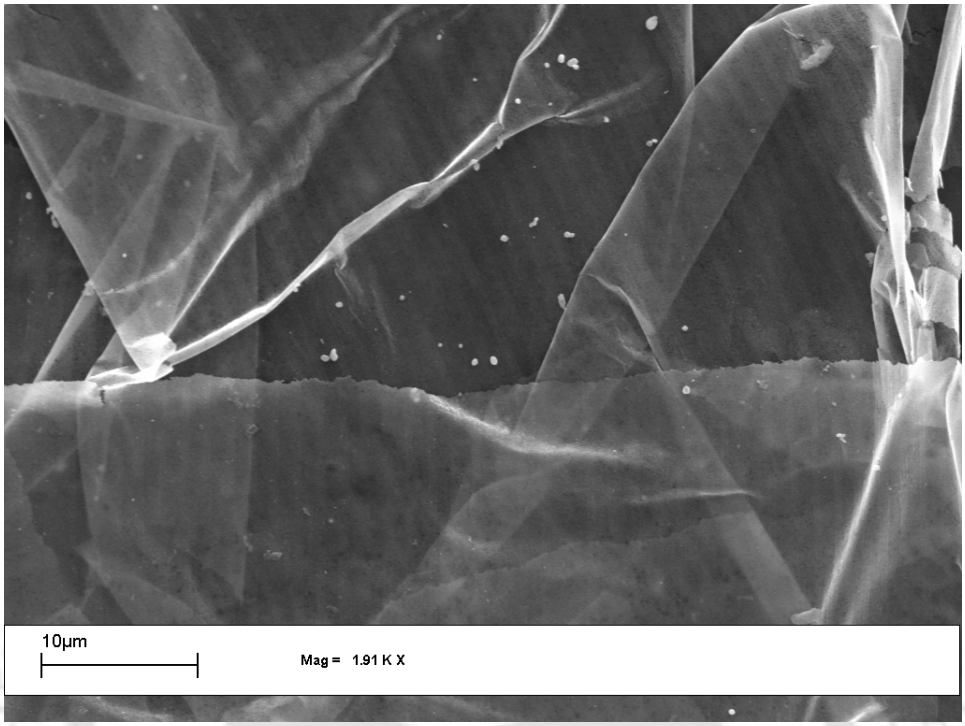

Figure 6. 1: Representative SEM image of AgAu NP film obtained by reacting $HAuCl_4$ with Ag foil from a CD.

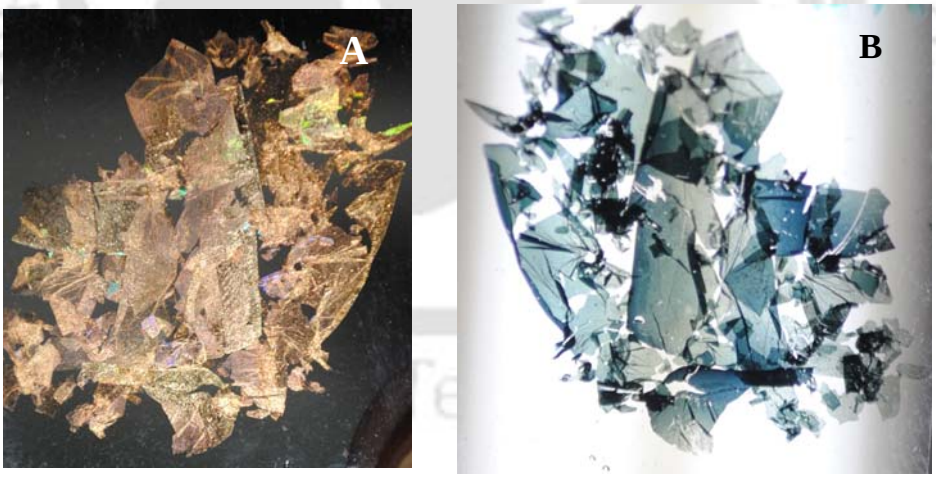

Figure 6.2: Representative image of the thin films generated from CDs transferred onto a glass cover slip recorded by a digital camera,(**A)** in the reflected light and **(B)** in the transmitted light.

photographed with illumination from the opposite direction it appears blue **Figures 6.2(B)** [76]. Also, the presence of interference fringes in the photograph recorded in reflected mode is apparent in **Figure 6.2(A)**. The appearance of different colors in reflected and transmission mode indicated the presence of Au NPs, the color of which are known to appear differently depending on the view especially blue in the transmittance mode of observation, especially when the particle sizes are large or assembly of smaller particles are present [76].

SEM images of the films obtained from CD and DVD are shown in **Figure 6.3**. As is clear from **Figure 6.3(A)**, a thin film was formed on top of the substrate (lacquer) of the CD, with clear indication of the presence of serrated lines in the film. It is important to mention here that similar lines were also observed in the films obtained from DVD, although of higher resolution. In addition, it is interesting to note that the particles (crystals!) which were present on the surface of the substrate could be observed through the film. Considering that the accelerating voltage of electrons (in SEM) was 20 kV the film must be sufficiently thin to help observe the particles present underneath both in the films generated from CDs and DVDs as shown in **Figures 6.3(A)** and **6.3(B)** respectively. Importantly, the particles could also be observed underneath the part of the film that was folded i.e. through two layers of the film as could be observed in **Figure 6.3(A).** This is interestingly indicative of the partial transparent nature of the films to the impinging electrons. A higher resolution image, shown in **Figure 6.3(C)**, indicated that primary structural motif of the original CD was maintained in the generated film. The crest-crest pitch was found to be 1.6 μm (**Figure 6.3(C)**), while in the films generated from DVDs crest-crest pitch of approximately 900 nm (**Figure 6.3(B)**)**.** In other words, the pitches of the films

matched with those of the templates present in the original CD and DVD films respectively. It may be mentioned here that overall integrity of the film formed was substantial with minimum presence of discernible deformation or damage. The observed cracks or damage probably occurred during handling (using forceps) and transfer for recording the images. Additionally, the film could be transferred to a glass slide or other substrate and measurements could be recorded. SEM image of a transferred film is shown in **Figure 6.3(D)**.

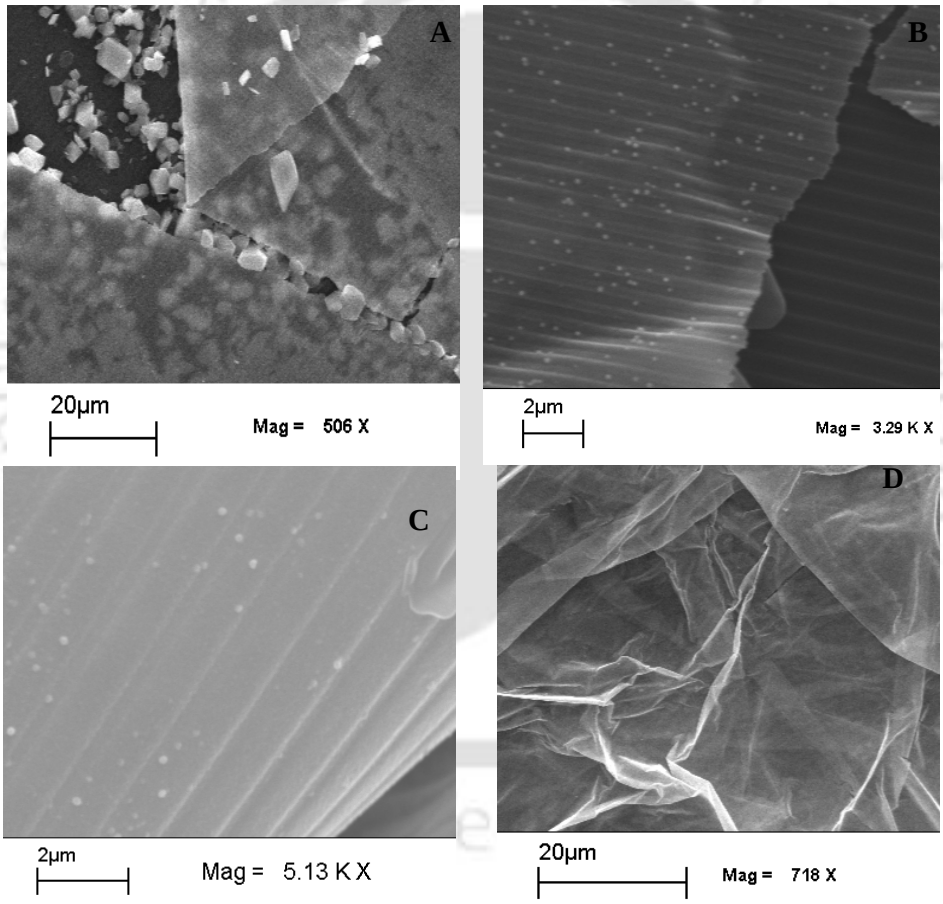

Figure 6.3: SEM images of the thin films generated from the silver foil of **(A)** CD as it is on the CD substrate **(B)** of a DVD **(C)** at a higher magnification showing the CD tracks having been transferred to the film; while **(D)** after being treated with saturated NaCl solution and transferred to an aluminum foil.

The EDX studies carried out along with the SEM images at different points of the film provided us with valuable information about the chemical composition of the films. In order to probe the details of chemical composition as prepared films were observed under SEM along with EDX experiments. **Figure 6.4** shows the SEM image of a thin film generated from an Ag foil of a CD by reacting with 2.2 X 10^{-4} M $HAuCl_4$ in the presence of 0.1 M CTAB and the EDX spectra of different spots in the image are shown in the accompanying figures. In the image (**Figure 6.4(A)**) the spots on which the EDX spectra were recorded are marked by the Roman numerals **(i, ii, iii)** and the same nomenclatures are used for labeling the spectra. **Figure 6.4 (i)** shows the spot EDX spectrum with the elemental percentage in parenthesis, of the thin film at spot **(i)** in **Figure 6.4(A),** where it is observed that the weight percentage of Ag and Au were 8.60% and 25.84% respectively along with those of with Br (5.25%) and C (60.31%). Although EDX spectral analysis does not provide actual quantitative measure of the concentration of the elements the relative abundance could be established for two elements when present together. Thus it is plausible that the film was made of Au and Ag and CTAB was bound to the film[77] which we will discuss a little later in this chapter (as confirmed by FTIR spectroscopy). There is the possibility of carbon from the CD substrate (the protective layer), which adds to the total carbon as the films are considerably transparent to the electron beams, EDX from the substances below the film is recorded simultaneously though it is unwanted. As the film is transparent to the electron beam it passes through the film and sees the substrate below generating X-rays reaching the EDX detector. The CD substrate contains high percentage of C (74.08%) as observed from **Figure 6.4 (iii)**. Also, one cannot rule out the presence of carbon in the film having been transferred from the

lacquer part during formation. On the other hand, the large cuboidal particles (with edge dimensions on the order of 1 μm) which are present on the surface of the CD

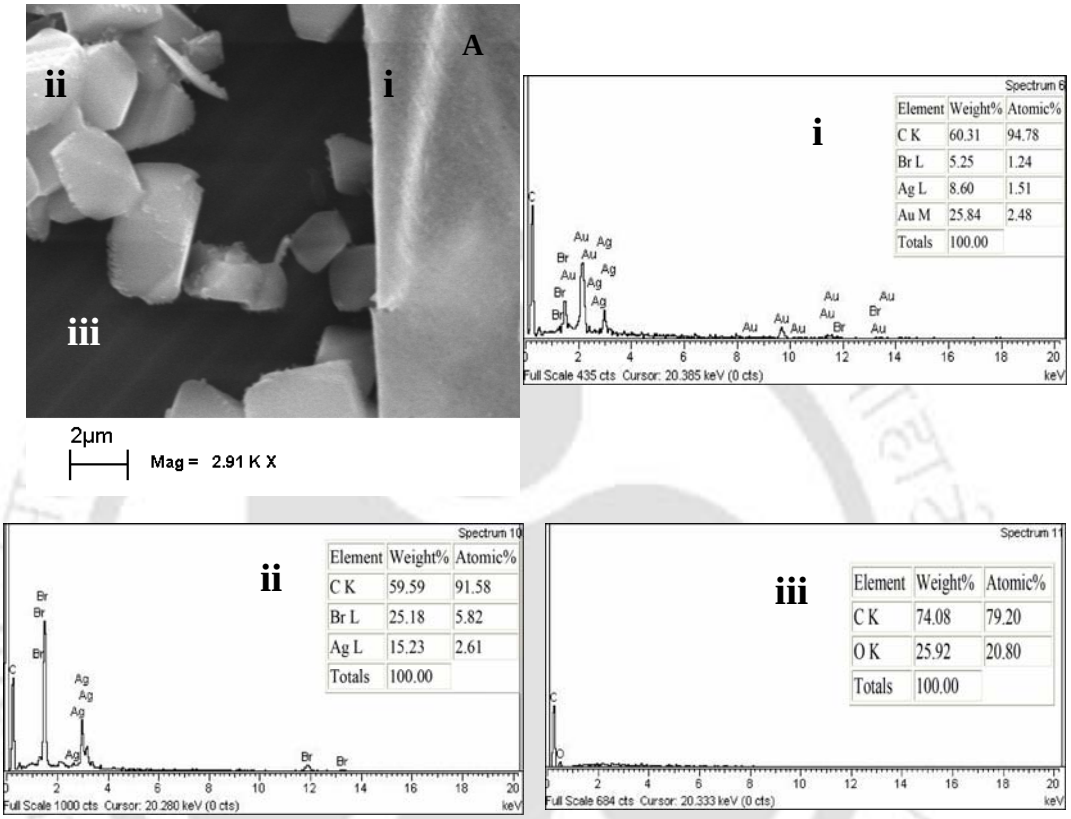

Figure 6.4: (A) SEM image of a part of a sample (from CD) directly viewed after initial washing with deionized water followed by drying. In the figure three spots which are marked (i, ii and iii) correspond to the spot EDX spectra recorded **(i)** on the thin film; **(ii)** on the bright particles and **(iii)** on the CD substrate.

consist of Ag and Br in addition to carbon. This could mean that these particles are made of AgBr crystals and possibly CTAB molecules are attached to the particles providing the source of carbon in the spectrum. It is plausible that the galvanic replacement of Ag by $HAuCl_4$ produced Ag and Au composite film, whereas AgBr crystals were generated from the oxidized Ag, in the presence of excess Br^- present in

the medium (from CTAB) in comparison to the concentration of Cl^- (from $HAuCl_4$). The EDX spectrum of the background consisting of the remainder of the CD indicated the presence of carbon (in addition to oxygen).

The galvanic replacement reaction involved may be as shown below..

$$3Ag + HAuCl_4 \longrightarrow 3AgCl + Au(0) + H^+ + Cl^-$$

As it is obvious that for solubility products of silver bromide (5.35×10^{-13}) is lower than silver chloride(1.77×10^{-10}) [78], silver bromide will be precipitated in preference to silver chloride which is observed in our SEM image and EDX studies as shown in **Figure 6.4** (**A)** and **Figure 6.4 (ii).** Also, the grey particles observed with the thin films contained Br and no Cl.

It can be seen from the XRD patterns of Ag foils obtained from CD (**Figure 6.5(A)**) and DVD (**Figure 6.5 (B)**) that they are composed of pure silver. It is evident from the figures that the patterns consisted of three major peaks (for both foils) occurring at 2θ values of 38.1°, 44.4° and 64.5°. These peaks correspond to (111), (200) and (220) planes of metallic Ag [79,80]. Though there is an extra peak in the XRD pattern for CDs (**Figure 6.5 (A)**) at 2θ value 42.7°, which we were unable to assign, however, can be attributed to the background protective layer of the CD. After treatment of the silver foils with $HAuCl_4$ at different concentrations in 0.1M CTAB thin films of AgAu could have been formed. Along with the film silver bromide might also have formed. **Figure 6.5 (C)** and **Figure 6.5 (D)** shows the representative XRD patterns of AgAu thin films generated from the CDs and DVDs respectively. Now, as metallic gold and silver have similar lattice constants, therefore they show identical X-ray diffraction peaks [79, 80]. In **Figure 6.5 (C)** we have peaks at 2θ values of 38.2°, 44.5°, 64.55° and in **Figure 6.5 (D)** at 38.15°, 44.35°. These peaks could be due to elemental

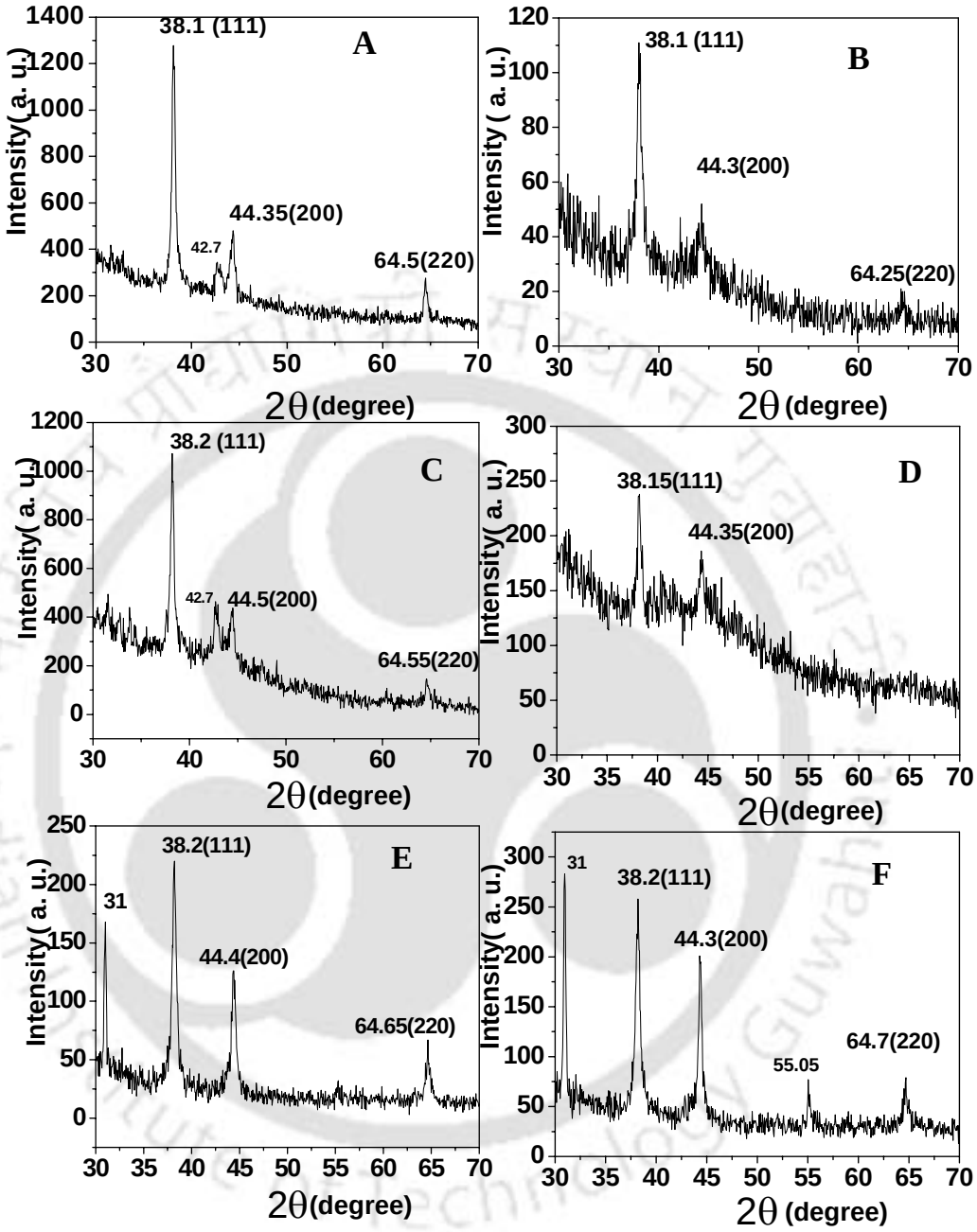

Figure 6.5: X-ray diffraction patterns, of the reflective layers from **(A)** CD and **(B)**, DVD without any further treatment, of Ag-Au thin films generated from **(C)** CD and **(D)** DVD reflective layers, by reacting with $HAuCl_4$ followed by washing with deionized water, of Ag-Au thin films from **(E)** CD and **(F)** DVD after treating with saturated NaCl solution and transferred to glass cover slip. Major peaks are identified with the 2θ values corresponding to places written in parentheses.

Ag or Au or due to both. But one point is sure that there is no other Ag or Au compound present in the film that can give a XRD peak. Again, considering the results from EDX spectroscopic studies (**Figure 6.4**) it can be said with reasonable certainty that a composite of Ag-Au bimetallic film was formed from the reaction of Ag film on the CD (or DVD) with $HAuCl_4$ in the presence of CTAB. Further, when the film was treated with saturated solution of NaCl and transferred to glass cover slips, peaks characteristic of AgBr [81] crystals appeared at 31^o (**Figure 6.5(E)**) and at 31^o and 55.5^o (**Figure 6.5(F)**). It is plausible that Br^- ions present as counter ions in CTAB which was adsorbed to the film were replaced by the Cl^- ions from NaCl for Cl^- is harder than Br^-. Now the released Br^- reacted with adsorbed Ag^+ ions to form less soluble AgBr in the form of crystals.

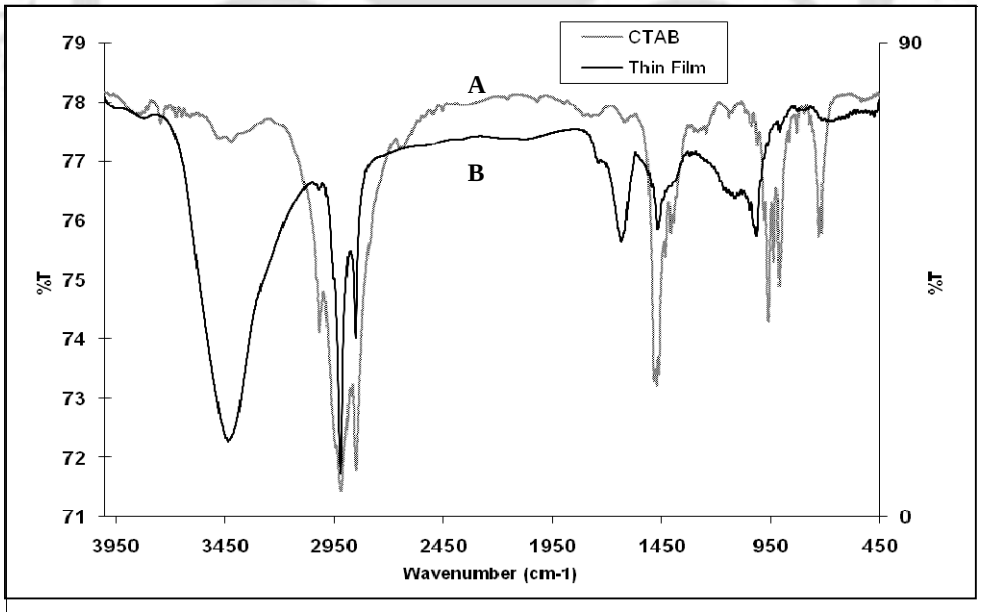

Figure 6.6: FTIR spectra of **(A)** CTAB and **(B)** of thin film obtained from DVD.

EDX studies have shown that carbon and bromine from CTAB were present on the thin films after being washed with deionized water. A comparison of the FTIR

spectra of thin film (palletized in KBr) with the pure CTAB (also palletized in KBr) as shown in **Figure 6.6**, supports the presence of CTAB in the thin films. The FTIR spectral features in the CH_2 symmetric and antisymmetric vibrational region (~3000-2800 cm^{-1}) appear similar for pure CTAB as well as for the thin film sample [77].

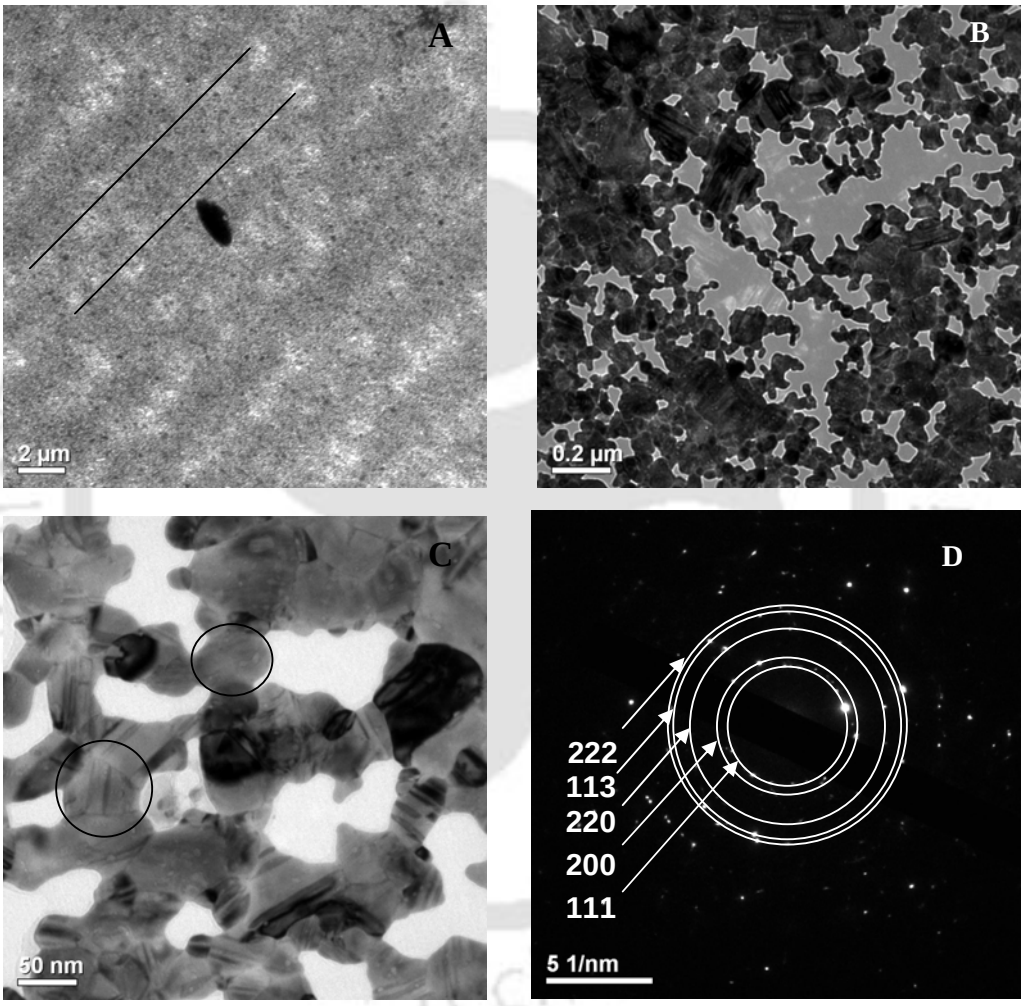

Figure 6.7: Transmission electron microscopic images at three different magnifications **(A)**, **(B)** and **(C)** of a film generated from a CD. **(D)** Selected area electron diffraction (SAED) results recorded on a part of the AgAu film generated from CD Ag foil, the image of which is shown in **(C)**.

TEM images of a AgAu film generated from CD are shown in **Figure 6.7**. The film was washed with water and then transferred to the copper grid for recording of the image. It may be mentioned here that for better clarity and structure of the films of images over different magnifications films from CD and DVD were imaged using TEM (as opposed to by SEM only). In the low magnification TEM image, **Figure 6.7(A)**, of film generated from CDs appear devoid of the original structures from the CD, but a careful observation shows that there are parallel tracks as marked by black lines. These lines are approximately 2 μm apart which is the same as the distance from centre of the crest-crest or trough - trough in the original CD. It may be possible that a slightly higher values of centre-centre distance than measured by SEM was due to expansion of the corrugated film upon transfer to the TEM grid. Higher magnification image in **Figure 6.7(B)** shows porous nature of the film. In **Figure 6.7(C)** we can see that the nanoparticles (NPs) constitute the film and the formation of the film was a result of fusion of the NPs. Also the NPs forming the film can be seen here as marked by black circles. Selected area electron diffraction (SAED) results of the film (**Figure 6.7(D)**) indicated metallic nature of the film with the presence of polycrystalline particles.

Figure 6.8 shows the representative images of a section of the film generated from DVD recorded at increasingly higher magnification. The images indicate that the film was rather thin so as to be able to record the TEM and the transparency of the film is further supported by the clarity of the images. **Figure 6.8(A)** indicates a rather continuous film that grew well according to the template of the original DVD. The lines are distinct with pitch length being 1.0 μm, further supporting the results

obtained from SEM studies. Interestingly, **Figure 6.8(B)** shows the presence of systematic perforation in the film. A careful examination reveals that the perforation

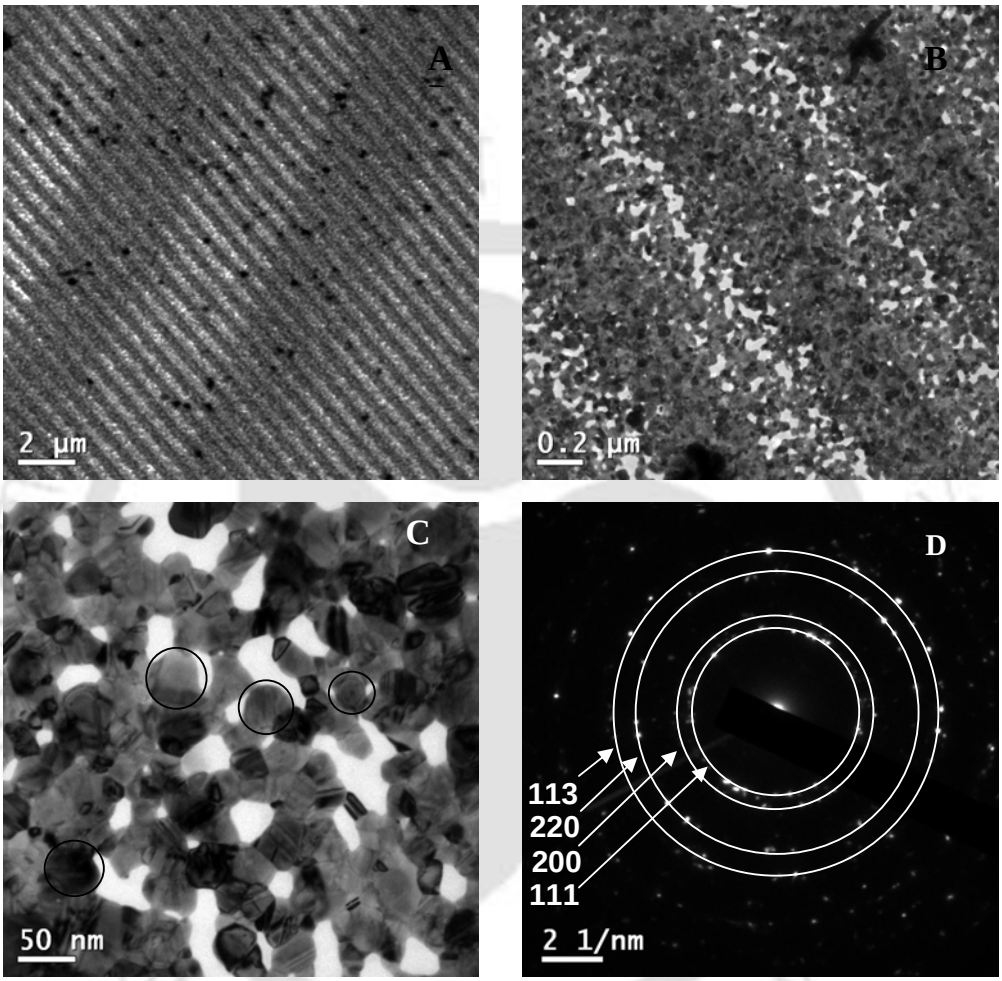

Figure 6.8: Transmission electron microscopic images at three different magnifications (**A),(B)** and **(C)** of a film generated from a DVD. (**D**) Represents selected area electron diffraction (SAED) results recorded on a part of the DVD, the image of which is shown in (**C)**.

primarily occurred at the troughs of the film and there were no discernible systematic perforations in the crests of the film, although the presence of a few holes could be observed. Imaging at higher magnification (**Figure 6.8(C)**) indicated the presence of

distinct holes in the film with sizes on the order of 50-100 nm. The holes did not have any distinct shapes in particular. In addition, discrete networks of nanoscale structures surrounding the holes could be observed. The presence of dark and lighter regions in the network possibly indicates merged particles of varying thickness with the darker ones representing thicker one. SAED results of the film (**Figure 6.8(D)**) indicated metallic nature of the film with polycrystalline particles that formed the network structures of the film.

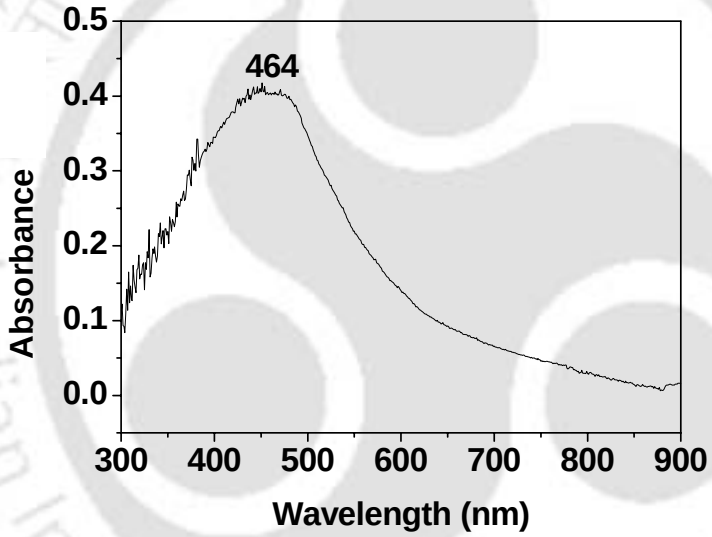

Figure 6.9: Representative UV- Visible spectrum of the film generated from CD

UV-visible spectra of the films showed the AgAu bimetallic nature of the films[24], as indicated by the absorbance in the range of 400nm to 500nm with maxima around 464nm in **Figure 6.9**. It must be mentioned here that UV-visible spectra of the films are often overlapped by the interference caused by the lines on the film as well as the thinness of the films [82].

AFM images of thin films generated from both CD and DVD recorded in contact mode with a silicon nitride tip are shown in **Figure 6.10. Figure 6.10(A)** and **Figure 6.10(B)** show the AFM topographic image of a thin film generated from a CD and DVD respectively. For the films generated from CD the original pattern of the CD tracks appeared somewhat distorted, although the tracks can be seen but with careful observation as marked by black lines in the **Figure 6.10(A)**. The tracks are separated by a distance of approximately 1.3 μm. This may be due to spreading of the film. A cartoon of the spreading process is shown in the inset of the same figure. In a CD the widths of the crest and trough are both 1μm each while the height difference between crest and trough is approximately 120 nm. Now after spreading of the film the desistance between crest to crest becomes 120nm+ 1μm+120nm≈ 1.3 μm as observed from the image as well as the height profile **Figure 6.10 (C)**. On the other hand the initial DVD pattern is well retained in the thin films generated from the DVD **Figure 6.10(B)**. Height profile of the films from DVD , **Figure 6.10(D)** shows the distinct crests and troughs with distance between centre of the crest to crest approximately 900 nm (width of the crest or trough ~400 nm + half from each crest 200 nm + 200 nm = 800 nm). The three dimensional views of the films from CD and DVD are sown in **Figure 6.10(E)** and **Figure 6.10(F)** respectively indicating the three dimensional nature of the films. Here both the original CD or DVD pattern and the nanoparticulate nature of the films are well observed. The nanoparticulate nature i.e. the NP building blocks of the films from CD and DVD are represented in the AFM topographic image of a smaller area of the films shown in **Figures 6.11 (A)** and **6.11(B)** respectively. Here particles of sizes ranging from 20-200 nm are observed. This matches well with earlier TEM imaging observations.

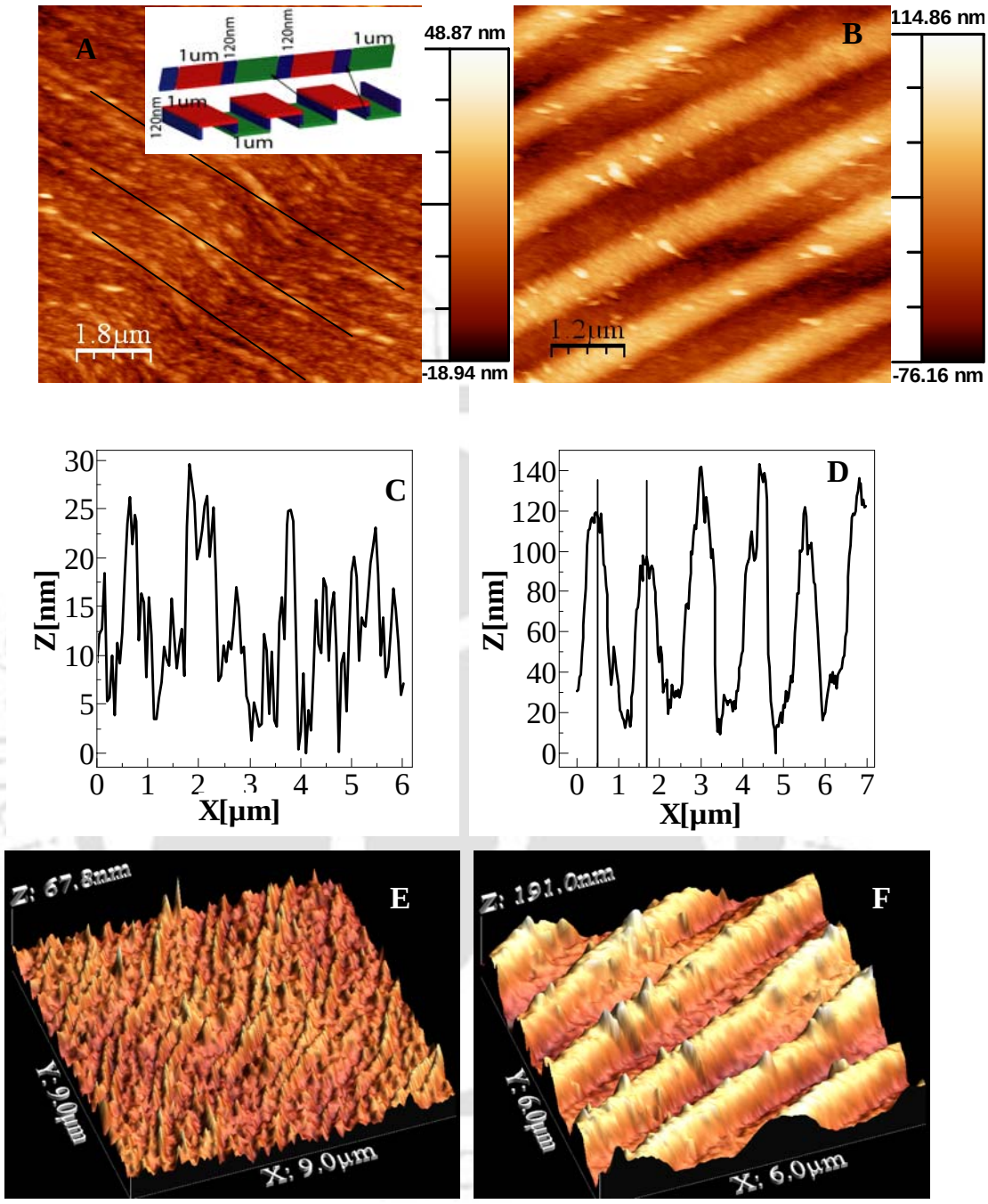

Figure 6.10. Representative AFM **(A)**, **(B)** topographic image, **(C)**,**(D)** height profile and **(E)**,**(F)** 3-dimensional view of a thin film generated from CD and DVD respectively after being transferred to glass cover slip.

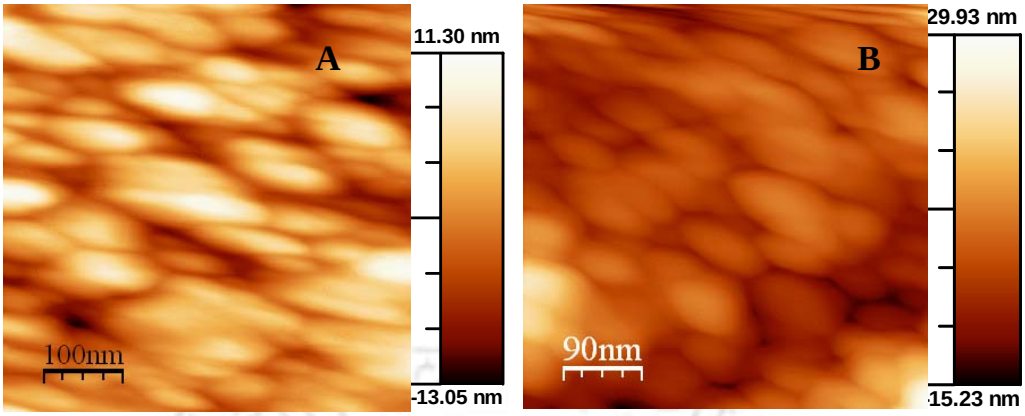

Figure 6.11: AFM topographic image of a smaller area in the films generated from **(A)** CD and **(B)** DVD.

These particles seem to have merged with each other resulting in the continuity of the structure. However, since reaction of the original Ag foil with $HAuCl_4$ led to the formation of the structure, it is plausible that partial etching of the film by galvanic replacement reaction in the presence of excess CTAB lead to formation of the film constituted by Ag and Au NPs. It is interesting to observe that a metallic film with corrugation would retain its surface and height profile upon reaction with $HAuCl_4$ and thus the role of CTAB in the retention of the structure of the film notwithstanding the reaction is of paramount importance. At lower concentrations of CTAB no film formation was observed. On the other hand at higher concentrations the reaction was very slow and film formation, if at all, took very long time and thus not pursued further.

In order to determine the thickness of the films we have recorded the AFM images of the films at the film-glass boundary in contact mode, shown in **Figure 6.12(A)** and **Figure 6.12(B)** for films generated from CD and DVD respectively. The average thickness of the film generated from CD was found to be 30± 5 nm as was seen in the

height profile, **Figure 6.12(C)** at the boundary of the film and glass. While the film from DVD was of approximate thickness 60 ± 5nm (**Figure 6.12(D)**).

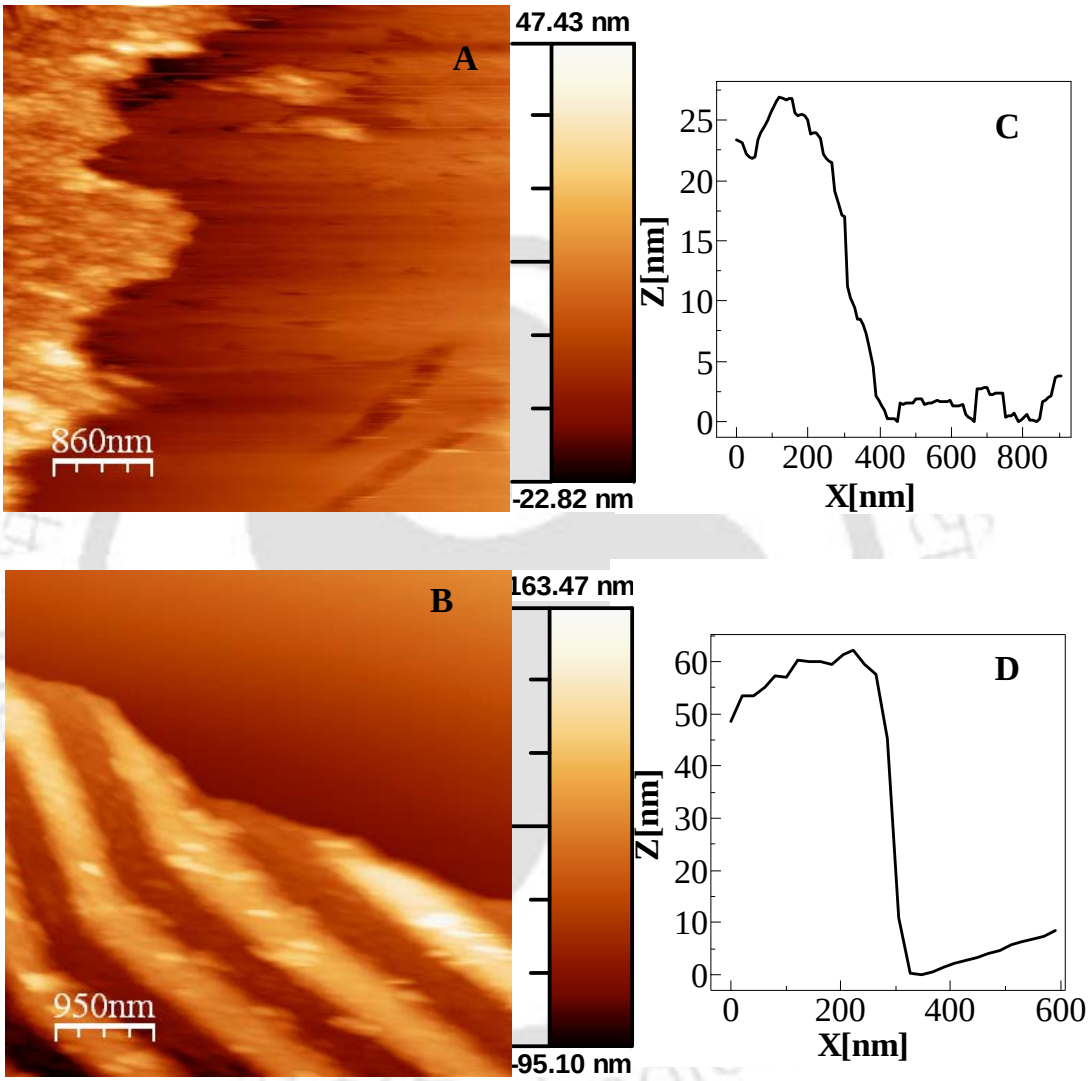

Figure 6.12: AFM topographic image of thin films generated from **(A)**, CD and **(B)** DVD silver foils at the glass film boundary, after transfer to glass cover slip. **(C)** and **(D)** are the height profiles at the film glass boundary for images **(A)** & **(B)** respectively.

We have also tried to transfer secondary structures apart from the primary CD/DVD tracks. For that we have had a CD written representing an ordinary data file and then

the same (the Ag foil) was reacted with $HAuCl_4$, in the presence of 0.1M CTAB, to see whether the writing patterns were transferred to the thin films. To our amusement the writing marks were transferred to the AgAu films. **Figure 6.13(A)** shows the patterns created by writing on a CD. The same patterns were transferred to the films as seen in **Figure 6.13(B)**. Here we see two films one on top of other, both of which

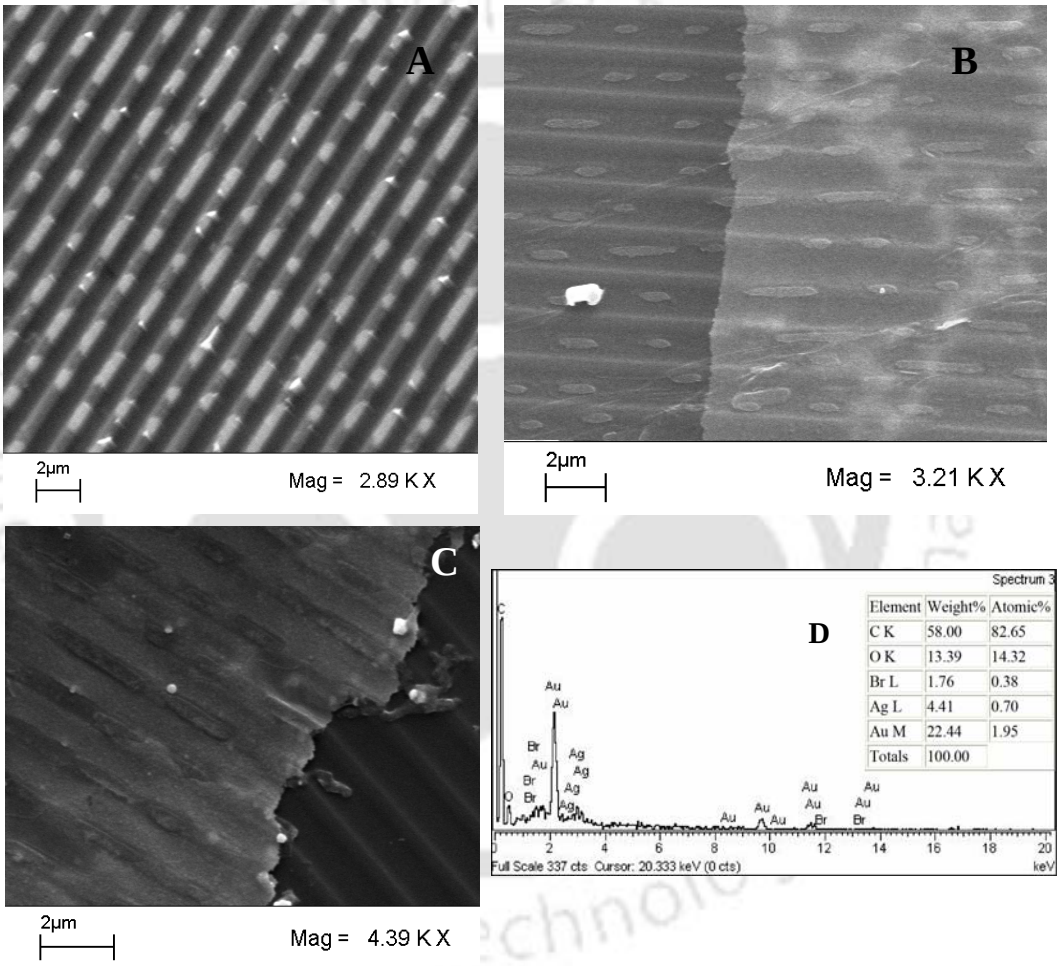

Figure 6.13: SEM images of **(A)** a written CD, **(B)** and (**C)** thin film generated from silver foil of a written CD. **(D)** EDX spectra and percentage composition of the film shown in **(C)**.

contain the written patterns. In **Figure 6.13(C)** it is clearly seen that the writing patterns were transferred to the film leaving no marks on the substrate containing the

tracks. The composition of the thin film is similar to the films obtained from the unwritten CD as shown by the EDX spectra and the percentage composition in **Figure 6.13(D).** Hence the present method could be an economic and efficient method for generating both primary and secondary patterns on Ag-Au NP thin films.

Conclusion

In this chapter we have demonstrated a novel method of generating bimetallic NP (of Au and Ag) thin films by using galvanic replacement reactions in presence of a surfactant (CTAB). The film contained the corrugated pattern of the substrate on which one of the metals, in the present case silver, was present as a bulk metallic thin film. We have also demonstrated that secondary patterns or marks generated on the bulk Ag film were also transferred to the final AgAu thin films. These films can be excellent materials for photonics and optoelectronics applications as well as porous membranes.

References

1. *Metal Nanoparticles*; Feldheim, D. L., Foss, C. A., Jr. Eds., Marcel Dekker, Inc.: New York, 2002.
2. Parak, W. J.; Manna, L.; Simmel, F. C. Gerion, D.; Alivisatos, P. Quantum Dots. In *Nanoparticles;* Schmid, G. Ed., Wiley-VCH Verlag GmbH & Co.: KGaA, Weinheim, 2004, pp 4-49.
3. Roucoux, A.; Schulz, J.; Patin, H. *Chem. Rev.* **2002,** *102,* pp 3757-3778.
4. Grisel, R.; Weststrate, K. J.; Gluhoi , A.; Nieuwenhuys, B. E. *Gold Bull.* **2002**, *35*, pp 39-45.

5. Zhou, B.; Balee, R.; Groenendaal, R *Nanotechnology law &business* **2005**, *2*, pp 222-229.

6. Hughes, M. D.; Xu, Y. J.; Jenkins1, P.; McMorn1, P.; Landon, P.; Enache, D. I.; Carley, A. F.; Attard, G. A.; Hutchings, G. J.; King, F.; Stitt, E. H.; Johnston, P.; Griffin, K. ; Kiely, C. J. *Nature*, **2005**, *437*, pp1132-1135.

7. Son, S. U.; Jang, Y.; Yoon, K. Y.; An, C.; Hwang, Y.; Park, J. G.; Noh, H. J.; Kim, J. Y.; Parkd, J. H.; Hyeon, T. *Chem. Commun.* **2005**, pp 86–88.

8. Luo, C.; Zhang, Y.; Wang, Y. *J. Mol. Cat. A* **2005**, *229*, pp 7–12.

9. Narayanan , R.; El-Sayed, M. A. *J. Phys. Chem. B* **2005**, *109*, pp 12663-12676.

10. Link , S.; El-Sayed, M. A. *Annu. Rev. Phys. Chem.* **2003**. *54*, pp 331–366.

11. Watanabe, K.; Menzel, D.; Nilius, N.; Freund, H. J. *Chem. Rev.* **2006,** *106*, pp 4301-4320.

12. Kelly, K. L.; Coronado, E.; Zhao, L. L.; Schatz, G. C. *J. Phys. Chem. B* **2003**, *107*, pp 668–677.

13. Stewart, M. E.; Anderton, C. R.; Thompson, L. B.; Maria, J.; Gray, S. K.; Rogers, J. A.; Nuzzo, R. G. *Chem. Rev.* **2008,** *108*, pp494-521.

14. Talapin, D. V.; Lee, J. S.; Kovalenko, M. V.; Shevchenko, E. V. *Chem. Rev.* **2010,** *110*, pp 389–458.

15. Mulvaney, P. *Langmuir* **1996,** *12*, pp788-800.

16. Daniel, M. C.; Didier Astruc, D. *Chem. Rev.* **2004**, *104*, pp 293-346.

17. Evanoff, D. D., Jr; Chumanov, G. *ChemPhysChem* **2005**, *6*, pp1221 – 1231.

18. Eustis, S.; El-Sayed, M. A. *Chem. Soc. Rev.* **2006**, *35*, pp209-217.

19. Gopinath, P.; Gogoi, S. K.; Chattopadhyay, A.; Ghosh, S. S. *Nanotechnology* **2008**, doi:10.1088/0957-4484/19/7/075104.

20. Toshima, N.; Harada, M.; Yamazaki,Y. Asakura, K. *J. Phys. Chem.* **1992**, *96*, pp 9927-9933.

21. Tokonami, S.; Morita, N.; Takasaki, K.; Toshima, N. *Phys. Chem. C* **2010**, *114*, pp 10336–10341.

22. Toshima, N.; Yonezawa, T. *New J. Chem.* **1998**, *22*, pp1179-1201.

23. Ferrando, R.; Jellinek, J.; Johnston, R. L. *Chem. Rev.* **2008**, *108*, pp 845-910.

24. Zhang, Q.; Lee, J. L.; Yang, J.; Boothroyd, C. Zhang, J. *Nanotechnology* **2007**, *18*, 245605 (8pp). doi:10.1088/0957-4484/18/24/245605

25. Murray-Methot, M. P.; Ratel, M.; Masson, J. F. *J. Phys. Chem. C* **2010,** *114*, pp8268–8275.

26. Major, K. J.; De, C.; Obare, S. O. *Plasmonics* **2009**, *4*, pp 61– 78.

27. Chen, J.; Wiley, B.; McLellan, J.; Xiong, Y.; Li, Z.-Y.; Xia, Y. *Nano Lett.* **2005**, *5*, pp2058– 2062.

28. Zhang, Q. B.; Xie, J. P.; Lee, J. Y.; Zhang, J. X.; Boothroyd, C. *Small* **2008**, *4*, pp1067-1071.

29. Srnova´-Sÿloufova, I.; Lednicky, F.; Gemperle, A. Gemperlova, J. *Langmuir* **2000,** *16*, pp 9928-9935.

30. Nagaraju, D. H. Lakshminarayanan, V. *J. Phys. Chem. C* **2009**, *113*,pp 14922–14926.

31. Chai, L.; Klein, J. *Langmuir* **2007**, *23*, pp 7777-7783.

32. Lu, Y.; Wang, Q.; Sun, J.; Shen, J. *Langmuir* **2005**, *21*, pp 5179-5184.

33. Grabar, K. C.; Allison, K. J.; Baker, B. E.; Bright, R. M.; Brown, K. R.; Freeman, R. G.; Fox, A. P.; Keating, C. D.; Musick, M. D.; Natan, M. J. *Langmuir* **1996**, *12*, pp 2353-2361.

34. Li, X.; Zhao, S.; Zhang, S.; Kim, D. H.; Knoll, W. *Langmuir* **2007**, *23*, pp 6883-6888.

35. Paul, S.; Pearson, C.; Molloy, A.; Cousins, M. A.; Green, M.; Kolliopoulou, S.; Dimitrakis, P.; Normand, P.; Tsoukalas, D.; Petty, M. C. *Nano Lett.* **2003**, *3*, pp 533-536.

36. Zheng, M.; Gu, M.; Jin, Y.; Jin, G. *Mater. Res. Bull.* **2001**, *36*, pp 853-859.

37. Lu, L.; Eychmuller, A.; Kobayashi, A.; Hirano, Y.; Yoshida, K.; Kikkawa, Y.; Tawa, K.; Ozaki, Y. *Langmuir* **2006**, *22*, pp 2605-2609.

38. Suyal, G.; Mennig, M.; Schmidt, H. *J. Mater. Sci.* **2003**, *38*, pp 1645-1651.

39. Musick, M. D.; Keating, C. D.; Lyon, L. A.; Botsko, S. L.; Pena, D. J.; Holliway, W. D.; McEvoy, T. M.; Richardson, J. N.; Natan, M. J. *Chem. Mater.* **2000**, *12*, pp 2869-2881.

40. Ou, M.; Lu, G.; Shen, H.; Descamps, A.; Marquette, C. A.; Blum, L. J.; Ledoux, G.; Roux, S.; Tillement, O.; Cheng, B.; Perriat, P. *Adv. Funct. Mater.* **2007**, *17*, pp 1903–1909.

41. Mulvaney, P.; Giersig, M.; Henglein, A. *J. Phys. Chem.* **1993**, *97*, pp 7061-7064.

42. Hu, W. P., Chen, S.-J., Huang, K.-T., Hsu, J. H., Chen, W. Y., Chang, G. L.; Lai, K. A. *Biosens. Bioelectron.* **2004**, *19*, pp 1465-1471.

43. Ren, M. L.; Meng, X. W.; Chen, D.; Tang, F. Q.; Jiao, J. *Biosens. Bioelectron.* **2005**, *21*, pp 433−437.

44. Niemeyer, C. M. *Angew. Chem., Int. Ed.* **2001**, *40*, pp 4128-4158.

45. Kamat, P. V. *J. Phys. Chem. B* **2002**, *106*, pp7729-7744.

46. Dinda, E.; Rashid, H. Md.; Biswas, M.; Mandal, T. K. *Langmuir* **2010**, *26*, pp 17568–17580.

47. Markovich, G.; Leff, D. V.; Chung, S.-W.; Soyez, H.; Dunn, B.; Heath, J. R. *Appl. Phys. Lett.* **1997**, *70*, pp 3107-3109.

48. Shipway, A. N.; Katz, E.; Willner, I. *ChemPhysChem* **2000**, *1*, pp 18-52.

49. Ozbay, E. *Science* **2006**, *311*, pp189-193.

50. Yu, A.; Liang, Z.; Cho, J.; Caruso, F. *Nano Lett.* **2003**, *3*, pp 1203-1207.

51. Fendler, J. H. *Nanoparticles and Nanostructured Films: Preparation, Characterization and Applications*; Wiley-VCH Verlag GmbH: Weinheim, 1998.

52. Biswas, P. C.; Nodasaka, Y.; Haruta, M. *J. Electroanal. Chem.* **1995**, *381*, pp 167-177.

53. Wang, H.; Huang, Y.; Tan, Z.; Hu, X. *Anal. Chim. Acta* **2004**, *526*, pp 13-17.

54. Zabet-Khosousi, A.; Dhirani, A. A. *Chem. Rev.* **2008**, *108*, pp 4072–4124.

55. Barnes, W. L.; Dereux, A.; Ebbesen, T. W. *Nature* **2003**, *424*, pp 824−830.

56. Ebbesen, T. W.; Lezec, H. J.; Ghaemi, H. F.; Thio, T.; Wolff, P. A. *Nature* **1998**, *391*, pp 667−669.

57. Cao, Y. W. C.; Jin, R. C.; Mirkin, C. A. *Science* 2002, *297*, pp 1536-1540.

58. Han, L.; Daniel, D. R.; Maye, M. M.; Zhong, C. J. *Anal. Chem.***2001**, *73*, pp 4441-4449.

59. Gordon, R.; Sinton, D.; Kavanagh, K. L.; Brolo, A. G. *Acc. Chem. Res.* **2008**, *41*, pp 1049– 1057.

60. Homola, J. *Chem. Rev.*, **2008**, *108*, pp 462–493.

61. Ray, C. P. *Chem. Rev.* 2010, *110*, pp 5332– 5365.

62. Li, Y.; Zhang, J.; Wang, T.; Zhu, S.; Yu, H.; Fang, L.; Wang, Z.; Cui, L.; Yang, B. *J. Phys. Chem. C*, **2010**, *114*, pp 19908–19912.

63. Gao, G. *Nanostructures and Nanomaterials, Synthesis Propreties and Applications*, Imperial College Press: London, 2004.

64. Xu, H.; Hong, R.; Wang, X.; Arvizo, R.; You, C.; Samanta, B.; Patra, D.; Tuominen, M. T.; Rotello, V. M. *Adv. Mater.* **2007**, *19*, pp 1383–1386.

65. Hao, E.; Tianquan Lian, T. *Chem. Mater.* **2000**, *12*, pp 3392-3396.

66. Xi, J. Q.; Schubert, M. F.; Kim, J. K.; Schubert, E. F.; Chen, M.; Lin, S.-Y.; Liu, W.; Smart,, J. A. Nat. Photonics **2007**, *1*, pp 176-179.

67. Huang, Y.-F.; Chattopadhyay, S.; Jen, Y.-J.; Peng, C.-Y.; Liu, T.-A.; Hsu, Y.-K.; Pan, C.-L.; Lo, H.-C.; Hsu, C.-H.; Chang, Y.-H.; Lee, C.-S.; Chen, K.-H.; Chen, L.-C. *Nat. Nanotechnol.* **2007**, *2*, pp 770 774.

68. Lee, D.; Rubner, M. F.; Cohen, R. E. *Nano Lett.* **2006**, *6*, pp 2305-2312.

69. Notsu, H.; Kubo, W.; Shitanda, I.; Tatsuma, T. *J. Mater. Chem.* **2005**, *15*, pp 1523–1527.

70. Feng, L.; Li, S.; Li, Y.; Li, H.; Zhang, L.; Zhai, J.; Song, Y.; Liu, B.; Jiang, L. ; Zhu, D. *Adv. Mater.* **2002**, *14*, pp 1857–1860.

71. Parker, A. R.; Townley, H. E. *Nature Nanotechnol.* **2007**, *2*, pp 347-353.

72. Hulteen, J. C.;Treichel, D. A.; Smith,T. M.; Duval, M. L.; Jensen, T. R.; Van Duyne, R. P. *J. Phys. Chem. B* 1999, *103*, pp 3854-3863.

73. Gates, B. D.; Xu, Q.; Stewart, M.; Ryan, D.; Willson,C. G.; Whitesides, G. M. *Chem. Rev.* **2005,** *105*, pp1171-1196.

74. Mazzola, L. *Nat. Biotechnol.* **2003**, *21*, pp 1137-1143.

75. Pan, C. T.; Lo, S. C.; Yang, J. C.; Chen, Y. J. *Opt. Quant. Electron.* **2007**, *39*, pp 693–705.

76. Ung, T.; Liz-Marzan, L. M.; Mulvaney, P. *Col. Surf. A* **2002**, *202*, 119-126.

77. Sau, T. K.; Murphy, C. J. *Langmuir*, 2005, *21*, pp 2923–2929.

78. Solubility product constants. In *CRC Handbook of Chemistry and Physics, 85th Edition;* Lide, D. R. Ed., CRC Press, Boca Raton, FL: 2005.

79. Srnova´-Sÿloufova, I.; Lednicky, F.; Gemperle, A. Gemperlova, J. *Langmuir* **2000,** *16*, pp 9928-9935.

80. Chen, D. H.; Chen, C. J. *J. Mater. Chem.*, **2002**, *12*, pp 1557–1562.

81. Sambhy, V.; MacBride, M. M.; Peterson, B. R.; Sen, A. *J. Am. Chem. Soc.* **2006**, *128*, pp 9798-9808.

82. Chakraborty, M.; Chowdhury, D.; Chattopadhyay, A., *J.Chem. Edu.* **2003**, *80*, pp 806-809.

Future Prospects

The work presented here opens up newer possibilities for theoretical understanding of the phenomena observed, further experimental probes for detailed understanding of the underlying mechanisms and the application of the process and products. As discussed earlier a detailed understanding of the interaction various nanomaterials with the biological system is important for predicting the future of our ecosystems when exposed extensively to nanoscale particles. Apart from the short term actions of the NPs (Ag NPs in this case) there may be some far reaching, long term consequences of use of these materials, which needs to be monitored and studied in greater detail for the better and controlled applications. Also, understanding the activities of NPs under biotic and abiotic conditions is crucial for future applications especially in their intended use for therapeutics or as antimicrobial agents. Whenever use of any nanomaterial with a human interface is involved, directly or indirectly, the possibilities of the human being exposed to the nanomaterials are considerable. Therefore, a detailed study of the biological activity of the nanomaterials is desired. In our case we have demonstrated the antimicrobial activity of Ag NPs using GFP expressing *E. coli* bacteria with the aim to study the mechanistic aspects of the bacteriacidal activity and at the same time providing an easy detection method facilitated by the GFP. Therefore, establishing the use of GFP expressing *E. coli* as a model system in the study of antimicrobial activities of Ag NPs or any other nanomaterial may serve as a convenient and superior method by using routine fluorescence microscopic studies. Furthermore, the Ag NPs synthesized in bacterial growth medium would serve the purpose of studies intended with bare NPs without

having to go through the complications of additional stabilizers used generally for the NP synthesis.

Similarly the synthesis of Ag NPs in cell growth medium to explore the cytotoxic effect of Ag NPs devoid of any external stabilizers is important. Cytotoxicity of Ag NPs is known but the application of Ag NPs in therapeutics is new. Our findings on the activity of the Ag NPs on mammalian cells suggest the possibilities of Ag NPs being used as therapeutic drugs in cancer treatments in conjunction with already established drugs. The results presented here, however, show the similar activities of the Ag NPs towards both cancerous and non cancerous cells; however, there is scope to minimize the cytotoxicity towards non cancerous cells via modifications leading to more targeted mode of action. Also, the test of Ag NPs in conjunction with other anticancer drugs is an attractive area remains much to be explored. These findings may lead to the development of a new class of anticancer drugs containing the organic –inorganic hybrid systems.

For many practical applications such as high density storage, photonics, electronics, plasmonics, biosensing chemical sensing, heterogeneous catalysis etc. the NPs bound to a surface especially in an organized fashion have the advantages of both macroscopic and the nanoscale objects together. In other words, macroscopic surface immobilization of NPs is helpful for easy handling of the macroscopic objects and at the same time for exploiting the properties of the nanoscopic materials. Our work on the development of surface bound AgAu NPs is an easy method to obtain the bimetallic AgAu NPs bound to a flexible plastic surface and the patterns generated due to the reaction diffusion rendered it to be an alternate to lithographic techniques. The materials generated by this method can serve as the substrates for surface enhanced spectroscopic techniques like metal enhanced fluorescence and the surface

enhanced Raman spectroscopy. There is the possibility of the AgCl bound to the surface being used as the photocatalyst for degradation of various organic dyes which we have explored to some extent and also would be useful in many photocatalytic organic transformations. Additionally the bimetallic nature of the surface bound NPs leaves plenty of scope for the tuning of the SPR frequencies of the AgAu NPs by changing the composition. Moreover, the arrangement of the AgAu NPs in the form of arrays is important from the point of view of the lithography, for lithographically patterned NP arrays have diverse range of applications. As the bimetallic NP patterns thus generated are dependent on the redox couple between Ag (0) and Au (III), other similar couples may be explored for the further understanding of the pattern generation process and newer applications. Finally, the composite film of Ag and Au generated from a template surface provides a fresh approach to the generation of metallic films with nanoscale components. Further, the corrugation and optical pattern transfer in the film make the application potential in the aforementioned fields appealing.